POLITÉCNICA

ESCUELA TÉCNICA SUPERIOR DE INGENIEROS INDUSTRIALES
UNIVERSIDAD POLITÉCNICA DE MADRID

José Gutiérrez Abascal, 2. 28006 Madrid
Tel.: 91 336 3060
info.industriales@upm.es

www.industriales.upm.es

Álvaro Quiles García

05 TRABAJO FIN DE GRADO

INDUSTRIALES

TRABAJO FIN DE GRADO

Concepción y Diseño de un Sistema de Medición del Perfil de Velocidades y del Nivel del Agua en un Canal de Pruebas

TRABAJO FIN DE GRADO PARA LA OBTENCIÓN DEL TÍTULO DE GRADUADO EN INGENIERÍA EN TECNOLOGÍAS INDUSTRIALES

NOVIEMBRE 2017

Álvaro Quiles García

DIRECTOR DEL TRABAJO FIN DE GRADO:
Emilio Migoya Valor

INDUSTRIALES
ETSII | UPM

POLITÉCNICA

Universidad Politécnica de Madrid

Escuela Técnica Superior de Ingenieros Industriales

TRABAJO DE FIN DE GRADO

GRADO EN INGENIERÍA EN TECNOLOGÍAS INDUSTRIALES

Concepción y Diseño de un Sistema de Medición del Perfil de Velocidades y Nivel de Agua para una Plataforma de Prueba de Canal

Álvaro Quiles García

Número de matrícula: 13370

Tutor: Emilio Migoya Valor

Noviembre 2017

Madrid

Tabla de Contenido Del Resumen en Español

1 Introducción y Motivación

El presente Trabajo de Fin de Grado forma parte de un proyecto de mayores dimensiones realizado en la universidad TU Darmstadt, dicho proyecto se basa en la modelización y simulación de una turbina mareomotriz mediante un canal de agua diseñado por (Hernandez, 2013) y mejorado por (Lehr, 2014), el objetivo del proyecto es calcular la eficiencia energética de la aplicación de una turbina mareomotriz real.

Más concretamente, el presente TFG se va a centrar en la concepción y diseño de un sistema de medición que sea capaz de medir parámetros que a posteriori serán necesarios para futuros trabajos dentro del proyecto anteriormente mencionado.

Dentro del departamento de fluidos (FST) de la universidad TU Darmstadt se ha diseñado un modelo para calcular el coeficiente de operatividad C_p para canales rectangulares hidráulicos con obstrucción completa tanto de altura como de anchura (Pelz, 2011).

A diferencia de las plantas hidráulicas convencionales, las turbinas mareomotrices se caracterizan por no tener una obstrucción completa. El presente trabajo estudiará turbinas con obstrucción completa de anchura, pero no de altura de manera que se consiga un flujo de derivación vertical.

El mayor problema a la hora de diseñar un sistema de medición para una turbina mareomotriz es la influencia de la superficie libre alrededor de la turbina, debido a la presencia de una cascada, salto de altura, la cual genera una diferencia de energía estática. El modelo analítico en el cual está basado el presente TFG se realizó mediante la conservación de la energía, la ecuación de continuidad y el principio de impulso lineal.

El sistema de medición diseñado debe ser capaz de medir la velocidad del flujo, la línea media y la anchura del tubo de corriente producido por la turbina y la altimetría del nivel del agua del canal.

Otra parte importante de este trabajo consiste en el diseño de un sistema que pueda mejorar el manejo de la turbina. Esto significa encontrar un sistema más automático que el actual, el cual a la hora de modificar el tipo de turbina o cambiar la posición de la turbina, está basado en un sistema de tornillos, siendo este muy incómodo a la hora de trabajar. En definitiva, se busca una estructura más manejable.

El experimento va a consistir en la modelización de una turbina real, donde se va a usar un plato perforado en vez de una turbina normal, debido al tamaño del canal de agua. Este plato perforado tendrá una anchura igual a la del canal de agua, lo que implica una obstrucción horizontal completa mientras que su altura será variable.

La elección de los platos perforados como “turbina” se debe principalmente a dos razones: En primer lugar, debido a que representa un flujo de derivación vertical, el cual es característico de las turbinas mareomotrices. La segunda razón es la no importancia del tipo de energía que se disipa ya que el resultado final a nivel de cálculo va a ser el mismo. En el presente caso, los platos perforados van a disipar calor en ved de energía mecánica.

La Figura 1 representa el modelo con el que se va a trabajar:

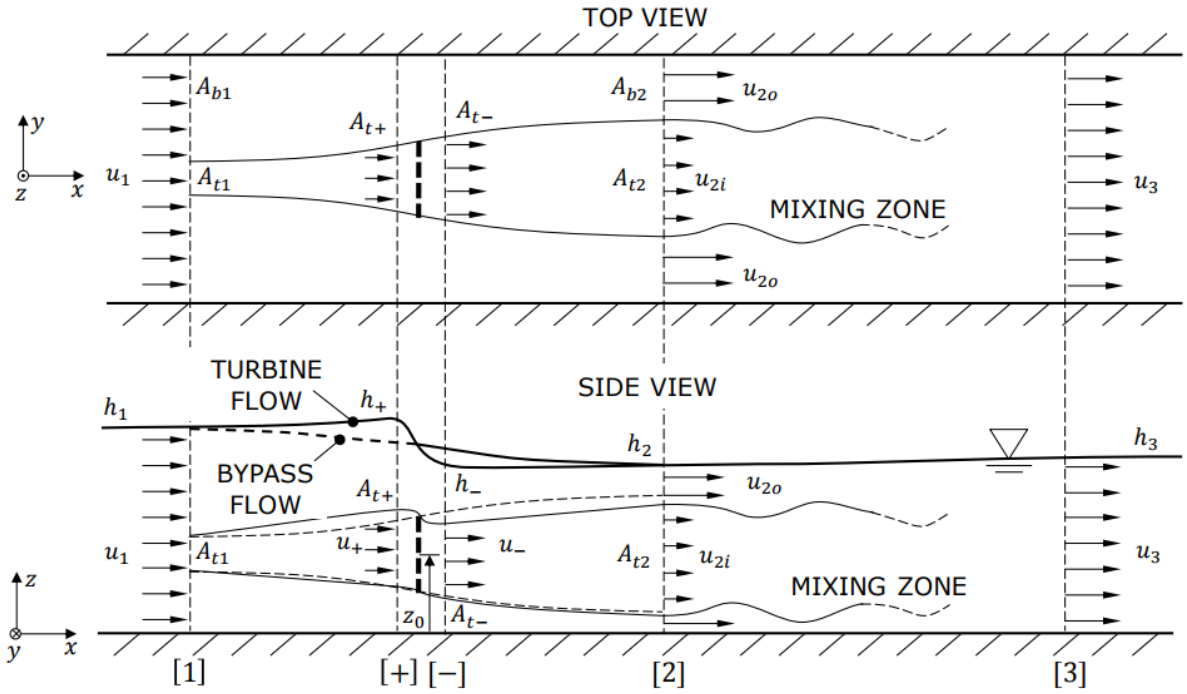

Figura 1: Simulación Experimental del Flujo

Como se puede observar, existen cinco puntos de interés a lo largo del canal, (1), (+), (-), (2) y (3). Este trabajo se centrará en la zona comprendida entre los puntos (+) y (2), ya que es el área de conflicto por la presencia de la cascada. Aun siendo cierto que este trabajo se centra en la zona entre los puntos (+) y (2), también se estudiará la zona entre (1) y (+).

Otra consecuencia relevante del uso de un flujo de derivación vertical reside en la diferencia de velocidades entre el agua que pasa por el plato perforado y el que pasa por el flujo de derivación ($u_{20} > u_{2i}$). Esto es interesante ya que el caudal volumétrico que pasa por el plato perforado se conserva hasta la zona de mezcla, como se puede apreciar en la Figura 1.

El canal de pruebas usado para la experimentación es el mostrado en las Figuras 2 y 3, se puede definir como un circuito cerrado debido a que el agua es la misma todo el rato, dicha agua viene de un tanque situado justo abajo del canal.

Figura 2: Canal de Pruebas 3D

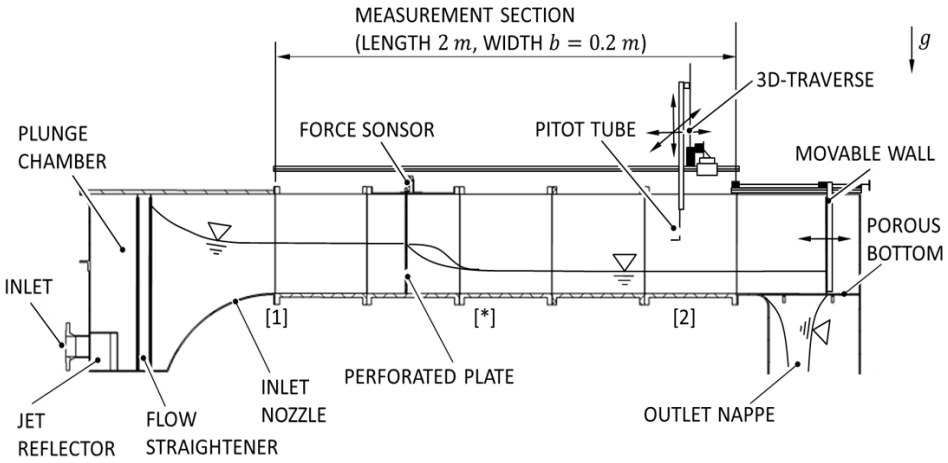

Figura 3: Canal de Pruebas 2D

La entrada del canal está fabricada de acero inoxidable y posee un filtro de agujeros redondeados, mediante el cual se consigue un desarrollo progresivo de la capa límite y un mejor perfil de velocidades en el canal. El canal de pruebas también posee un homogeneizador y un control del caudal volumétrico en la entrada.

Otro aspecto que considerar es el material del cristal del canal, vidrio acrílico, el cual fue escogido por (Hernandez, 2013) debido a su transparencia. Este material puede ser muy útil a la hora de usar técnicas de medición de carácter óptimo como lo son PIV o PTV, estas técnicas serán importantes a la hora de la elección final del sistema de medición

Antes de empezar con el estudio del diseño del sistema de medición es necesario estudiar la variación de ciertos parámetros.

El caudal volumétrico máximo con el que la bomba puede trabajar es de 82 m^3 /h. El número de Froude, $Fr = \frac{Q}{b\sqrt{g \cdot h^3}}$ considerado va a depender de la zona del canal de pruebas, donde Q es el caudal, b es la anchura y h es la altura de agua en el punto estudiado.

En la entrada se buscará un número de Froude comprendido entre los valores 0 y 0.3, mientras que en la salida estará comprendido entre 0 y 0.5. El número máximo de Froude al que se podrá enfrentar el canal de pruebas es de 1.4 en la zona de la cascada. Con lo que se puede afirmar que el flujo de agua es subcrítico en todo el canal menos en la cascada donde es supercrítico.

Sabiendo el caudal y el número de Froude, se calcula el rango de velocidades en el que se puede trabajar, mediante la siguiente expresión:

$$u = (\, Fr \sqrt{g \frac{Q}{b}}\,)^{2/3}$$

Donde se obtienen velocidades en el canal entre 0.2 y 1.3 m/s. Es conveniente tener en cuenta que los perfiles de velocidad justo después de la turbina no son homogéneos. Por tanto, como se estudió previamente en (Nieschlag, 2016), ver sección 2.2, es necesario multiplicar por un factor de 1.3. Resultando en que la velocidad máxima del canal previamente explicado será de 1.7 m/s.

El número de Reynolds también es necesario calcularlo, y se puede calcular mediante la siguiente expresión para canales abiertos con forma rectangular (Pelz, 2011).

$$Re = \frac{4 \cdot u_o \cdot h_0}{(1 + 2\frac{h_0}{b})\nu}$$

Se obtiene un número de Reynolds a lo largo del canal de $Re\left(Fr = [0.1,\ 1.4]\right) = [7.3 \cdot 10^4,\ 2.4 \cdot 10^5]$. Con lo que se obtiene un flujo de carácter turbulento en el canal de pruebas.

Otros cálculos de menor relevancia han sido calculados en la sección 2.2.

2 Estado del Arte

La primera parte del trabajo se centra en el estudio completo de las diferentes técnicas de medición existentes a día de hoy en el mercado. Más concretamente en las principales técnicas de medición para velocidades de flujo y para la altimetría de este. Este apartado esta detallado en la sección 4.

Para la medición de la velocidad se han encontrado ocho posibles técnicas: PIV, PTV, Tubo de Pitot, Sondas de Múltiples Agujeros, Sondas de Alambre Caliente, Laser Doppler Anemometry, Molecular Tagging Velocimetry y Visualización del Flujo. Estas técnicas están ampliamente explicadas en la sección 4.1. En la tabla 2 se puede observar una comparativa entre ellas.

Para la medición del nivel del fluido en el canal de pruebas se han encontrado también ocho posibles técnicas: Cámara de Alta resolución, Láser, Conductive Level Altimetry, Capacitive Level Altimetry, Medida Directa, Ultrasonido, Radar y Magnetostrictive Level Transmitters. Estas técnicas están ampliamente explicadas en la sección 4.2. En la tabla 3 se puede observar una comparativa entre ellas.

Tras realizar el estudio de los posibles métodos se tendrá que buscar combinaciones entre las diferentes técnicas para satisfacer todos los objetivos que tiene el diseño del sistema de medición. Estos son los comentados en la sección 3., medición de la velocidad del flujo, la línea media, la anchura del tubo de corriente producido por la turbina y la altura del flujo en el canal de pruebas.

Tabla 1 y Tabla 2: Técnicas de Medición de Perfil de Velocidades y Altimetría respectivamente

	Camera	Laser	Conductive Level Altimetry	Capacitive Level Altimetry	Direct Measurement	Ultrasonic	Radar	Magnetostricitive Level Transmitters
A	NO	NO	NO	NO	NO	NO	NO	NO
u (cascade)	NO	NO	NO	NO	NO	NO	NO	NO
u (rest)	NO	NO	NO	NO	NO	NO	NO	NO
h (cascade)	YES	YES	YES	Part	YES	YES	YES	YES
h (rest)	YES	YES	YES	YES	YES	YES	YES	YES
z	NO	NO	NO	NO	NO	NO	NO	NO
p (cascade)	Part	Part	Part	Part	Part	Part	Part	Part
p (rest)	Part	Part	Part	Part	Part	Part	Part	Part
Economic	YES	NO	YES	NO	YES	Medium	Medium	NO
Accuracy	Medium	High	Medium	Medium	Low	High	Medium	High

	PIV	PTV	Pitot	Multi-hole Probe	Hot Wire Probe	LDA	MTV	Flow Visualization
A	YES	YES	YES	YES	YES	Partially	YES	YES
u (cascade)	YES	YES	NO	NO	YES	YES	YES	YES
u (rest)	YES	YES	YES	YES	YES	NO	YES	YES
h (cascade)	NO	NO	NO	NO	NO	NO	NO	NO
h (rest)	NO	NO	YES	YES	NO	NO	NO	NO
z	YES	YES	YES	YES	YES	Partially	YES	YES
p (cascade)	Partially	Partially	NO	Partially	Partially	Partially	Partially	Partially
p (rest)	Partially	Partially	YES	YES	Partially	NO	Partially	Partially
Economic	NO	NO	YES	Medium	YES	NO	NO	YES
Accuracy	High	High	Medium	Medium	Medium	High	High	NO

3 Diseño del Sistema de Medición

Las combinaciones seleccionadas son las coloreadas en las Tablas 1 y 2, las cuales describimos a continuación:

1. Tubo de Pitot + Conductive Level Altimetry
2. Visualización del Flujo + Cámara + Tubo de Pitot
3. PIV/PTV + Cámara

Es conveniente leer detenidamente las técnicas de PIV, PTV y Visualización de flujo para entender las posibles combinaciones, las cuales se encuentran respectivamente en las secciones 4.1.1, 4.1.2, y 4.1.8., ya que son las técnicas en las que se va a basar este trabajo.

3.1 Combinación 1: Tubo de Pitot + Conductive Level Altimetry

La primera combinación es el sistema de medición implementado anteriormente en este canal. Este se basa en la utilización del Tubo de Pitot para la medición del perfil de velocidades y la técnica *Conductive Level Altimetry* para la medición del nivel de agua del canal.

Antes de empezar cualquier proyecto es necesario analizar los problemas del anterior sistema de medición utilizado en el canal y de la anterior estructura de la turbina empleada.

El problema principal en el sistema de medición actual es la falta de precisión en el área de interés (cascada). El tubo de Pitot debe de estar posicionado perpendicularmente a la superficie del fluido. En este proyecto es prácticamente imposible posicionarlo perpendicularmente a la superficie debido a la existencia de una cascada. La primera consecuencia de no posicionar perpendicularmente el tubo de Pitot es la producción de una superposición entre la presión dinámica y estática, esto conduce a un error de precisión bastante considerable.

En el caso de la medida del nivel del agua se utiliza como se ha comentado la técnica *Conductive Level Altimetry,* la cual está detallada en la sección 4.2.3. Este método también presenta problemas de precisión en la cascada como se estudió en el departamento previamente.

Debido a la poca precisión de ambos métodos, el cálculo del perfil de velocidades, de la línea media y anchura del tubo de corriente producido por la turbina, se propone mejorar el ya comentado sistema de medición. Por tanto esta combinación no será considerada.

3.2 Combinación 2: Visualización del Flujo + Cámara + Tubo de Pitot

En la segunda combinación se usará la técnica de Visualización del Flujo y el Tubo de Pitot para medir el perfil de velocidades del flujo, mientras que la cámara de alta resolución será la encargada de medir la altitud del nivel del fluido.

En cuanto a la técnica de visualización, como se explica en la sección 5.1.2.1., primero se optó por un concepto basado en el uso de láminas de baja densidad de polietileno con el objetivo de ser capaces de observar la forma del tubo de corriente producido por la turbina. Esta idea fue desechada tras debatirla con Prof. Pelz debido a que la presencia de las láminas puede producir fuerzas sobre ella incontrolables y no despreciables.

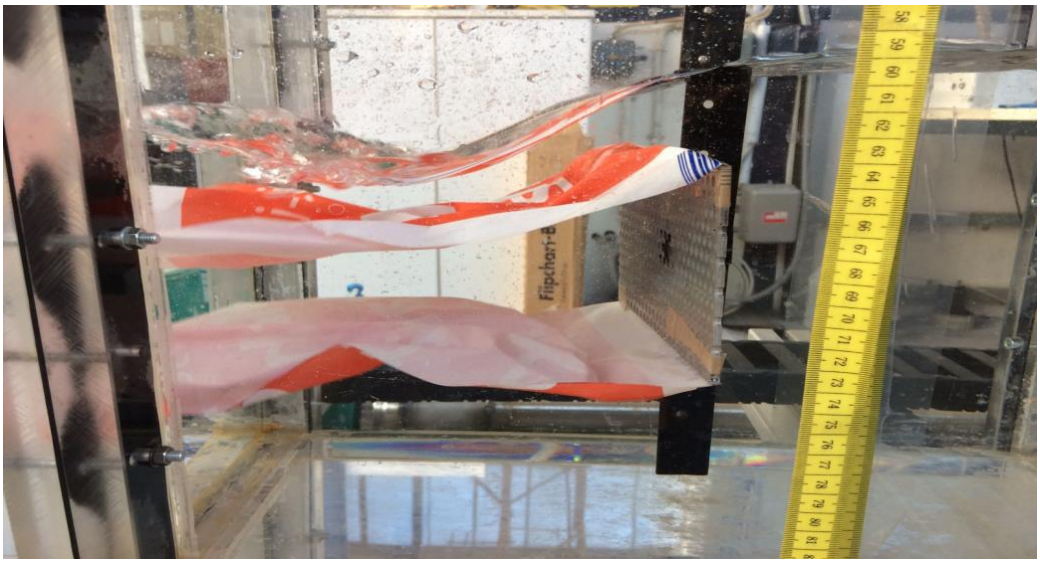

Figura 4: Visualización del Flujo mediante Láminas

Tras desestimar este primer prototipo, se decidió usar una técnica que consiste en la generación de burbujas de hidrógeno para observar el comportamiento del flujo. La idea es generar burbujas por electrólisis y tomar fotos desde la cámara de alta resolución, por tanto, la cámara tendrá dos funciones: tomar fotos de las burbujas de hidrógeno y medir el nivel del fluido en el canal de pruebas.

En este sistema de medición el tubo de Pitot se usará para medir el perfil de velocidades de la zona previa a la turbina, (1) hasta (+).

La generación de burbujas se realizará con el esquema electrónico mostrado en la Figura 5:

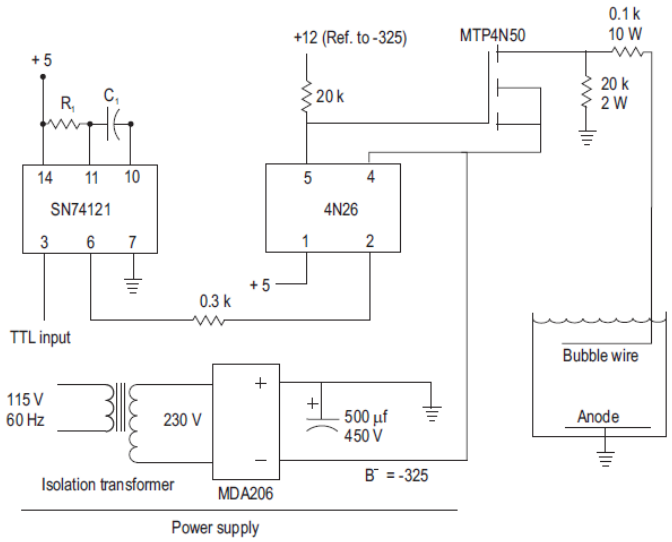

Figura 5: Circuito Electrónico para la Generación de Burbujas de Hidrógeno

Dicho circuito está compuesto por un transformador aislado, un rectificador, de manera que se trabaja en corriente continua, un "*Opto-isolator*", un multivibrador monoestable un transistor MOSFET el cual se encargará de generar un pulso para crear líneas de burbujas en distintos tiempos, una señal de entrada TTL y una sonda que hace de cátodo.

El funcionamiento y la lista de materiales necesarios para construir la consola eléctrica están detallados en la sección 5.1.2.2. Una de las ventajas de la posibilidad de crear un pulso de voltaje es la determinación de la velocidad media directamente de la frecuencia del pulso.

Debido a que la seguridad es primordial, se necesita un elemento que cortocircuite a 2 A con el objetivo de evitar daños producidos por la corriente que circula. Todos estos elementos, además de las resistencias necesarias, los aislantes necesarios y el transformador pertinente están detallados con sus proveedores y precios en la sección 9.3 (Presupuesto).

Para mejorar la calidad de la visualización de las burbujas, es altamente recomendable añadir una cantidad de 0.12 gramos de sulfato de sodio por litro de agua. Este componente crea una concentración electrolítica, la cual mejora la visualización de las burbujas. Otras posibilidades, si no se dispone de sulfato de sodio, podrían ser el uso de sal común o de una cantidad muy pequeña de ácido clorhídrico.

Nótese la importancia de la calibración de los aditivos por prueba y error, pues una baja concentración llevaría a la necesidad de un mayor voltaje, mientras que una alta concentración puede llevar a tamaños de burbujas muy grandes, lo cual no es deseable ya que el flujo utilizado en este proyecto es de carácter turbulento.

Otro punto que requiere su estudio es la elección del alambre generador de burbujas, la cual está detallada en la sección 5.1.2.2., se termina eligiendo como material el platino, de diámetro 50 μm y longitud 250 mm. El diámetro es de 50 μm debido a que se requieren

burbujas de pequeño tamaño ya que el fluido tiene un carácter turbulento. Un alambre de diámetro 25 μm sería excesivamente pequeño y podría romperse con facilidad.

Dicho alambre generador de burbujas será vertical debido a que de este modo es posible no solo medir la velocidad, sino también la línea media y la anchura del tubo de corriente producido por la turbina. Además que se evitan las turbulencias que crea un alambre generador de burbujas horizontal.

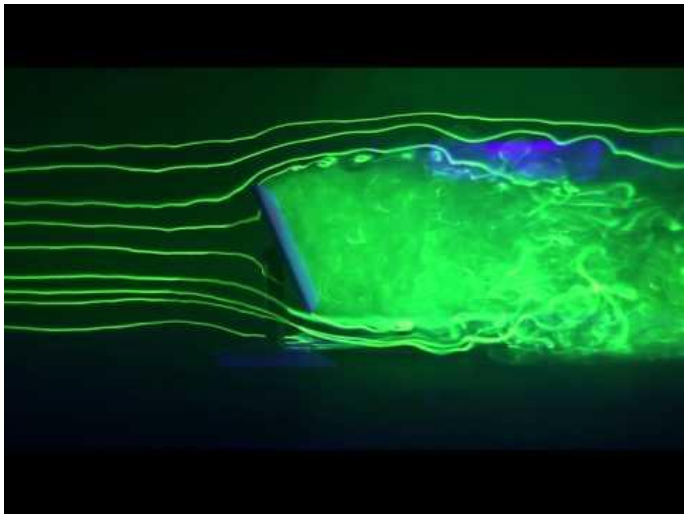

Figura 6: Visualización del Flujo

El soporte del generador de burbujas es de latón y su estructura es mostrada en la Figura 7:

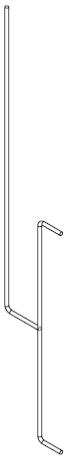

Figura 7: Soporte para Sonda Vertical

Es importante mencionar la necesidad de calibrar la tensión mecánica con la que el alambre generador de burbujas es ajustado al soporte, además de la necesidad de utilizar un aislamiento de manera que se pueda evitar que las burbujas de hidrógeno se produzcan en sitios indeseados.

Otro aspecto de alta relevancia es la iluminación, en este experimento usaremos LED's de alta potencia ya que requieren poca potencia y proporcionan una iluminación de calidad. Los cálculos realizados están detallados en la sección 5.1.2.2. Se decide posicionar 2 LEDs de 400 lúmenes de manera oblicua y otro LED posicionado en la parte baja del canal de 1.120 lúmenes. Otra opción de iluminación podría ser mediante láminas de láser, en este trabajo no ha sido posible su estudio, pero se plantea como posible mejora para siguientes trabajos.

El tubo de Pitot será implementado de la forma mostrada en la Figura 8:

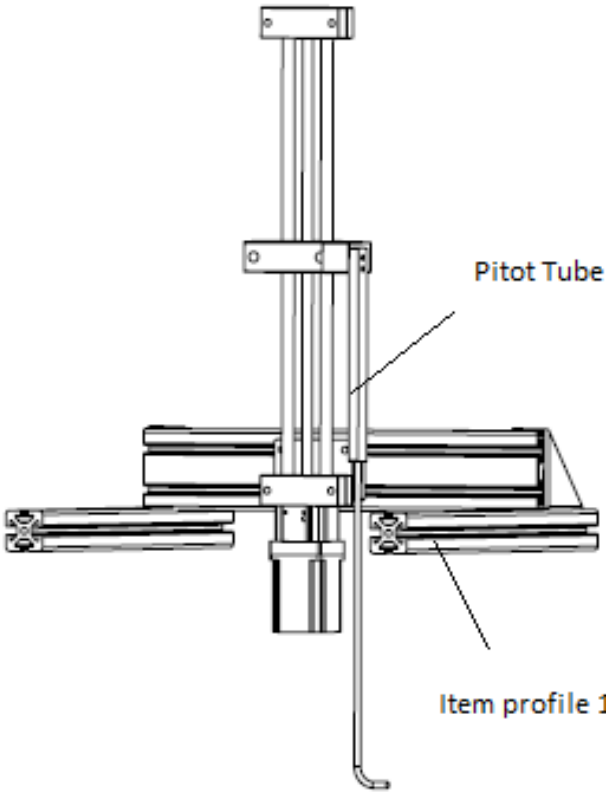

Figura 8: Estructura del Tubo de Pitot

Como se puede observar en la Figura 8, el tubo de Pitot se puede desplazadar verticalmente mediante el uso de un motor paso a paso y de un husillo de bolas. Este mecanismo será explicado detalladamente más adelante. Los planos de las piezas de todos los conjuntos de este trabajo se pueden encontrar en la sección 10. Anexos.

En la Figura 9 se puede observar el conjunto de los alambres de platino usados para la generación de burbujas de hidrógeno. Este conjunto está detalladamente explicado en la sección 5.2.

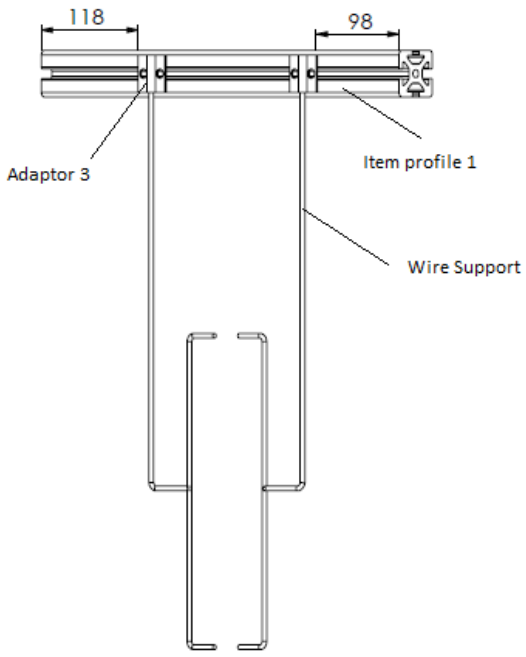

Figura 9: Estructura de los Soportes de los Alambres

Esta segunda combinación se propondrá como diseño definitivo del sistema de medición ya que mediante su uso se consiguen todos los objetivos previamente fijados y su coste no es muy elevado.

3.3 Combinación 3: PIV/PTV + Cámara

Aun así, existe una tercera combinación que daría un salto de calidad al proyecto, esta consiste en el uso de las técnicas de visualización PIV o PTV. Como se explica posteriormente en las secciones 4.1.1. y 4.1.2. una de las grandes desventajas de estas técnicas es el precio, el cual no sería un problema debido a la disponibilidad del material en la universidad TU Darmstadt.

Lo que si supondría un problema sería la enorme dificultad de su implementación, calibración y análisis. Para sobreponerse a estas dificultades será necesario un gran conocimiento de la materia y de la instrumentación, el cual en el departamento no se dispone por el momento.

Se han realizado diferentes cálculos (sección 5.1.3.) con el objetivo de calcular el número de Strokes, para observar si las partículas de PTV son capaces de seguir el flujo del fluido sin desviarse. Se ha llegado a la conclusión de que se podría usar esta técnica solo para turbinas de gran altura y números de Froude muy bajos. De esta manera se podrá conseguir números de Strokes cercanos a 0.1. Con valores cercanos a 0.1 se consigue que las partículas sigan al fluido sin desviarse.

$$Stk = \frac{t_0 \cdot u_0}{l_0} = \frac{0.0625 \cdot (0.22 \div 0.465)}{0.05 \div 0.25} = 0.055 \div 0.58$$

Donde t_0 es el tiempo de relajación de la partícula, u_0 es la velocidad de la partícula en condiciones normales y l_0 es la longitud característica de la turbina. Para información más detallada mirar sección 5.1.3.

4 Diseño de la Estructura de la Turbina

El principal problema de la estructura de la turbina anterior a este trabajo era el arduo trabajo que se necesita para operar con el plato perforado, esto significa que, a la hora de cambiar la posición de la turbina, cambiar su resistencia o su tamaño es necesario la utilización de tornillos, implicando unos mayores tiempos de preparación de los experimentos al cambiar alguna característica de la turbina.

Por tanto, el objetivo será encontrar un sistema que sea más automático con el objetivo de acelerar el proceso de recolección de datos cuando la turbina esté posicionada en diferentes posiciones y con diferentes características.

Se propone una estructura compuesta por un husillo de bolas, un motor de paso a paso y una caja de cambios. Mediante el uso de este sistema se consigue fácilmente controlar el cambio de posición del plato perforado mediante código en Labview y usando un controlador que estará posicionado fuera del canal de pruebas. Programar en Labview está más allá de este trabajo y será responsabilidad de la persona encargada de llevar a cabo el experimento.

Este mecanismo permite recolectar datos no solo en una posición, sino en diferentes posiciones del plato perforado en menor tiempo que la estructura actual la cual a diferencia de un sistema automático se basa en atornillar y desatornillas el plato perforado al soporte de la turbina. (Sección 2.3.)

Con este sistema propuesto solo es necesario atornillar a la hora de cambiar el tamaño del plato perforado, por lo que el procedimiento de la recolecta de datos debería consistir en tomar todos los datos acordes a un tamaño de plato perforado determinado en diferentes posiciones y con diferentes resistencias y después cambiar el tamaño del plato, y así sucesivamente. Con la anterior estructura, era necesario atornillar siempre que se quiera cambiar la posición, la resistencia o el tamaño del plato perforado.

Otra ventaja de este mecanismo es el hecho de poder posicionar el plato perforado por encima del canal de pruebas de manera que al cambiar el tamaño de los platos perforados sea más cómodo y no haga falta atornillar dentro del canal de pruebas como era necesario anteriormente. Para ello es necesario que el soporte de la turbina (ver sección 5.1.2.1. y sección 10) sea más largo que el actual.

Los planos de las piezas del adaptador L y el adaptador 1 se pueden encontrar en la sección 10. El resto de piezas deben de ser compradas a los proveedores indicados en la sección 6.1. Además, en dicha sección están indicadas las funcionalidades de cada pieza.

Posicionando el husillo de bolas lateralmente al flujo, se evita que la estructura balancee, ya que la superficie normal al flujo es menor que la superficie transversal, lo cual da más rigidez a la estructura. Aunque está opción es eficiente, posee una desventaja y esta es la aparición de un momento indeseado. Este momento no es muy grande ya que se ha diseñado de manera que la distancia entre el soporte de la turbina y el husillo de bolas sea menor de 5 cm.

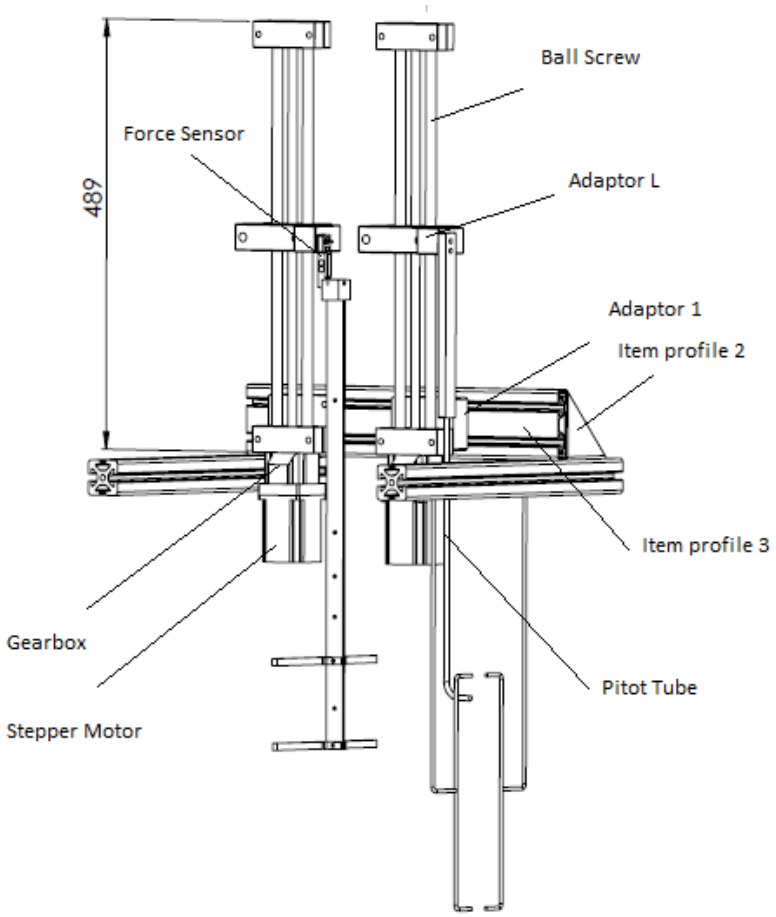

Figura 10: Estructura de la Turbina Lateral

Existe otra opción, la cual consiste en que el husillo de bolas sea frontal al flujo, esta finalmente no ha sido considerada ya que la estructura podría balancear modificando la posición de la turbina constantemente, véase la sección 6.1. Figura 50.

Aunque el mecanismo seleccionado ha sido la opción lateral al flujo, ambos mecanismos, lateral y frontal, poseen prácticamente las mismas piezas, por lo que podría ser una buena idea experimentar con ambos mecanismos.

5 Elección de Resistencias de la Turbina sobre el Flujo

Para la elección de resistencias el objetivo es intentar disipar la mínima energía posible, esto significa buscar un coeficiente de resistencia lo más bajo posible. En la siguiente ecuación se relaciona el coeficiente de resistencia con el coeficiente de sección transversal. (Idel'chik. Handbook of Hydraulic Resistance [Coefficients of Local Resistance and of Friction]. , 1966.)

$$\xi = (0.707\sqrt{1-\Phi} + 1 - \Phi)^2 \cdot \frac{1}{\Phi^2}$$

$$\Phi = \frac{A_{open}}{A_{close}}$$

Esto significa que, a mayor coeficiente de sección transversal, menor será el coeficiente de resistencia. Por lo tanto, será más conveniente usar platos perforados con agujeros cuadrados que con agujeros redondos, ya que un plato perforado con agujeros redondos posee una mayor área cerrada y consecuentemente un menor coeficiente de sección transversal.

Por ello finalmente, se fabricarán tres resistencias con agujeros cuadrados de lado 5, 8 y 10 mm y con una distancia entre centros de 8, 12 y 15 mm respectivamente.

Se fabricarán cinco diferentes tamaños de platos perforados, la anchura será la misma que la del canal de pruebas para conseguir una obstrucción completa (200 mm) pero la altura tomará los valores de 50 mm, 100 mm, 200 mm, 250mm y 400mm.

Los materiales y su coste están detalladamente explicados en la sección 6.2., la siguiente figura refleja la forma de las resistencias con agujeros cuadrados.

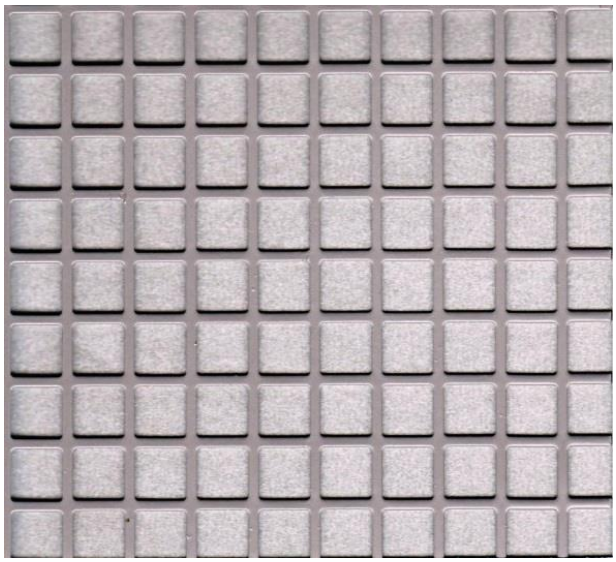

Figura 11: Resistencia de la Turbina

6 Conclusiones y Trabajos Futuros

En vista de todo lo mencionado anteriormente, es conveniente realizar varias conclusiones acerca del presente TFG. El sistema de medición se puede dividir en la medición de la velocidad y la medición del nivel de altimetría del fluido en el canal.

La velocidad será medida mediante una técnica de Visualización del Flujo, más concretamente con el método de generación de burbujas de hidrógeno, la consola eléctrica usada para generar las burbujas por electrólisis es la mostrada en la Figura 5, el alambre generador de burbujas será de platino y su soporte de latón, la longitud del alambre será de 250 mm con el objetivo de cubrir toda la altura del canal y la iluminación del área de interés se realizará mediante un sistema de LEDs. Con este sistema será posible medir la distribución de velocidades, la línea media y la anchura del tubo de corriente generado por la turbina entre los puntos (-) y (2). Se usará un tubo de Pitot para medir el perfil de velocidades en la zona entre los puntos (1) y (+).

La medición del nivel del agua se realizará mediante la misma cámara de alta resolución usada en el método de las burbujas de hidrógeno. En la TU Darmstadt se dispone de la cámara Sensicam.qe. Realizando un número considerable de fotos e interpolando no será de gran dificultad medir la altimetría del nivel del fluido. Se considera innecesario usar otras técnicas de mayor dificultad como láseres o métodos ultrasónicos.

La estructura de la turbina diseñada en este trabajo consiste en un husillo de bolas, un motor paso a paso, una caja de cambios y un controlador. El movimiento vertical de este sistema será codificado mediante Labview. Este mecanismo permite medir los parámetros requeridos en diferentes alturas y con diferentes resistencias sin el uso de tornillos. El único momento donde será necesario el uso de tornillos será a la hora de cambiar el tamaño del plato perforado.

Con este mecanismo se gana rapidez a la hora de recolectar datos y comodidad a la hora de manejar la estructura de la turbina.

Dicha estructura tendrá el husillo de bolas posicionado lateralmente al flujo, de manera que se pueda evitar el balanceo de la estructura. La distancia entre el husillo de bolas y el soporte de la turbina será mínima con objeto de evitar un momento indeseable. Todas las piezas de estos conjuntos están detalladas en la sección 10.

Aunque la técnica de la generación de burbujas de hidrógeno es eficiente, si se quiere dar un salto de calidad en el proyecto, es recomendable usar técnicas como PIV o PTV, las cuales son mucho más precisas. Por tanto, el siguiente paso podría ser la implementación de una de estas técnicas. Si este no es el camino a seguir y se decide usar la técnica de la generación de burbujas de hidrógeno, sería conveniente iluminar el área de interés con láminas de láser en vez de con LEDs.

La persona responsable en la realización del experimento deberá calibrar los aditivos y la señal de entrada al multivibrador TTL mediante los parámetros R_1 y C_1 explicados en la sección 5.1.2.2. Además es recomendable probar las dos estructuras propuestas en el presente trabajo: la opción lateral y frontal, ya que poseen piezas bastante similares.

Tabla de Figuras Del Resumen en Español

S286

Conception and Design of a Velocity and Water Level Profile Measurement System for a Channel Test Rig

Konzeption und Auslegung einer Messeinrichtung zur Messung von Geschwindigkeits- und Pegelprofilen an einem Gerinnenprüfstand

Álvaro Quiles García, Supervisor: Christian Schmitz, M.Sc.

Bachelor Thesis, Darmstadt, 12.07.2017

TECHNISCHE UNIVERSITÄT DARMSTADT

FLUID SYSTEM TECHNIK

Prof. Dr.-Ing. Peter Pez.

Erklärungen

Hiermit versichere ich, die vorliegende Diplomarbeit ohne Hilfe Dritter nur mit den angegebenen Quellen und Hilfsmitteln angefertigt zu haben. Alle Stellen, die den Quellen entnommen wurden, sind als solche kenntlich gemacht worden. Diese Arbeit hat in gleicher oder ähnlicher Form noch keiner Prüfungsbehörde vorgelegen.

(Ort,Datum) (Unterschrift)

Acknowledgments

I would like to express my sincere thanks to Prof. Dr.-Ing. Peter Pelz, Principal of the Department, for providing me with all the necessary facilities for the research.

I place on record, my sincere thanks to Christian Schmitz, who has been the supervisor of this bachelor thesis. I am extremely thankful and indebted to him for sharing expertise and valuable guidance, also for his continuous encouragement.

I take this opportunity to express gratitude to all of the FST Department members for their help and support. I also thank my family for the unceasing encouragement, support and attention, they made possible that I had the opportunity to do my bachelor thesis in TU Darmstadt.

Finally I want to thank the support of my Erasmus family from Darmstadt, which have support me in the good and the bad times throughout this year.

Table of Contents

List of Symbols

Base System

The first column in the following list shows the symbols used in the text for the occurring physical and mathematical quantities. The meaning of the symbol is described in the second column. The dimension formula of each physical quantity is given in the third column as the power product of the basis variables length (L), mass (M), time (T), temperature (Θ), quantity of substance (N), current (I) and light intensity (J)

Symbol	Description	Dimension
u	Velocity of the flow	$L\,T^{-1}$
h	Water level	L
A_t	Streamtube wide	L
Z_t	Streamtube medium line	L
$\dot{m}$	Mass flow	$M\,T^{-1}$
ρ	Density	$M\,L^{-3}$
V	Volume	L^3
A	Area	L^2
t	Time	T
e	Internal energy	$L^2\,T^{-2}$
k	Kinetic energy	$L^2\,T^{-2}$
q	Heat flux	T^{-3}
R_h	Hydraulic raidus	L
p_w	Perimeter wetted	L
Re	Reynolds number	1
ν	Kinetic viscosity	$L^2\,T^{-2}$
μ	Dinamic viscosity	$M\,T^{-1}\,L^{-1}$
b	Width of the channel	L
a	Height of the channel	L
g	Gravity	$L\,T^{-2}$
D_h	Hydraulic Diameter	L

Fr	Froude number	1
δ	Distance between turbine and channel	L
Stk	Stokes number	1
l	Characteristic dimension of turbine	L
d	Diameter	L
H	Hydraulic head	L
Q	Volume Flow	$L^3\,T^{-1}$
p_s	Static pressure	$M\,L\,T^{-2}$
σ	Dimensionless turbine width position	1
ζ	Dimensionless turbine height position	1
α	Dimensionless streamtube width	1
ξ	Dimensionless streamtube height	1
R	Gas constant	$L^2\,M\,T^{-2}\;\Theta^{-1}\,N^{-1}$
s	Wall depth	L
U	Voltage	$M\,L^2\,I^{-1}\,T^{-3}$
R	Resistance	$M\,L^2\,T^{-2}\,I^{-2}$
ε	Permittivity	$M^{-1}\,L^{-3}\,T^4\,I^2$
C	Capacitance	$M^{-1}\,L^{-2}\,T^4\,I^2$
$\bar{f}$	Cross-section coefficient	1
ξ	Resistance coefficient	1

Subscripts	Definition
1	Entrance of the channel
+	Just before the perforated plate
-	Just after the perforated plate
2	Beginning of the Mixture Zone
3	Homogeneous fluid
2o	Outside the streamtube
2i	Inside the streamtube
CV	Control Volume
0	Far from the perforated plate
P	Tracer particle
C	Critic

Abbreviation	Definition
TU	Technische Universität
HDP	High Density Polyethylene
LDP	Low Density Polyethylene
DC	Direct Current
TTL	Transistor-Transistor Logic

1 Introduction

After decades using fossil fuels to generate electricity, the principal organisations, which defend the environment, are starting to encourage governments to use green energy from renewable energies. In the following picture it can be observed the final consumption of the Renewable Energies in the world at the year of 2015.

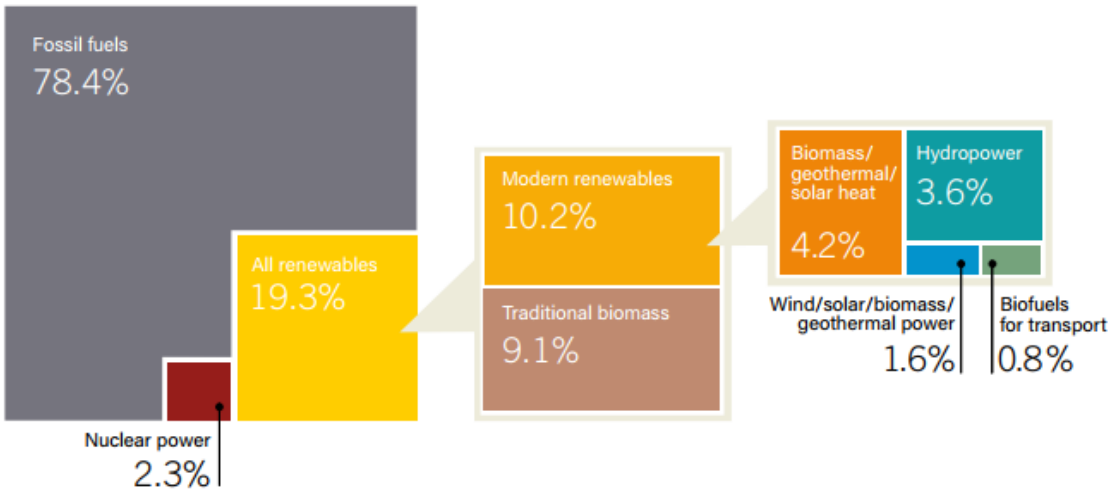

Figure 1: Final Energy Consumption 2015 [1]

The present thesis is going to be focused on the hydropower energy, which is only the 3.6% of the total energy consumption of the world. More concretely it will be focused on Tidal turbines. Talking about Tidal energy, it is worthy to mention that experts assure that the future of this energy looks really consistent due to the more efficient underwater turbines which will appear in the following years. [2]

The main problem nowadays is the high cost involved in the whole process, because of that during these days it is difficult to compete against the traditional electric companies, which offer a really competitive price. The main objective in the following years should be to come down the high construction costs due to a better efficiency of the materials. [3]

In [4], it is designed a model to calculate the performance factor C_p for a hydroelectric power station in a rectangular channel with complete obstruction in width and height. There have been several studies about it, for instance [5], where the developed method is extensively extended in such a way that the turbine has a complete obstruction in height but at the same time is bypassed horizontally by a bypass.

In contrast to conventional power plants, tidal turbines are placed freely in the flow and do not have a complete obstruction. The present thesis studies a complete obstruction in width but not in height, leading to a vertical by-pass flow.

The influence of the free surface on the turbine is the main problem at the time of designing the measurement system, due to the cascade produced by the presence of the turbine, which generates a difference of static energy. The analytical model, which is the basis of this thesis, was done by using energy conservation, continuity equation and the principle of linear momentum [6].

The construction of the test rig was designed in [7] and improved in [8]. The main objective of the present thesis is to improve the measurement system designed by [9] and [8]. The concept should be able to measure the velocity of the flow, the medium line and the width of the streamtube and finally the water level altimetry.

Another important part of the thesis will consist in designing a system which can improve the management of the turbine changes, that means a more automatic system instead of a manual system that is principally based in screwing when is necessary to change any position or characteristic of the turbine.

The present thesis will therefore focus on the research, design and implementation of a measurement system which fulfils the requirements and the design of a more manageable turbine structure.

2 Motivation

2.1 Experiment Technical Fundamentals

2.1.1 Basic Explanation of the Flow Simulation

This experiment consists in the modulation of the flow from a real Tidal Turbine, where a perforated plate will be use instead of a normal turbine. The perforated plate will have a complete width but a variable height, which will produce a vertical by-pass flow.[6]

It has been chosen this kind of "turbine" due to different reasons:

- Although the perforated plate dissipates heat instead of mechanic energy, which will be later convert in electricity, this prototype is used due to the fact that it does not matter which kind of energy it dissipates, the final results will be exactly the same.

- It represents a By-pass flow, which is characteristic of a tidal turbine in comparison to conventional hydro-power stations where there is not by-pass flow.

Figure 2 represents the flow model of the experiment, with a vertical by-pass flow generated due to the perforated plate previously commented.

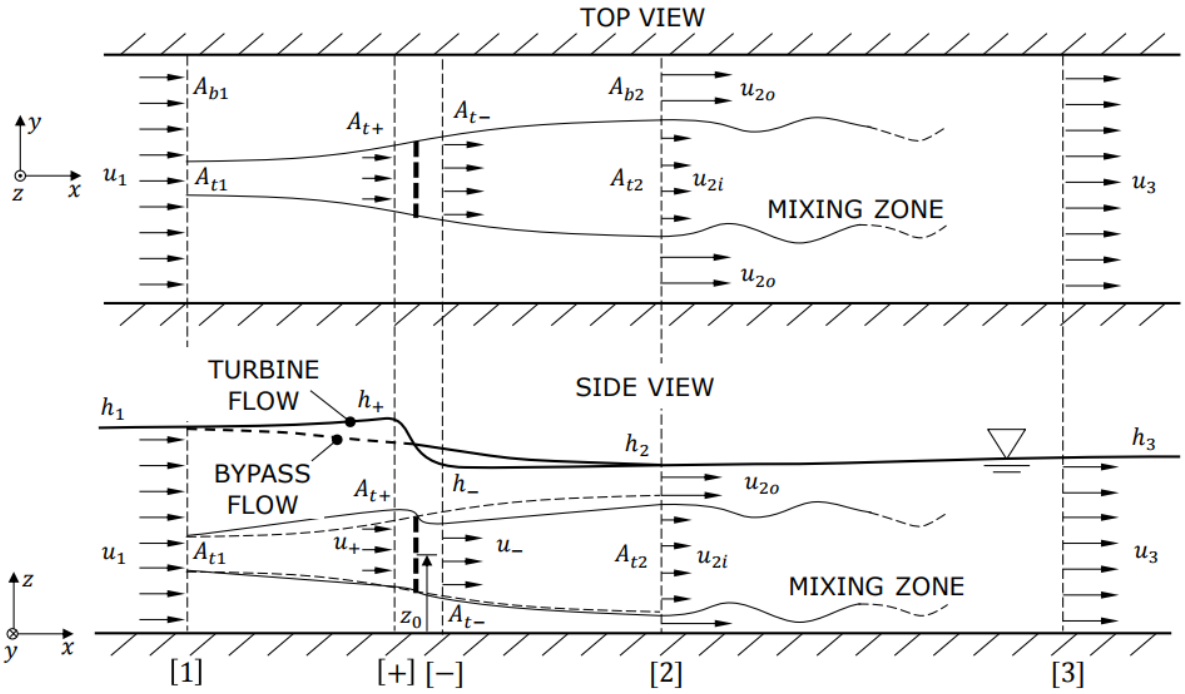

Figure 2 Flow Simulation of the Experiment [10].

As it can be observed in the Figure 2, there are 5 important points along the channel test rig. (1),(+),(-),(2) and (3). The area of interest of this thesis consists of the interval between points (+) and (2). This area is what it is called: "*Area of interest"* only in this thesis.

The Area of interest includes a cascade produced by the presence of the perforated plate, this cascade will lead to a difference of static energy due to the difference of heights between the points (+) and (-). This difference of static energy is going to be a relevantt part of the dissipated energy, which the perforated plate produces, so it is of great importance.

Another relevant consequence of using a by-pass flow turbine is the difference of velocity between the water which passes through the turbine and the one from the by-pass flow ($u_{20} > u_{2i}$). This fact is interesting because there will be a conservation of the volume flow until the mixing zone as it can be seen in Figure 2.

2.1.2 Conservation of Mass

The principle of mass conservation assures that for a closed system, the mass of the entire system should remain constant without any variation along the time. There is a popular statement which says that "*mass can neither be created nor destroyed*". This statement means that if the mass added is the same as the mass removed in a control volume the variation of mass flow in the control volume is cero. [11] $\frac{dm_{cv}}{dt} = 0$ (Steady-flow process).

$$\dot{m}_{in} - \dot{m}_{out} = \frac{d\dot{m}_{cv}}{dt} = 0 \quad \text{(Eq. 1)}$$

If a mass balance is done to a steady-flow process like the one it is used in this thesis the mass that flows in or out of the channel must be the same.

Usually this principle is represented as in the Eq.2 but in this case we only have one possible entrance and one possible exit so it is possible to eliminate the summations. [11]

$$\sum \dot{m}_{in} = \sum \dot{m}_{out} \quad \text{(Eq. 2)}$$

As it is known from the Reynold's transport theorem [11] the mass flow in the control volume is constant.

$$\left.\frac{dm}{dt}\right|_{CM} = \frac{d}{dt}\int_{CV} \rho dV + \int_{CS} \rho(\vec{u}_{rel} \cdot \hat{n}) dA \quad \text{(Eq. 3)}$$

It is possible to simplify this equation: [11]

- As it was said before: $\left.\frac{dm}{dt}\right|_{CM} = 0$

- It is considered that the fluid is incompressible, in the case of this experiment the fluid will be water, and hence the density of the water between different sections is constant.
  $\frac{d}{dt}\int_{CV}\rho dV = 0$

So finally the principle of mass conservation leads to the following formula with the conditions of the experiment ρ is constant due to the incompressibility of the liquid. [11]

$$0 = \int_{CS}\rho(\vec{u}_{rel}\cdot\hat{n}dA) = \rho\cdot u_{out}\cdot A_{out} - \rho\cdot u_{in}\cdot A_{in} = \sum Q_{in} - \sum Q_{out} \quad \text{(Eq. 4)}$$

In the Figure 3 it can be observed a Control Volume in a steady-flow with a variant cross section. Eq. 5 and Eq. 6 are the formulas applied from Eq.4 to this case, which is the same as our experiment.

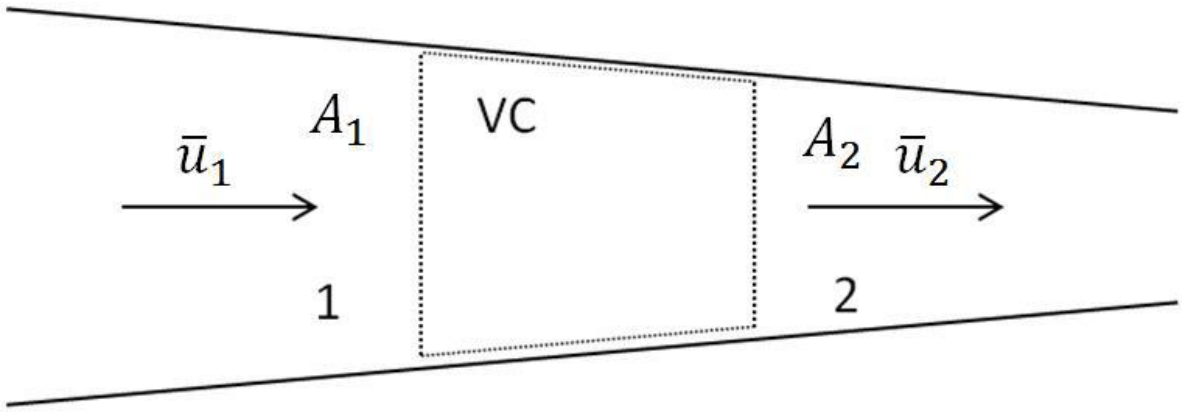

Figure 3: Control Volume with variant cross-section [7]

$$\sum Q_1 = \sum Q_2 \quad \text{(Eq. 5)}$$

$$u_1\cdot A_1 = u_2\cdot A_2 \quad \text{(Eq. 6)}$$

It is important to notice that there is continuity in the equations and that the velocities are proportional to each other by a relationship between the cross sections of the entrance and exit of the control volume.

This mass conservation principle will lead to a volume flow conservation and it will be important in the Measurement Concept election as it will be explain in the following sections.

2.1.3 Conservation of Momentum and Energy.

These two principles are not that relevant, as the principle of mass conservation, for this thesis, even so they should be mentioned because they were very important for the modelling process. By using these principles it is possible to get some equations of interest for the modelling.

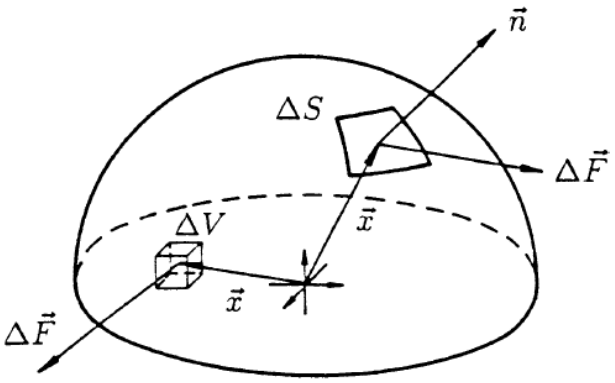

Figure 4: Volume and Surfaces Forces. [7]

The Figure 4 shows the depiction of the two kinds of forces that appear in the formula of the momentum conservation, surface forces and volumetric ones.

The principle of energy conservation states that within some domain, the energy is neither created nor destroyed but it remains constant. That means that energy can be transformed in other kind of energies but the energy of the whole system must be constant. [12]

$$\frac{D}{Dt}\iiint_{V(t)}\left[\frac{u_i u_i}{2}+e\right]\rho dV = \iiint_V u_i k_i \rho dV + \iint_S u_i t_i dS - \iint_S q_i n_i dS \quad \text{(Eq. 7)}$$

The momentum can be defined as the mass of an object multiplied by its velocity. The principle of momentum conservation states that the momentum is neither created nor destroyed. It remains constant within a domain. It can only be changed by the action of some forces. The main complexity of this principle in comparison with the mass and energy conservation resides in the fact that the momentum is a vector quantity. This means that the conservation must be in the three directions at the same time. [12]

After using the Reynold's transport theorem it is obtained: [13]

$$\iiint_V \frac{\partial(\rho\cdot\vec{u})}{\partial t} dV + \iint_S \rho\cdot\vec{u}(\vec{u}\cdot\vec{n})dS = \iiint_V \rho\vec{k}dV + \iint_S \vec{t}dS \quad \text{(Eq. 8)}$$

2.1.4 Dimensionless Numbers

2.1.4.1 Number of Reynolds

Before defining the Reynolds number it is necessary to take into account that the experiment is done in an open channel test rig. Consequently, there is a characteristic value called the hydraulic radius: [13]

$$R_h = \frac{A}{p_w} \quad \text{(Eq. 9)}$$

A means the Area and p_w means the wetted perimeter.

In our channel the perimeter is 1.000 mm and the cross-section is 80.000 mm^2. Resulting:

$R_h = 80$ mm

The number of Reynolds can be defined as a relationship between the inertial forces and the viscous forces. This dimensionless number is defined in the following equation [13]

$$Re = \frac{\rho \cdot U \cdot R_h}{\mu} = \frac{U \cdot R_h}{\nu} \quad \text{(Eq. 10)}$$

An important issue about this number is that it can define the behaviour of the flow as laminar flow or turbulent flow. [13]

A laminar flow appears in an open channel when the Reynolds number is low ($Re < 500$), this means that the viscous forces are dominant in comparison with the inertial forces. This kind of flow is characterized by a constant and smooth fluid motion. Normally this behaviour happens when the velocities are really low.

Talking about the turbulent flow, which appears in a typical open channel test rig, it is necessary to have a Reynolds number higher than in the laminar flow ($Re > 2000$). A turbulent flow is characterised by the domination of inertial forces in comparison with viscous forces in addition to the many vortices and flow instabilities in the fluid.

It is important bearing in mind that there is a transition state when the Reynolds number is between the laminar flow and the turbulent flow.

A more accurate formula for open channel test rigs is the following equation: [10]

$$Re = \frac{4 \cdot u_o \cdot h_0}{(1+2\frac{h_0}{b})\nu} \quad \text{(Eq. 11)}$$

By using this formula depending on the volume flow which is introduced to the channel, it is obtained a range of the Reynolds number between $7 \cdot 10^4 \div 3 \cdot 10^5$. In section 2.2 is detailed this calculation

This means that the flow of the experiment is going to have always a turbulent behaviour.

2.1.4.2 Froude Number

The Froude number can be defined as the relationship between the inertial forces and the gravity forces. It is a dimensionless number which defines whether the flow is critical or uncritical. [13]

In open channels there is a characteristic value:

$$D_H = \frac{4 \cdot a \cdot b}{2a+b} \quad \text{(Eq. 12)}$$

The Froude number is defined as the following equation: [13]

$$Fr = \frac{\bar{u}}{g\sqrt{D_h}} \quad \text{(Eq. 13)}$$

As it has been mentioned before, the Froude number can delimitate when the flow state is critical: [13]

- $Fr < 1$: The flow is subcritical, which means a tranquil and slow fluid, where the gravity forces dominate over the inertial forces.
- $Fr = 1$: The flow is critical, it will be more detailed in section 2.1.5
- $Fr > 1$: The flow is supercritical, which means a fast rapid fluid, inertial forces dominate in comparison with gravity forces.

In our experiment the Froude number at the entrance of the channel is between 0-0.3 m/s, at the end of the channel is between 0-0.5 m/s, but just after the perforated plate, in the cascade the flow is supercritical with a maximal Froude number around 1.4.

So the flow has a subcritical behaviour in the whole channel except for the area close to the perforated plate where is produced the hydraulic jump.

Figure 5 shows a graphic implicating the Reynolds number and the Froude number and the different possible states of the flow in an open channel test rig.

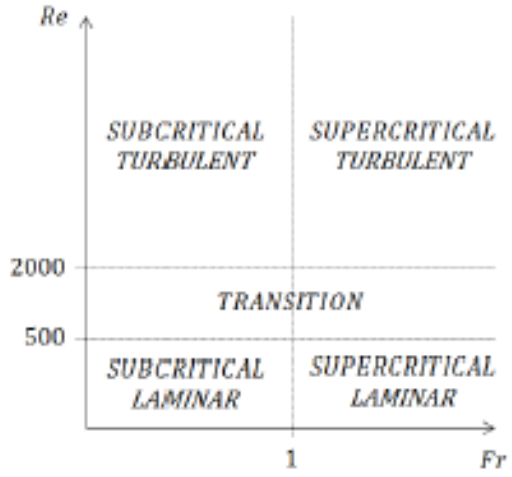

Figure 5: Flows state depending on Re and Fr

Also it is necessary to mention what Jonas Nieschlag [6] study in his thesis. As it is observed in the Figure 6, the Froude number and the distance between the turbine and the ground are relevant for the size of the waves produced by the turbine.

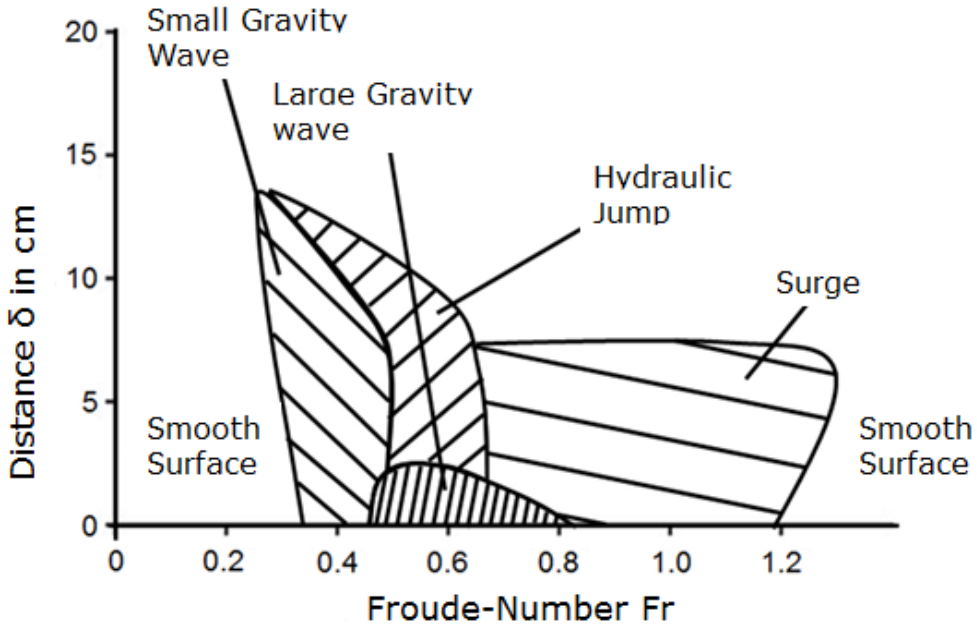

Figure 6: Overview of the occurrence of various surface phenomena [6]

In this experiment the idea is to work between the small, large gravity wave and hydraulic jump depending on the distance where the perforated plate is positioned.

The main aspect of Figure 6 is that the picture can show the relevance of the turbine's position in the test rig, because the results differ a lot in different positions.

Figure 7, Figure 8 and Figure 9 show three different types of waves explained in Figure 6*:* Small gravity waves, large gravity waves and hydraulic jump.

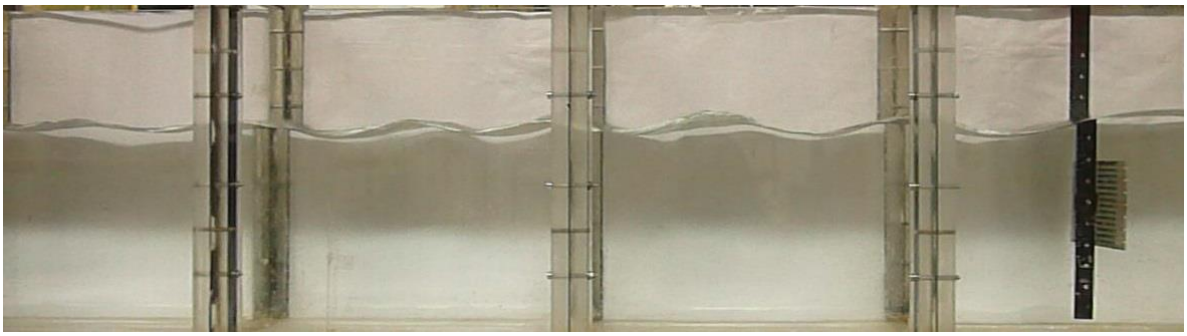

Figure 7: Small Gravity Wave [6]

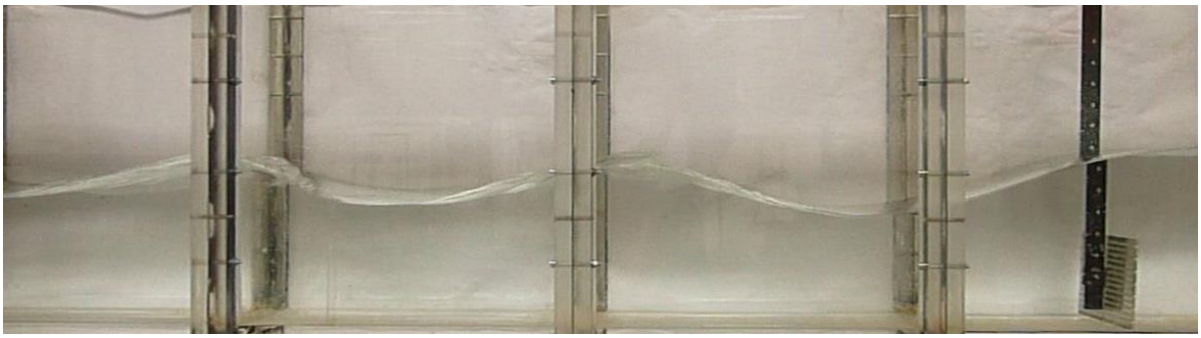

Figure 8: Large Gravity Wave [6]

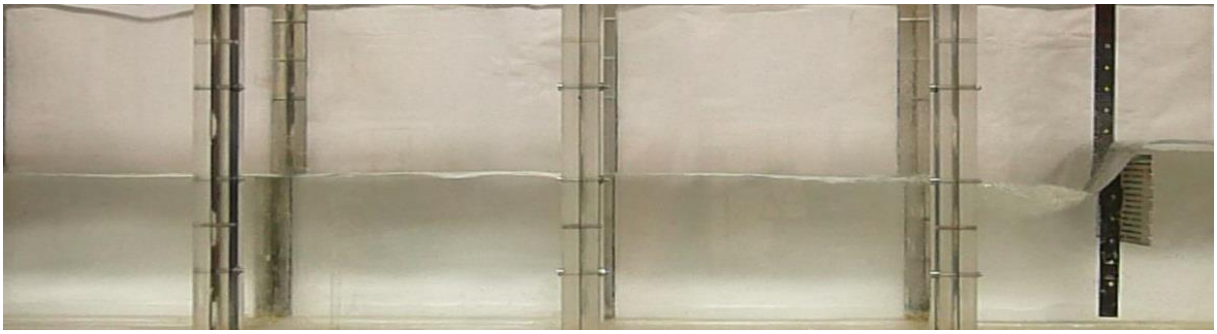

Figure 9: Hydraulic Jump [6]

2.1.4.3 Stokes Number

The Stokes dimensionless number (Stk) is defined as the ratio between the characteristic time of a particle and the characteristic time of the flow through an obstacle. [14]

$$Stk = \frac{t_0 \cdot u_0}{l_0} \quad \text{(Eq. 14)}$$

The parameter t_0 is called as the relaxation time or stopping time of the particle, conventionally it is computed applying the Stokes (linear) drag law to a particle initially moving with the free stream velocity. The parameter u_0 is the fluid velocity of the flow in normal conditions and the parameter l_0 is the characteristic dimension of the obstacle, in our case it would be the height of the perforated plate. [14]

If the particles Reynolds is lower than 1, it means that the particles follow a stokes flow, and the relaxation time parameter can be defined as follows: [14]

$$t_0 = \frac{\rho_p \cdot d_p^2}{\mu_{H20}} \quad \text{(Eq. 15)}$$

In case of using optical methods as PIV or PTV with particle tracers it is necessary to have a low stokes number, a low stokes number $Stk \ll 1$ means that the particles will follow the fluid streamlines, whereas if the stokes number of a particle is too large, it continues along its initial trajectory. [14]

The idea is to get stokes number lower than 1 and if it is possible, lower than 0.1, which leads to an error between the streamlines of the flow and the particles lower than 1%.

In the following picture, it is observed three cases depending on the strokes number between a solid particle and a liquid flow like water. In the first case the particle and the flow have the same stream line, whereas in the third case they have completely different streamlines as it was explained before.

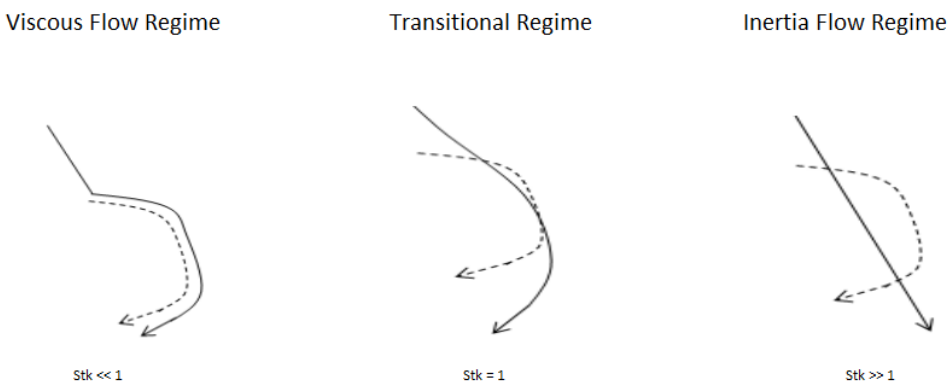

Figure 10: Stokes Number Behaviour of the Flow

2.1.5 Specific Energy and Critical Flow

The specific energy of the flow in the open channel is composed by a part of kinetic energy (velocity) in addition to a part of potential energy (depth). Usually in an open channel it is necessary to determinate the energy of the fluid in a particular section of the test rig. [11]

$$H = h + \frac{\bar{u}^2}{2g} \quad \text{(Eq. 16)}$$

In our case the energy of the fluid at the entrance of the channel is $H_1 = 250\ \text{mm}$ [15].

Where h means depth and $\bar{u}$ the average velocity [13], note that the velocity depends on the volume flow and the cross-section.

$$u = \frac{Q}{b \cdot h} \quad \text{(Eq. 17)}$$

This dependence is important because the specific energy will depend on the depth in both addends. Figure 11 shows a graph between the specific energy and the depth of the fluid. [13].

This specific energy will be of interest when designing the dimensions of some pieces which are in touch with the water.

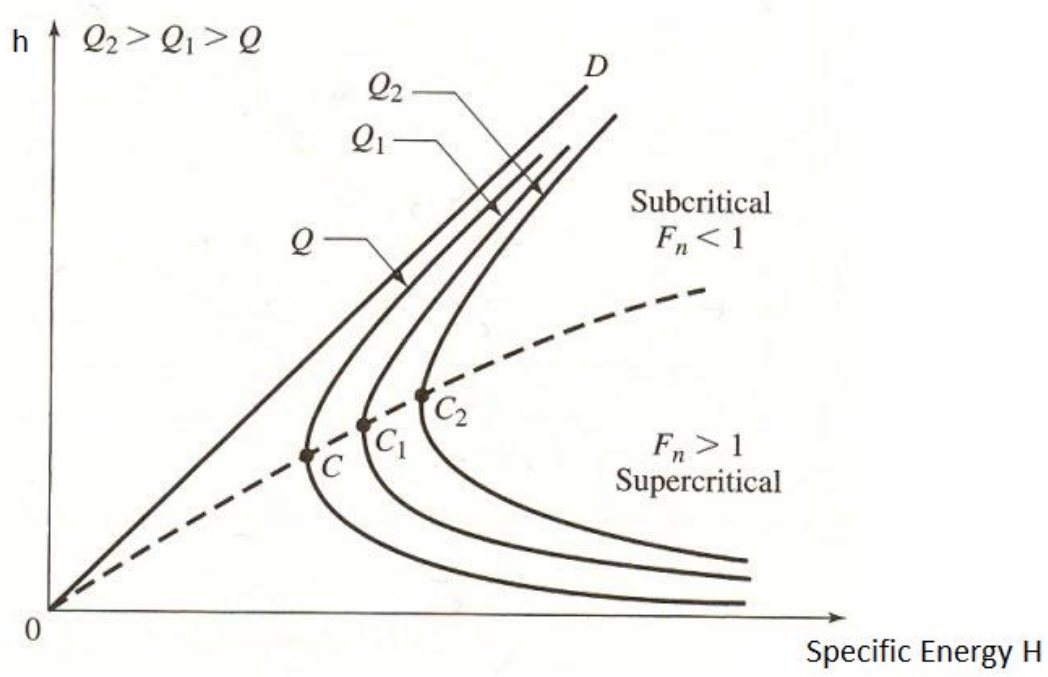

Figure 11: Specific energy with Fluid depth

There should be done some comments about Figure 11*:* [9]

- The line of 45º defines $H = h$
- For any point on the curve (H,h) the horizontal distance between the h-axis and 45º-line is the potential energy, whereas the horizontal distance between the 45º-line and the mentioned point of the curve is the kinetic energy
- It is important to talk about the point in the curve, where the specific energy is minim, this occurs in the moment of critical flow $Fr = 1$.
- At the critical state it can be found the critical depth h_c

The critical depth defines if the fluids flow is supercritical or subcritical. In the case that $h < h_c$ the flow behaves supercritical, whereas if $h > h_c$ the flow behaves subcritical.

As it is observed in Figure11, in the curve (H-h) there are two points with the same specific energy but the difference between them relies on the fact that the one above the critical depth produces a subcritical flow, while the point below the critical depth produces a supercritical flow. [13].

2.2 Test rig

The test rig used in this experiment is the one shown in the Figure 12 and Figure 13, it can be defined as a closed loop because the channel is provided by the same water all the time. An important element of the test rig is the electric water pump, which provides water to the channel. This water comes from a water tank, which is below the outlet of the channel.

Figure 12: Test rig 3D [10].

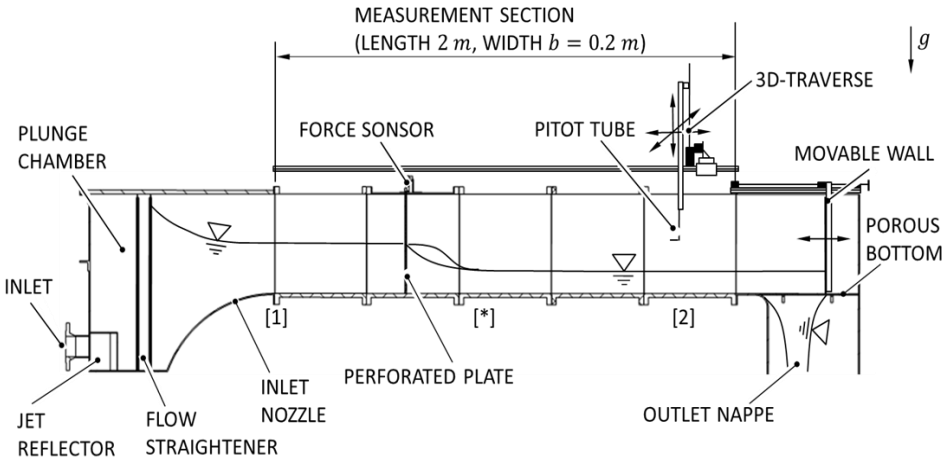

Figure 13: Test rig 2D [10]

There are some relevant aspects which are important to comment briefly:

The inlet part of the channel is made of stainless steel and it has a round-shaped bottom so that there can be a progressively develop of the boundary layer and also a better velocity profile which is going to arrive later to the turbine. [7]

Also in the inlet part, as it can be observed in Figure 13 there is a baffle plate and a homogenizer which provides the channel a balance flow, moreover it affects in a good way to the velocity profile by which will be more realistic due to the importance of having a homogenized flow. [7]

The volume flow rate through the channel is controlled by changing the position a movable wall in the outlet section. The volume flow (Q) in addition to the Froude number (section 2.1.4.2.) and some other parameters, such as the position ($z_t = \zeta \cdot H_1$) (Figure 6*)* and width ($A_t = h_1 \cdot b \cdot \sigma$) of the turbine are relevant when controlling the flow of the experiment.

Another relevant aspect of the test rig is the material of the channel. This material is acrylic-glass, this material has been chosen due to its transparency. The usage of this material is interesting because it allows working with optical techniques of measurement such as PIV, PTV or even Flow Visualization; this information will be relevant for the election of the measurement system.

It is also important to talk about the measurement section of the channel; D. Hernández worked on the construction of the test rig in his Bachelor Thesis [7], the maximum height was calculated in this work by relating the height with the Froude number in order to decide which channels height would be sufficient.

By using Eq.13 and Eq.17 we arrive to Eq.18 and Eq. 19.

$$h = \left(\frac{\dot{V}^2}{Fr^2 g b^2}\right)^{1/3} \quad \text{(Eq. 18)}$$

$$u = \left(Fr\sqrt{g\frac{Q}{b}}\right)^{2/3} \quad \text{(Eq. 19)}$$

By considering a Froude number of 0.5 and the volume flow 82 m^3 /h. The result of the maximal height is h= 0.174 m, but as one of the most important aspects of construction is the flexibility it was decided to make it over dimensional with a maximum height of 40 cm. [7]

Now it is possible to calculate the velocity for a Froude number of 0.1 by using Eq. 17 $u = \frac{\dot{V}}{b \cdot h} = 0.22\ \mathrm{m}/s$

A more interesting value is the velocity in the point of supercritical flow (Fr=1.4) just after the cascade. In this case the velocity will be the maximum one $u_{max} = 1.29\ \mathrm{m}/s$ with $h(Fr = 1.4) = 0.087\ \mathrm{m}.$

By using this data and Eq.11 the maximal Reynolds in the area of interest just after the turbine is $Re_{max} = 2{,}4 \cdot 10^5$, which is clearly a turbulent behaviour of the flow. (See section 2.1.4.) $Re(Fr = 0.1 \div 1.4) = 7.3 \cdot 10^4 \div 2.4 \cdot 10^5$

One of the improvements that the department is involved is in buying a more powerful water pump, which could provide the channel a volume flow of 132 m^3/s.
This new Volume flow will lead to a maximal velocity of $u_{max} = 1.52.$

It is also worth bearing in mind that the velocity profile is not homogenous after the perforated plate, normally in the centre of the channel there is a factor that raises the velocity of 1.3. So if the turbine has a volume flow of 82 m^3/s, the max. velocity using the factor of 1.3 will be $u'_{max} = 1.677\ \mathrm{m}/s$. And if the volume flow is 132 m3/s,, the max. velocity will be $u'_{max} = 2\ \mathrm{m}/s$

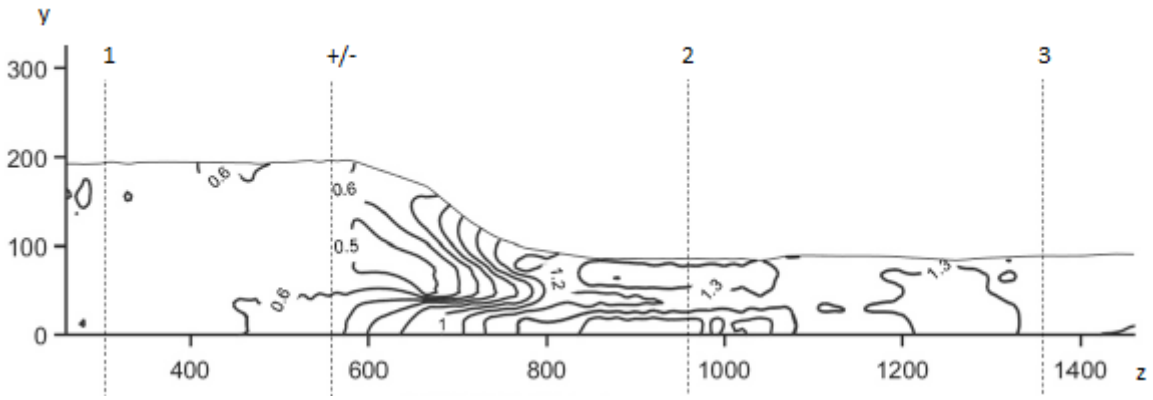

Figure 14: Velocity Map in the channel for Fr=1.4 [6]

The length of the channel is 2 m and it was implemented by using a modular concept, which is shown in the Figure 15. This figure shows five different modules of 40 cm each one, which are fixed in order to get the whole channel. This concept enables in a future to modify the length of the channel. In fact, nowadays Oliver Starke [15] is amplifying the length of the measurement section in order to get a more stable velocity profile.

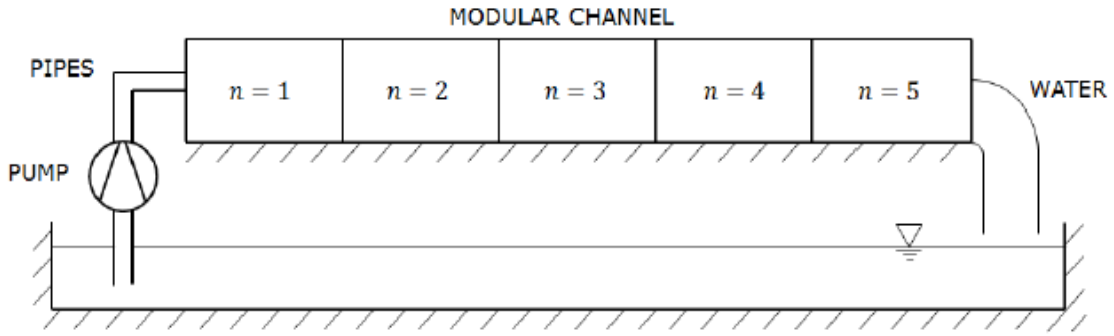

Figure 15: Modular Concept in an Open Channel

Finally, it is also important to mention that it is installed a bending beam load sensor above the turbine in order to know to forces and possible deflection produced by the flow. This sensor is really accurate with a measurement uncertainty of 0.1%. [16]

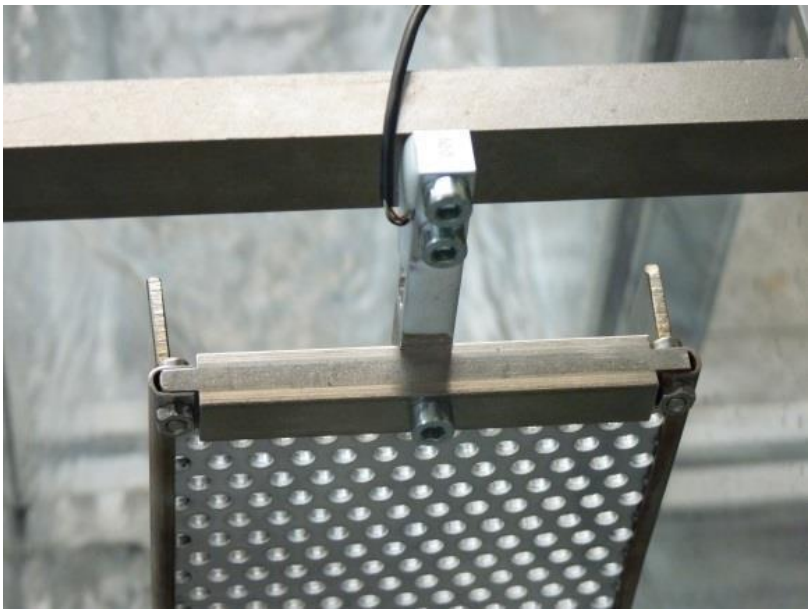

Figure 16: Bending Beam Load Sensor [8]

2.3 Current Problems

The first thing that it should be done at the beginning of each project resides in analysing the possible current problems of the experiment, and consequently, after this task, settled the objectives.

The Current problems have been divided in two parts: Measurement system and Turbine system.

2.3.1 Measurement system

The main problem of the actual measurement system is the lack of accuracy in the area of interest, which is the cascade; this is the area where the measurement system will be implemented.

To measure the velocity, a Pitot tube is used. The Pitot tube is already implemented in the test rig. This is not the best option to measure the velocity in a cascade because a Pitot tube should be positioned perpendicular to the surface of the fluid, which in this case is not possible due to the fact that a cascade is not a smooth surface.

The first consequence of using a Pitot tube in such cases is the superposition of the dynamic and static pressure, this statement will provide a wrong result of the velocity in the area of interest. In the thesis done by Mathias Lehrer [8] it is done some calibration to reduce the error, even this technique could work with some errors, one of the main objectives of this thesis is to improve the velocity measurement system.

In the water lever measurement, it is currently used the Conductive lever altimetry method, which also has some problems of accuracy at the time of measuring it in the cascade. This measurement was proposed also by Mathias Lehrer [8]. As it can be observed in the Figure 17, there is a lot of scattering. [10]

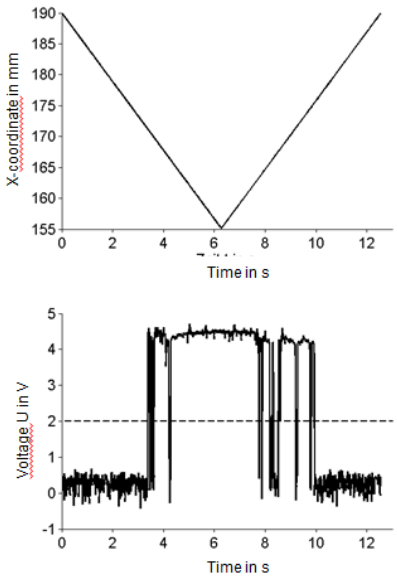

Figure 17: Test results of the Conductive Level Altimetry technique

As the velocity and the water level measurements are not accurate, it is complicated to assure accurate results in the calculation of the pressure. By using this measurement system it is also too complicated to calculate the medium line and the width of the streamtube, which are some objectives that are commented in section 3.

In light of the above mentioned, the idea is to change both measurement systems in order to improve the accuracy of the final results. These errors are important in some aspects of the test rig experiment. Both measurements will be explained in more detail in the sections 4.1.3 and 4.2.3.

2.3.2 Turbine System

The main problem of the Turbine system is the hard-work needed when operating with the perforated plate. That means changing the position of the turbine, changing its resistances or removing the turbine for another with different size.

In all these cases it is necessary to use screws and also it is really uncomfortable due to the fact that the turbine is fixed inside the test rig. As it can be observed in the Figure 18 there are some holes in the turbine support, which are used in order to change the position of the turbine.

Figure 18: Channel test rig, side view.

So the objective is to improve the current manual performance in order to speed up all the process of collecting data in different turbine positions and make the work easier for the people in charge of carrying out the experiment measurements.

3 Objectives

After considering the main problems of the current Measurement and Turbine Concepts, it is necessary to make a *Functional Specific Document.*

A *Functional Specific Document* is a document which reflects the different objectives, which will be necessary to achieve at the end of the Thesis, this document reflects not only the objectives but also some extra information which is important for understanding all the requirements that the chosen concepts should have.

Table 1 is divided in two parts: On the one hand the Measurement Concept in order to improve the current measurement system due to its lack of accuracy and on the other hand a Turbine Concept where it is important to make the turbine operating and removing systems automatically instead of manually.

Note that in the part of the Measurement concept that the pressure calculated, is the static one, so if the water level is known with the following formula we can easily get the pressure.

$$p_s = \rho g h \quad \text{(Eq. 20)}$$

Some other formulas used at the time of filling Table 1 were:

$$\sigma = \frac{A}{b \cdot H_1} \quad \text{(Eq. 21)}$$

$$\zeta = \frac{Z}{H_1} \quad \text{(Eq. 22)}$$

$$\alpha(x) = \frac{A_t(x)}{b \cdot H_1} \quad \text{(Eq. 23)}$$

$$Z_t(x) = \frac{Z_t(x)}{H_1} \quad \text{(Eq. 24)}$$

Eq. 21 and Eq.22 represents the ratio of the turbine width and height, whereas Eq.23 and Eq.24 represents the ratio of the width and the medium line of the streamtube generated by the turbine.

By knowing that b = 0.2 m and H_1 = 0.25 m, the ranges shown at Table 1 were calculated.

The velocity range written in the table has been done with Froude Numbers between 0.2-1.4 which is the range that we are working with along the channel. (See Eq. 19)

The Factor 1.3 previously explained is added when calculating velocities closely to the turbine.

Concepts	Requirements	Symbol	Points of Measurement	Range	Type of Information	Extra Information
Concept Measurement	Measure velocity	u	u_1 u_+ u_- u_2 u_3	0.35-1.68 m/s	BF	
		u(x,y)		0.35-1.68 m/s	BF	Distribution between 1 and 2
		u(x,y)		0.35-1.68 m/s	W	Distribution between 2 and 3
	Measure Pressure	p	p_1 p_+ p_- p_2 p_3	980-3920 Pa	BF	
		p(x)		980-3920 Pa	BF	Distribution between 1 and 2
		p(x)		980-3920 Pa	W	Distribution between 2 and 3
	Mesure water level	h	h_1 h_+ h_- h_2 h_3	0.1-0.4 m	BF	
		h(x,z)		0.1-0.4 m	BF	Distribution between 1 and 2
		h(x,z)		0.1-0.4 m	W	Distribution between 2 and 3
	Measure of the width of the Streamtube	α(x)	Turbine to 2	0.2-1	BF	Distribution between 1 and 2
	Measure Medium line of the Streamtube	ʒ(x)	Turbine to 2	0.1-1	BF	Distribution between 1 and 2
	Measure of the width of the Streamtube	$A_t(x)$	Turbine to 2	0.01-0.05 m^2	BF	Distribution between 1 and 2
	Measure Medium Line of the Streamtube	$Z_t(x)$	Turbine to 2	0.025-0.25m	BF	Distribution between 1 and 2
	Economical Limitations				W	Material available in TU Darmstadt
Concept Turbine	Turbine width	σ	Turbine	0.2-1	BF	
	Turbine height	ʒ	Turbine	0.1-1	BF	
	Turbine width	A	Turbine	0.01-0.05 m^2	BF	
	Turbine height	Z	Turbine	0.025-0.25 m	BF	
	Number of Turbine width	# σ	Turbine	4+	BF	
	Number of Turbine height	# ʒ	Turbine	4+	BF	
	Different Resistances	R	Turbine	3+	BF	
	Economical Limitations				W	Material available in TU Darmstadt

Table 1: Functional Specific Document

BF: Fixed Requirement for a determined range

W: Wish

The points of measurement (1), (+), (-), (2) and (3) are referred to the Figure 2.

To sum up, the main objectives are:

Measurement concept:

- Measure velocity
- Measure water level altimetry and static pressure
- Measure the medium line and the width of the streamtube

Turbine Concept

- Automatic change of turbine height position
- Easier change and election of the turbine resistances
- Easier change of turbines size

4 Research

The research of the measurement concept is divided in two parts: Velocity Measurements (4.1.) and the Water Level Measurements (4.2.).

4.1 Velocity Measurements

The first step, in the measurement concept, has been a research of possible techniques for the velocity measurement. They have been placed in *Table 2* in order to compare them and analyse if they achieve the objectives of the *Measurement Concept.*

	PIV	PTV	Pitot	Multi-hole Probe	Hot Wire Probe	LDA	MTV	Flow Visualization
A	YES	YES	YES	YES	YES	Partially	YES	YES
u (cascade)	YES	YES	NO	NO	YES	YES	YES	YES
u (rest)	YES	YES	YES	YES	YES	NO	YES	YES
h (cascade)	NO	NO	NO	NO	NO	NO	NO	NO
h (rest)	NO	NO	YES	YES	NO	NO	NO	NO
z	YES	YES	YES	YES	YES	Partially	YES	YES
p (cascade)	Partially	Partially	NO	Partially	Partially	Partially	Partially	Partially
p (rest)	Partially	Partially	YES	YES	Partially	NO	Partially	Partially
Economic	NO	NO	YES	Medium	YES	NO	NO	YES
Accuracy	High	High	Medium	Medium	Medium	High	High	NO

Table 2: Evaluation of Velocity Measurement Techniques

4.1.1 Particle Image Velocimetry (PIV)

This technique can be classified as an optical method. The main characteristic of this kind of measurements is that they are non-invasive in the flow, which means no probe would be in the flow; hence it should be more accurate than an equivalent technique using a probe inside the flow. [17]

This method requires a light source in addition to a recording medium for its implementation. It is important to mention that inside the family of optical methods, there are two subgroups:

- Tracer base methods
- Non-tracer base methods

PIV is definitely a tracer base method. The Figure 19 shows how the method functions. At the beginning, some tracer particles are introduced in the channel, also it there is a laser implemented, which will make a sort of light sheet where the tracer particles pass through. Then the camera will take double-pictures depending on the pulse duration of the laser and the frequency of the PIV camera. The last and more important step of the whole process is to analysis of all the data collected by using a computer. [17]

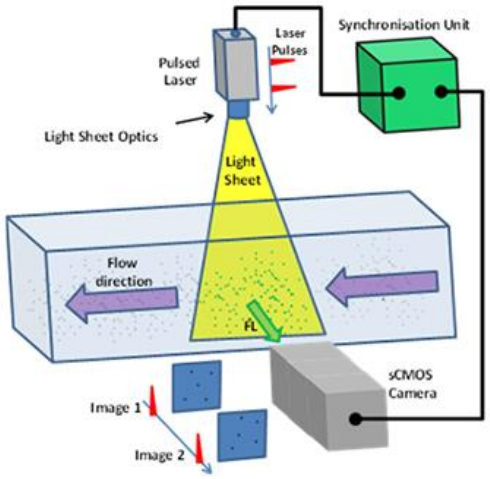

Figure 19: PIV Functioning [20]

In PIV it is normally used glass microspheres or particles of polystyrene as tracers, which are empty inside, with a similar density than the water. This density issue should be considered, so that the tracers would not be unstable in the water flow. Furthermore, it is necessary a transparent glass (acrylic-glass) and a high-resolution camera to take pictures and compare the velocity of the tracers and the flow. [7]

It is also necessary to know the relation of the flow velocity and the tracer particles velocity if it has not been possible to find particles of the same density as the water.

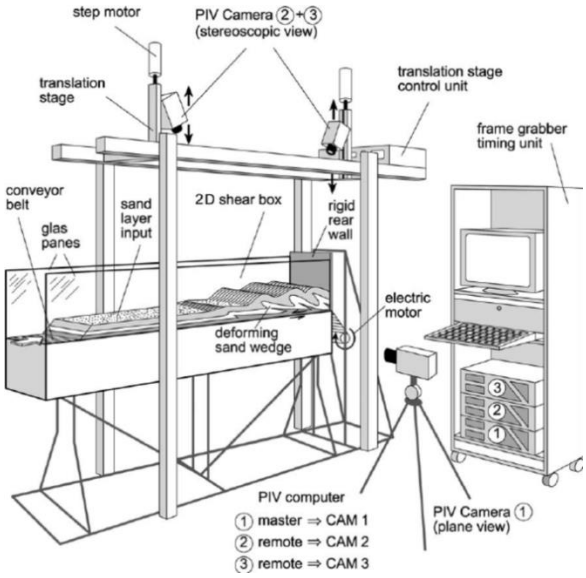

Figure 20: PIV 3D

There are several kinds of PIV techniques, for instance it exists 3D PIV Figure 20, which works with more than one camera. By using 3D PIV, it is possible to know not only the scalar velocity but also the vector field of the water flow. [18]

This kind of PIV technique allows not only knowing the vector field, but also the position and the form of the turbulences. The only disadvantage of this type of PIV is the highly expensive price of the equipment and the hard implementation. It will not be necessary this kind of PIV in order to achieve the objectives settled in section 3. By using a 2D PIV camera is more than sufficient. [18]

In TU Darmstadt there is a PIV system with a double-pulsed-laser and 1280x1024 pixels of resolution and CCD camera. This means that the only disadvantage is the hard implementation of the system.

Talking about the measurement system, PIV would be a nice solution to know the velocity of every single point after the “turbine”, also the camera could be profited for other uses.

4.1.2 Particle Tracking Velocimetry (PTV)

This second technique is really similar to the PIV method, and consequently it is also an optical method with really similar characteristic.

This method is normally used in order to measure the velocity of particles that are inside a flow, tracer base method, usually it is used a CCD Camera in order to make the pictures in order to analyse the behaviour of the tracer particles in the flow. [18]

There are some differences between PTV and PIV. In PTV individual particles are tracked, that means that it follows a Lagrangian approach, whereas in PIV the approach is Eulerian and consequently the density of tracer particles in PTV is so much lower than in PIV. If there are less tracer particles, there are also lower vector fields. [21]

One advantage of PTV is that apart from the vector field of the velocity we can know the streamtube shape, which would be great information for the thesis because two of the objectives are measuring the width and the medium line of the streamtube.

As well as in PIV, there are two methods of measuring in PTV:

- 2D-PTV where we measure the flow field in two dimensions by illuminating with a laser sheet and with lower quantity the particles than in PIV we can track each particle individually for some frames.

- 3D-PTV is based on several cameras, 3-dimensional illumination and tracking of flow tracers, which can be also different from solid particles, this technique is based on photogrammetric principles.

A common 3D-PTV consists of several digital cameras, usually three or four, with an angular installation. These cameras should be synchronous recording the light from the tracers particles in the water flow. As in PIV the flow is illuminated by a laser, the light has not restriction, which means that it can be coherent, monochromatic, etc. It is worth bearing in mind that the more consecutive frames that the particles are tracked, the better for the experiment. [21]

In the current case, it is not necessary the accuracy of 3D-PTV, so 2D-PTV would be quite enough. PTV is a great solution for the improvement of the measurement system. It would help not only to know the velocity in each point but also the shape of the streamtube, which is also an important requirement. The implementation and the costs will be discussed in the section 4.2.

4.1.3 Pitot Tube

This type of technique focuses in a pressure measurement; thanks to this instrument it is possible to know the dynamic pressure p_t. [8]

$$p_t = \frac{1}{2}\rho u^2 \qquad \text{(Eq. 25)}$$

It is a really common method of measuring in aerodynamic and hydraulic applications, however it carries with some problems of accuracy when the flow is unstable. In this particular case, it is worked with waves produced by the turbine, and consequently there will be a superposition between the static pressure and the dynamic pressure, if the probe is not placed perpendicular to the surface.

In this technique there is influence of some parameters such as the measured difference of pressure, the pipe geometry, surface tension, trapped air mass and the temperature as it can be seen in the calculations made by M.Lehr. [8]

$$p_t = \frac{m_{air} \cdot R_s \cdot T}{V} - \frac{2s}{R} - \rho g x \qquad \text{(Eq. 26)}$$

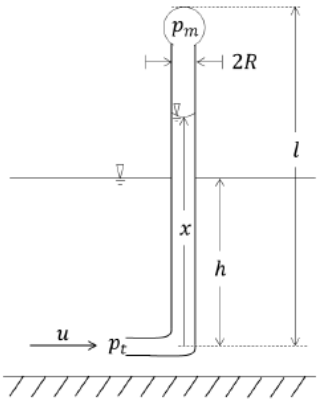

Figure 21: Pitot Tube

Although it has some problems of accuracy, one of the requirements is to know the velocity before the turbine, in this part of the test rig would be a good idea to use a Pitot tube due to the fact that it is already implemented in the laboratory.

4.1.4 Multi-hole Probe

This technique is a concept really similar to the Pitot tube, but extended to a more than one dimension. The holes could be between three and seven depending on the type of the probe. The more holes the probe has, the better measurements would be done in the other directions. [22]

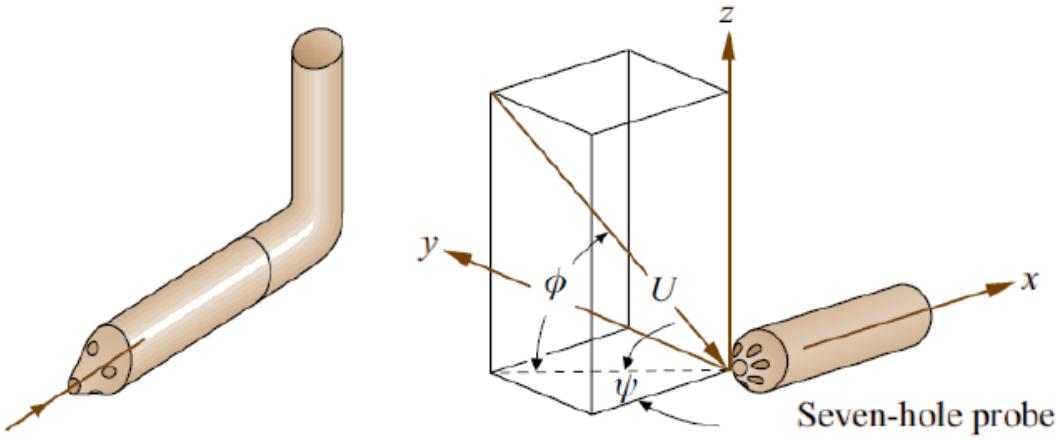

Figure 22: Multi Hole Probe [8]

For instance, whereas a three-hole probe can only measure the velocity in two directions, the five-hole prove allow to measure the three-dimensional velocity vector.

The main disadvantage of multi-hole probe in comparison with Pitot tube is that Pitot tube is already implemented in the laboratory, whereas a multi-hole probe should be bought.

4.1.5 Hot Wire Probe

The hot wire anemometer has been used for many years in experiments related with the fluid field, although some new techniques, like the optical methods, have appeared being more accurate, it is worth keeping in mind the great advantages and the operational principle that hot wire probes provide.

First of all, nowadays it is still used this kind of technique due to the electronics improvement and also due to its detailed results in turbulent flows, which is the case in the area of interest of this thesis. [7]

The geometry of a hot wire anemometer consist of an small heated wire, a sensor, which gets the electrical signal of the wire and by using an electronic equipment we are able to convert these signals in real values. It is important to make clear that it will not be possible to measure all the vector fields of the flow, this technique works punctually owing to the dimensions of the sensor. [23]

Talking about the operational principle, it is based on thermal methods. The clue resides in getting the flow velocity from the relationship of the local flow velocity and the heat transfer from the hot wire to the fluid by using the relationship of these two parameters.

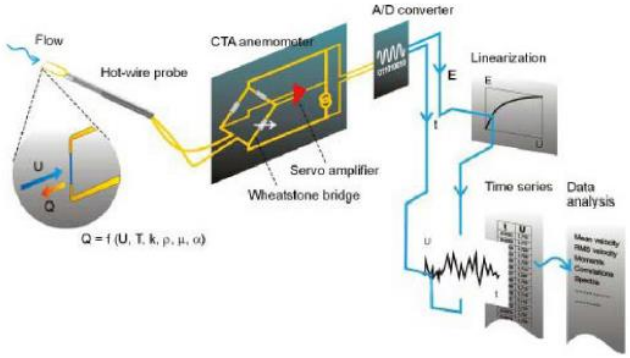

Figure 23: Measurement principles of CTA [23]

In the hot wire anemometer, two different systems can be used: CCA (Constant Current) and CTA (Constant Temperature).

In the current case it is preferable to use the Constant Temperature Anemometer for our test rig than the CCA, the circuit would be like the following one:

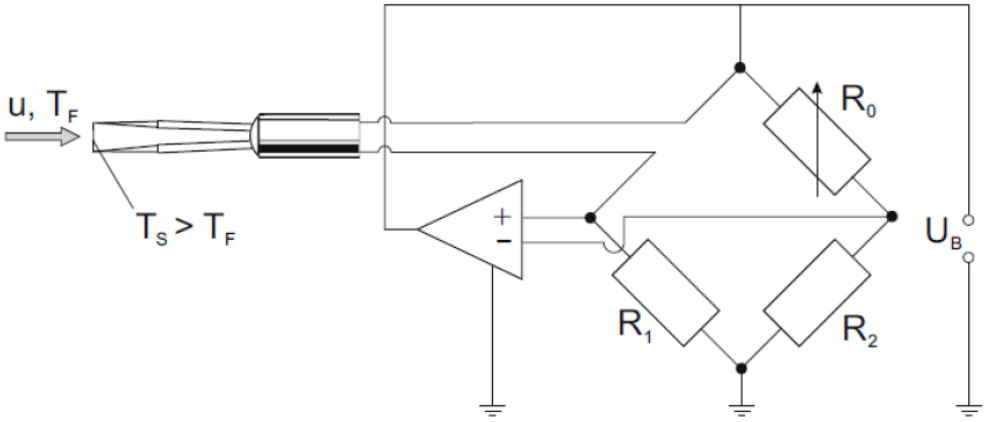

Figure 24: Circuit of a hot wire probe [24]

Using the CTA system implies providing a controlled amount of electrical current, whereas maintaining the wire temperature constant, implies a variation of the heat transfer.

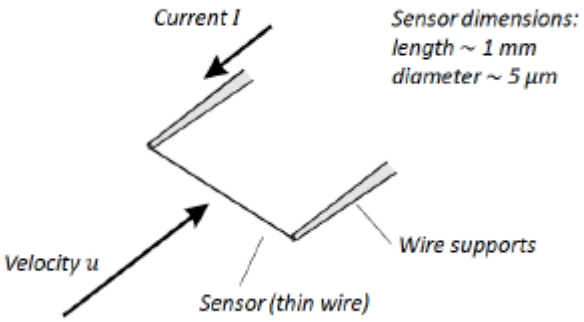

Figure 25: Operation principle of a hot wire probe [22]

It is also important to talk about the sensor that it is used in this method, it is said that a proper sensor for a hot wire anemometer need the following characteristics: [23]

- High value of the temperature coefficient resistance.
- An electrical resistance, which can be heated with a common voltage and current levels.
- Small size of the wire.
- High resistance in order to resist the stresses of the hydraulic flow.

The most common hot wire sensor is the tungsten coated with a thin platinum layer. It provides a much more resistance to oxidation. [24]

There are plenty of different types of probes. In Figure 26 are shown the three types of probe more relevant, which are the most popular in our field of measurement. [23]

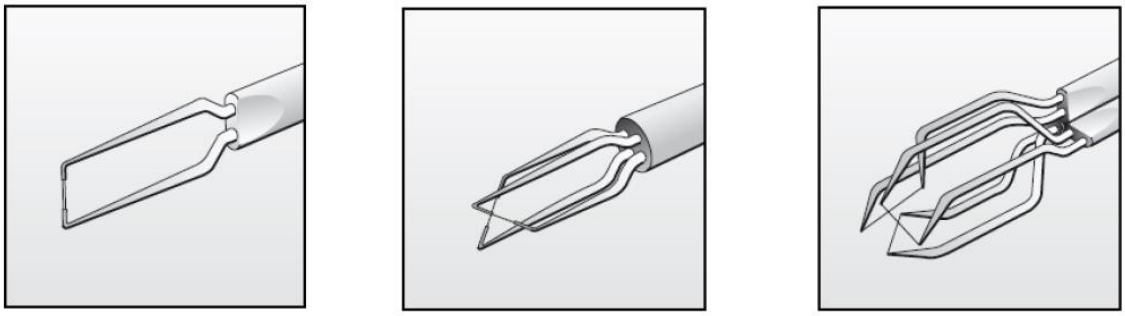

Figure 26: Different Types of Hot Wire Probes [23]

In the left picture it can be observed a Fiber-film probe, in the central picture a X-wire probe and in the right side a tri-axial probe for 3D-flows.

This method can be used either in air or in water, in this thesis it is worked in water so in order to perverse the quartz coating, it is necessary to make sure that grounding water takes place. In this case we protect the hot wire from damage due to voltage differences. [23]

The last important point about this technique is the calibration, it is possible to do a calibration in-situ in the test rig, but it would be really complicated, so usually it is done in another canal.

4.1.6 Laser Doppler Anemometry

LDA is a tool used in many fluid dynamic investigations in gases or liquids in order to know the flow velocity. As well as PIV or PTV is an optical method with a non-intrusive principle, it is also necessary some tracer particles. [27]

It is known as the technique of using the Doppler shift in a laser beam in order to measure the velocity in transparent or semi-transparent fluid flows. It is important to remark that LDA is linear with velocity and needs no pre-calibration, what makes this technique interesting. [26]

The basis of this technique is as it has been said the Doppler shift, it exists also the Doppler shift with light not only sound, in the case that light is reflected from a moving object, the frequency is shifted by a proportional amount to the speed of that object. Consequently, if the frequency shift is achieved, it is possible to estimate the velocity. [26]

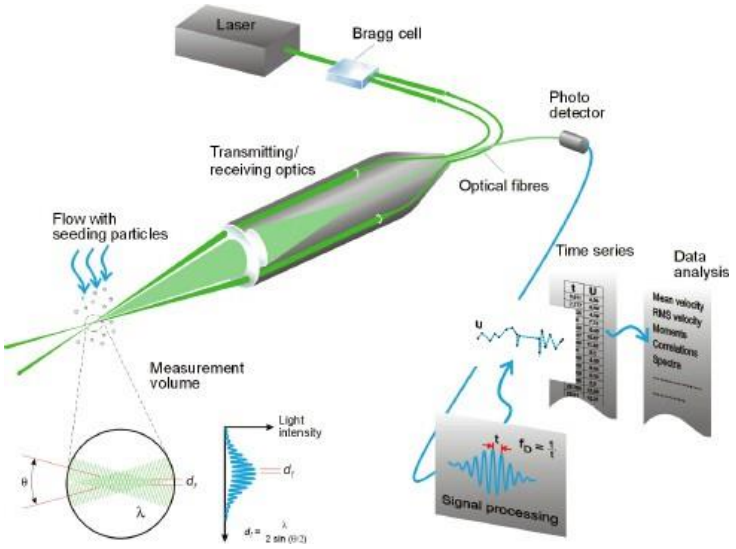

Figure 27: Functioning of Laser Doppler Anemometry [27]

So, the main idea is to make pass through the test rig some neutrally buoyant particles which could scatter light. The particles will be illuminated by a known frequency of laser light. In order to detect this scattered light, it is normally used a PMT (photomultiplier tube). This kind of instrument generates current in proportion to absorbed photon energy to amplify that current. What it is commonly called the Doppler shift is just the difference between the incident and scattered light frequencies. [26]

So, it is a simple process, it is necessary only a continuous wave laser and use some transmitting optics (beam splitter and focusing lens), later the signal is received by a photodetector and after that the last step is to process all the information.

Some advantages that this technique has are: non-intrusive measurement, high spatial and temporal resolution and the no need for calibration. [27]

The main disadvantages of this method are the high cost implementation and the complexity of measuring in the whole distribution of the flow, it is usually easier to measure in a punctual point. In the case of this experiment it is needed to measure the velocity in the whole area of interest.

4.1.7 Molecular Tagging Velocimetry

MTV is a new technique, which is mainly used when all the previously mentioned methods are not suitable due to tough conditions.

The idea of MTV relies on molecules that can be turned into tracers by excitation with photons. There should be inserted some tracer particles in the test rig, then in the region of interest is where by using a pulsed laser, the particles are “tagged”. Then another second laser is in charge of reading the movement of the “tagged particles”. [28]

The theoretical part of this technique allows us to estimate the velocity vector field due to the Lagrangian displacement vector.

This method has plenty of advantages, depending on the tracer properties and the method of implementation, MTV can be used not only used for knowing the velocity vector flow but also the flow visualization. [28]

Although it has several advantages, the implementation and high cost of the equipment turn the method in almost impossible for this experiment.

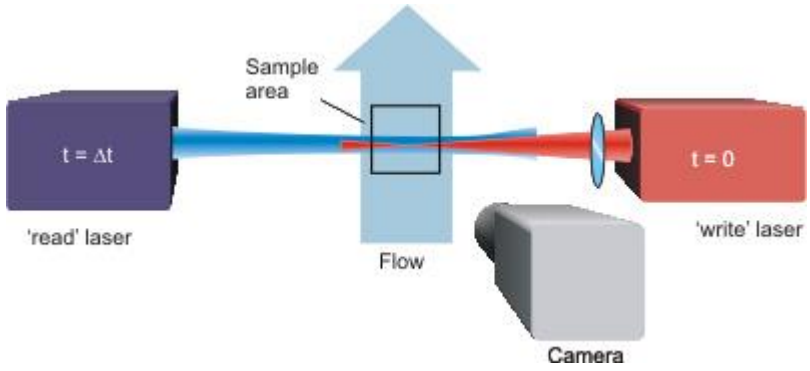

Figure 28: Funcitoning of MTV

4.1.8 Flow Visualization

Flow Visualization is a method which takes information from images taken by a camera in order to get knowledge about the behaviour of the flow. In the case of this thesis it could be used to measure the velocity, the width and the medium line of the streamtube.

There are many types of flow visualization, for instance smoke injections, smoke wires, dye or hydrogen bubble-wire. [29]

Another option could be to position some foils at the upper and bottom part of the perforated plate as it is shown in Figure 29. The idea of this concept resides in measuring the distance of the foils which consists in the width of the streamtube.

As the volume flow which is passing through the perforated plate is constant, by knowing the distribution of the distance between the foils. It is trivial to calculate the velocity of the flow which has passes through the turbine by using Eq. 27.

Also it would be necessary to measure the velocity in the entrance of the perforated plate, this velocity could be measured by using a Pitot tube or a hot wire anemometry, which have been explained before.

$$Q_{turbine} = u \cdot A_{streamtube} \quad \text{(Eq. 27)}$$

It is worth bearing in mind that the velocities of the water flow from the by-pass flow and the water flow which passes through the turbine are different; this means that the volume flow, which passes through the turbine, is going to remain constant until the mixing zone see Figure 2. Just by knowing the area of the stream tube in each point it is easy to know the velocity between the points (-) and (2).

One of the very first ideas was to use foils of polyethylene with bands of polystyrene, which will fit together with the “turbines” in order to visualize the streamtube of the flow like in Figure 29. It was decided to use this material because it has a density similar to water, it is totally necessary to work with materials with the same density as water in order to have a stable prototype. The main problems of using this kind of foils will be commented in section 4.2.

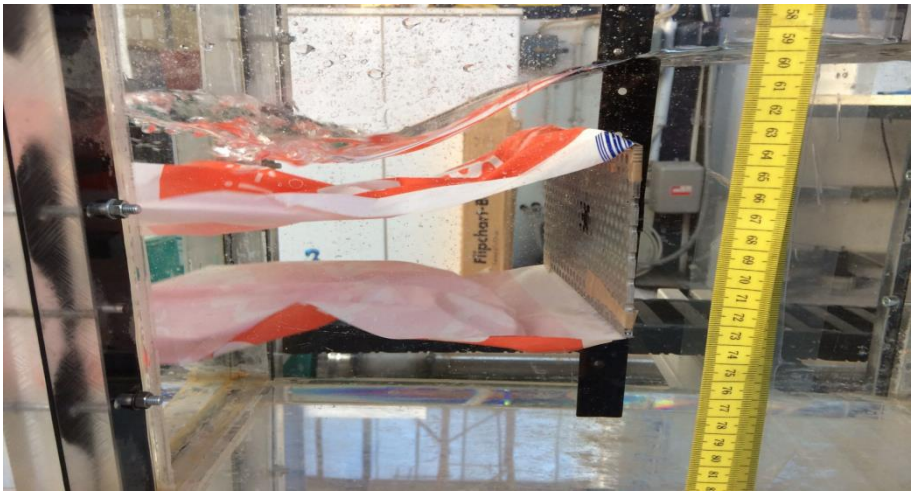

Figure 29: Flow visualization with foils.

The other type of Flow Visualization, which has been studied in this thesis, has been Hydrogen Bubble generation. The technique relies on the generation of hydrogen bubbles by electrolysis, the hydrogen bubbles are produces in a thin wire (25-50 µm), which acts as the cathode of the DC circuit. The anode terminal of the circuit is commonly a metal located in the bottom part of the channel. [30]

Note that the wire should be the cathode in order to generate small hydrogen bubbles. If the anode is the one chosen, oxygen bubbles would be generated instead of hydrogen bubbles. Generally oxygen bubbles are not desirable because they normally nucleate easily, and have larger size than the hydrogen bubbles, which are around half size the wire diameter. [31]

Although the hydrogen bubbles have not the same density as water, as the wires are really small in size, the buoyancy forces are negligible in comparison with the drag forces, this fact means that the bubbles will not produce a disturbance of the flow conditions.

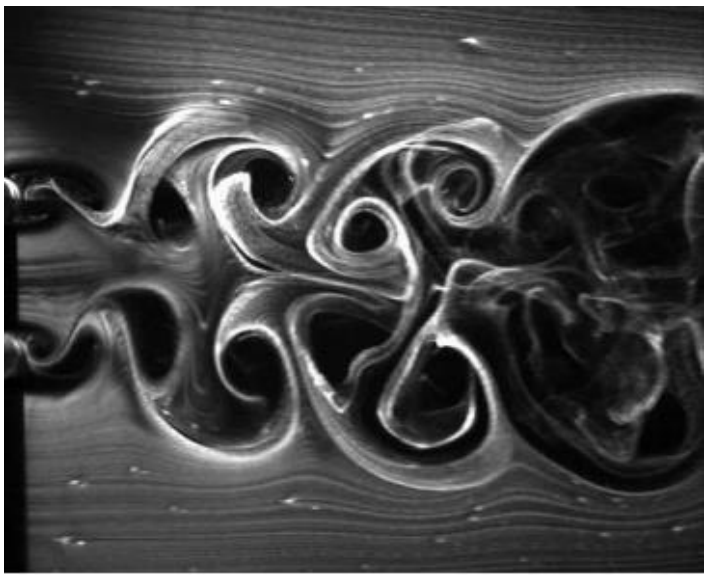

Figure 30: Hydrogen Bubble

One of the most important advantages of this technique is its versatility; they can be located almost anywhere. Other good points of this method are simplicity, quick experimentation and cost effectiveness. [32]

On the other hand, this method has some limitations, the principal one relies on its effectiveness for low Reynold numbers. In our case maximum Reynolds number, which occurs in the cascade with $Fr = 1.4$ and $Q = 82\mathrm{m}^3/s$ (worst case) is approximately $Re = 2.6 \cdot 10^5$. This means turbulent flow and leads to some necessary calibrations and dimensions of the wire, which will be commented in section 4.2.

If the flow is turbulent, it is normally used wires probes of 25-50 µm because the diameter of the bubbles is directly proportional to the diameter of the wire. In turbulent flow it is necessary to use low bubble diameter in order to have a nice visualization. Wire probes larger than 50 µm will lead to poor quality visualization. However, the smaller the wire is, the more possibilities of breakage of the wire. [33]

Another important limitation is the high degree of trial and error involved, the calibration is really tough. In fact after calibration it is possible to visualize complex flows successfully.

The system of hydrogen bubble generation consists of a DC-power supply, with a voltage range of minimum 70 V, this voltage depends on other parameters which will be discuss later, a current capacity of at least 1 A. In order to create DC voltage can be used a transformer and rectifier. Another possibility is an off-the-shelf switching power supply. [34]

It is also necessary to have a pulse generator which enables to measure the local velocity by creating series of time lines of hydrogen bubbles. It will be detailed in section 5.2.

It should be noticed that a safety system is necessary when working with this method, contact with the wire probe, the anode or the water flow can result extremely dangerous. Typically is used a circuit breaker to limit the electrical current. [33]

It is important to notice that the bubbles which are generated in the wake of a bubble wire move a little bit slower than the local velocity due to the wake effect of the wire, which can be quantitatively account as did Lu & Smith (1991) [35]

Normally salts are added to tap water, which contains dissolved electrolytes to facilitate a good electrolytic process, for instance common salt, sodium sulphate or hydrochloric acid. It is important that there is not a big concentration of electrolytes in order to avoid nucleation of the bubbles at lower voltage levels and corrosion of metals. [32]

Talking about the wires, it is necessary to comment that wires often fail (wire breaks), one has to be skilled when constructing this kind of structures. There are different types of wires: horizontal and vertical as it can be observed in Figure 31.

As it has been previously mentioned conductive wires consists of 25-50 µm welded between two metal and conductive supports as it can be observed in Figure 31. It is necessary that the wire is under tension to provide a clean sheet of bubbles, however too much tension will result on the breakage of the wire. The material, geometry and insulation of the wire probe and the supporting parts will be discussed in section 5.2.

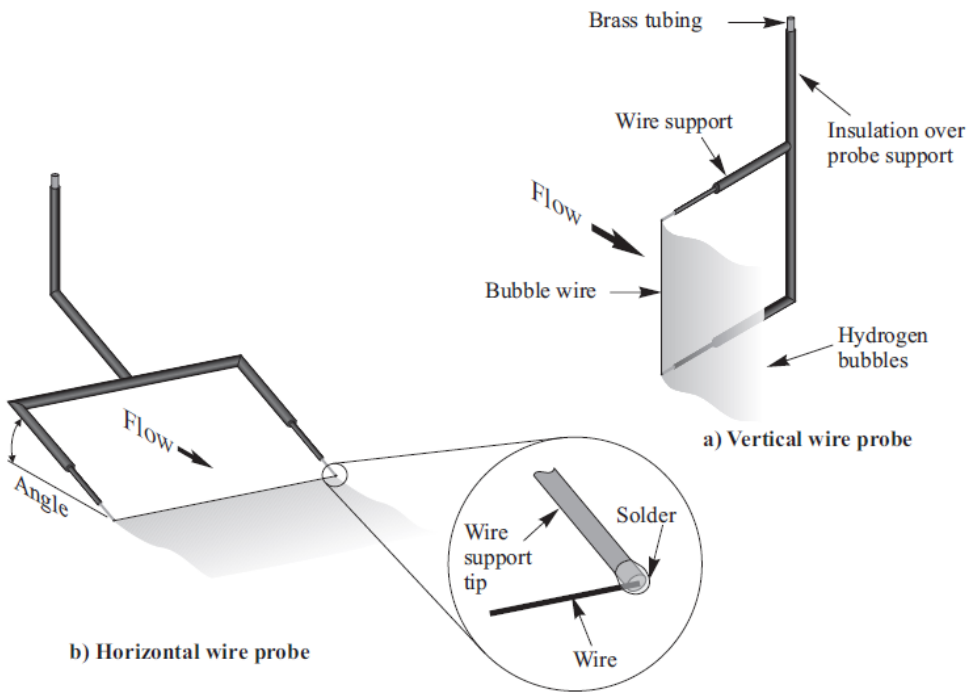

Figure 31: Types of wire probes [32]

Another common problem is the contamination of electrolytes produced on the wire, which can be cleaned by momentary reversal of the electrical polarity by the incorporation of a switch in the power supply circuit. It is necessary to "clean" the wire for approximately 8 seconds with an operating voltage lower than 50 V. [33]

Illumination is necessary in hydrogen bubbles generation to create a clear visualization of the flow and consequently nice pictures which can be analysed. A high-power light emitting diode (LED) is effective. It is available and provides light output like common lamps with small power requirements and infrared emissions. In section 5.2 will be commented the positioning of the LEDs in the test channel. It is also used a contrast background in order to improve the image quality. A simple solution is the usage of a black poster board behind the area photographed. [32]

Figure 32: High Power LED

Another important parameter of the picture quality is the clearance of the water. It is possible to maintain clean the water by filtering it and by using chlorine, which can facilitate the ion concentration of hydrogen in the water in addition to preventing organic growth in the water.

Apart from normal illumination with standard lamps or LEDs it is also possible to create thin light sheets. If well-defined cross-sections are desired, it is possible to use laser and generating optics in order to create the light sheets. [36]

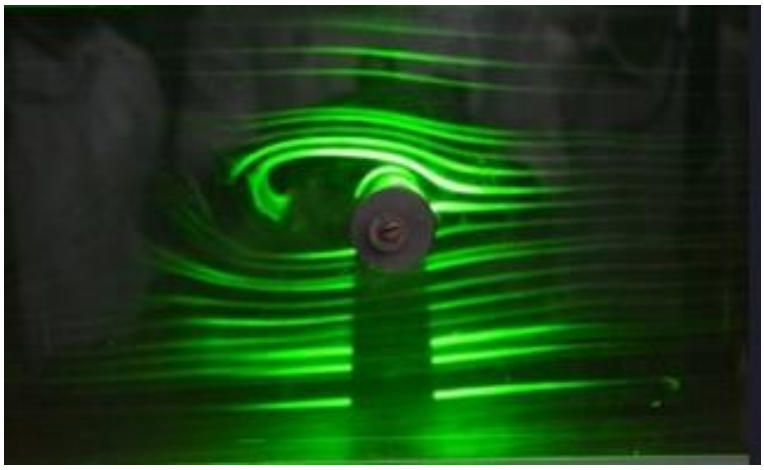

Figure 33: Laser Light Sheets

4.2 Water Level Measurements

In this part of the project, it has been found eight possible techniques in order to measure the water level altimetry of the flow. As it has been done in section 4.1., all the possible techniques have been placed in a table with the parameters which need to be measured.

	Camera	Laser	Conductive Level Altimetry	Capacitive Level Altimetry	Direct Measurement	Ultrasonic	Radar	Magnetostrictive Level Transmitters
A	NO	NO	NO	NO	NO	NO	NO	NO
u (cascade)	NO	NO	NO	NO	NO	NO	NO	NO
u (rest)	NO	NO	NO	NO	NO	NO	NO	NO
h (cascade)	YES	YES	YES	Part	YES	YES	YES	YES
h (rest)	YES	YES	YES	YES	YES	YES	YES	YES
z	NO	NO	NO	NO	NO	NO	NO	NO
p (cascade)	Part	Part	Part	Part	Part	Part	Part	Part
p (rest)	Part	Part	Part	Part	Part	Part	Part	Part
Economic	YES	NO	YES	NO	YES	Medium	Medium	NO
Accuracy	Medium	High	Medium	Medium	Low	High	Medium	High

Table 3: Evaluation of the Water level Measurement techniques

4.2.1 Camera

This might be one of the simplest methods of the level water measurement, it consists just in taking a lot of pictures of the area of interest with a high resolution camera, or even with a

good camera, and get an average of the water level altimetry, it is an interesting method because for this measurement is not necessary a high accuracy.

In the case that PIV/PTV or flow visualization, the same camera could be used for both measurements. At TU Darmstadt there is already a Charge Coupled Device (CCD) Camera: Sensicam qe.

Figure 34: CCD Camera (Sensicam qe)

4.2.2 Laser Distance Sensor

In this technique it is necessary a laser sensor and a float, which is the one pointed by the laser in order to know the water lever altimetry.

This kind of method work on the simple principle of leaving a buoyant object with a lower density than water so that it will be placed in the middle between air and water, then it is necessary a mechanical device to read out the position of the float (laser), a good option to get all the information read by the laser is to use a detector (CCD line sensor) and finally process all the information in a computer. [24] Figure 35 shows a triangular path of the laser wave.

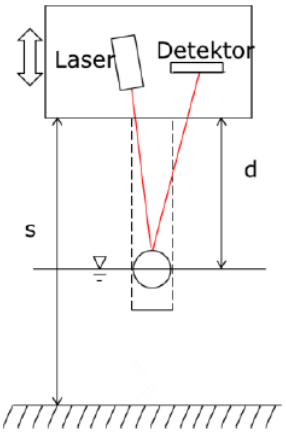

Figure 35: Functioning of the Laser Distance Sensor [29]

By knowing the position of the laser and detector (s) and the distance between the detector and the surface (d) it is possible to get the water level height (h). This is a basic explanation; a further explanation of this method can be found in reference [8]

$$h = s - d \qquad \text{(Eq. 28)}$$

If we get in detail, the laser diode produces a dot in the float, this light is scattered, and it passes through some lens to finally arrive to the sensor (detector). The measurement error in this kind of triangular sensor methods is less than 0.1 mm. [37]

Some advantages of this technique are the high accuracy, the low invasiveness, acceptable price and easy implementation. [37]

The main disadvantages are the difficult functioning of this method in the cascade, which generates much turbulence and the difficulty of passing over the turbine. This fact lead to the rejection of this concept.

4.2.3 Conductive Level Altimetry

As it was previously explained in section 2.3 this method is currently used to measure the conductive level altimetry. The operational system depends on the electrical conductivity between two electrodes, which is function the filling height of the test rig.

So in this method it is used a needle electrode in order to scan the surface and achieve the level height. The theoretical property that is used is that the electrical conductivity of the water is much higher than the one from the air. [37]

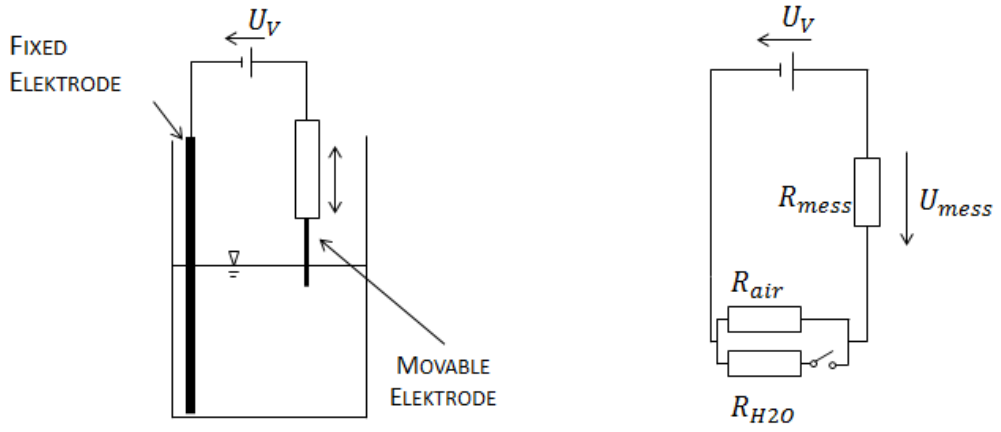

Figure 36: Scheme of the Conductive Level Altimetry method [8]

The geometry of the measurement system can be observed in Figure 36. It consists of a fixed electrode already immersed in water. The sensing electrode is moved perpendicular to the water surface with a stepper motor and a ball screw. At the moment that the needle electrode touches the water the electric flow is detected and consequently the water level altimetry of the test rig, if the needle electrode does not touch the water there would not be an electrical continuity. [37]

This measurement has an important disadvantage, the large invasiveness of the method; this fact provides a lower accuracy than other methods. Other students did some tests about this technique and there were large scattering at the cascade point, which is the area of interest, see section 2.3. [8]

4.2.4 Capacitive Level Altimetry

The operational principle of this technique resides in the fact that the capacitance of a capacitor is a function of the relative permittivity, which is quite different in the water than in the air. By using this property it is possible to calculate the water level by using the following formula: [9]

$$C_{total}(h) = \epsilon_0 \frac{b}{d}\left(\varepsilon_{r,air} \cdot L + \left(\varepsilon_{r,H2O} - \varepsilon_{r,air}\right) \cdot h\right) \qquad \text{(Eq. 29)}$$

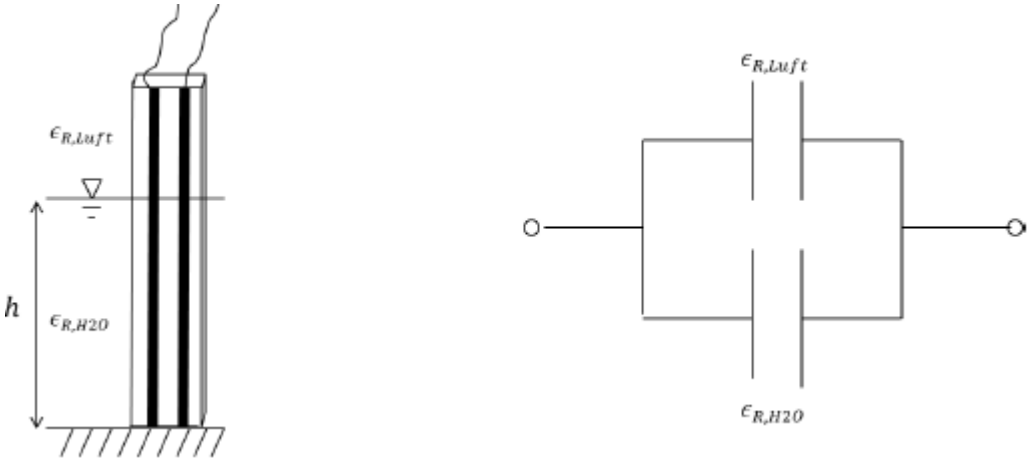

Figure 37: Description of Capacitive Level Altimetry method [29]

After some calculations done in [9], it is achieved the asset that this technique is not that accurate for commercial capacitor up to $1\,pF$, hence it would be necessary to buy special capacitor, so much more expensive.

In this measurement systems there are a few aspects that should be considered, for instance there is a problem with the fluctuations of the temperature, it is important to consider this fact because the

relative permeability changes a lot with the temperature. This is not a problem due to the constant temperature of the laboratory were the test rig is placed.

Another important aspect to comment is the capillary, if we use a big invasive sensor, it will make the water level rise in the gap between the electrodes of the capacitor. Here there are two options:

- Use a smaller sensor with the disadvantage of requiring a capacitor with lower capacitance, which means more expensive.
- Use a big sensor assuming that there could appear the capillary phenomena.

To sum up, it will not be one of the most suitable techniques for the experiment due to the large invasiveness and the high cost of the special capacitors. Also the measurement will not be really accurate in the area of interest.

4.2.5 Direct Measurement

This method is the simplest one and also the least accurate. It consists just in measuring with a normal ruler in a transparent glass the water level of the test rig. It is not a measurement that we should consider seriously. The lack of accuracy is too high so this technique should be rejected because there are so many options better than this one.

4.2.6 Ultrasonic Level Transmitter

This technique measures the water level altimetry by using ultrasonic waves. The idea is to measure the distance between the transducer and the water surface by using the ultrasonic pulse, which travels from the transducer to the surface and comes back, (TOF). [38]

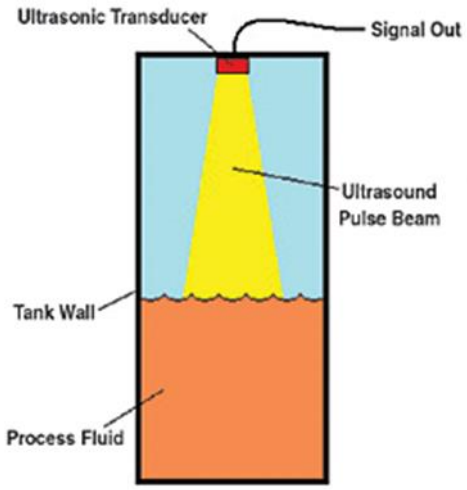

Figure 38: Ultrasonic Measurement [38]

Figure 38 explains graphically how the system works. These systems works perfectly for flat surfaces like a tank, but in a cascade the accuracy is not that high. Another disadvantage is the possible false echoes of the walls or the structures that could appear. As the area of interest is not flat, this method should be rejected. [38]

4.2.7 Radar Level Altimetry

This technique requires an air radar system beam microwaves downward from an antenna, which will be placed at the top of the test rig.

The idea is that the signal provided form the transmitter is reflected off the liquid surface back to the antenna, by knowing the timing circuit it is possible to calculate the distance to the fluid surface by measuring the round-trip time (TOF).[38]

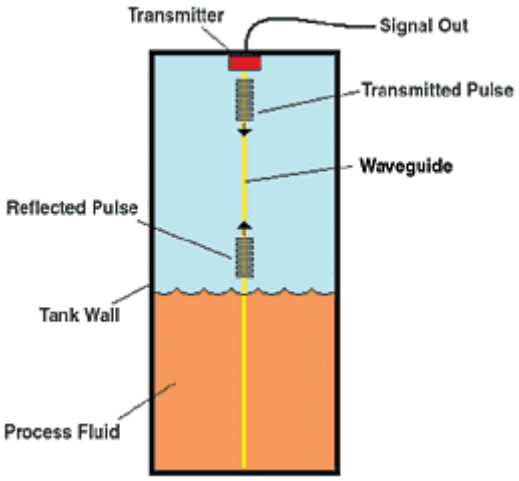

Figure 39: Radar Level Altimetry measurement

This method could have measurement problems if the dielectric constant of the fluid is low, the reason of this fact is that the amount of reflected energy frequencies depends on the dielectric constant. If it is low, it means that the radar's energy enters or passes through. In our case, water ($\varepsilon_r = 80$) there are no continuity problems. [38]

Some other problems related to this system are the divergence of the beam that could provide erroneous readings. In order to overcome this problem, it can be incorporated complex algorithms using fuzzy logic to the transmitter, although this is not a simple solution, another simplest solution could be to use Guided Waver Radar (GWR) systems, it consists of a flexible cable antenna system, which guides the microwave down from the top of the test rig to the surface water and back to the transmitter, this system is 20 times more efficient that normal radar systems [38]

Although it works better than the ultrasonic measurement, it is quite similar, due to the difficulty of measuring in the area of interest, which is not a smooth surface. It should be also rejected for this experiment.

4.2.8 Magnetostrictive Level Transmitter

The main concept of this method relies on the usage of magneto-strictive transmitters instead of mechanical links, using the speed of a torsional wave along a wire to find the float and get the position of it. [38]

In this system the float carries some permanent magnets, and a sensor wire is connected to a piezo ceramic sensor at the transmitter. Consequently, a determined tension will be attached in the opposite way in the end of the sensor tube. This tube could run through a hole in the centre of the float as it shows Figure 40 or could be adjacent to the float.

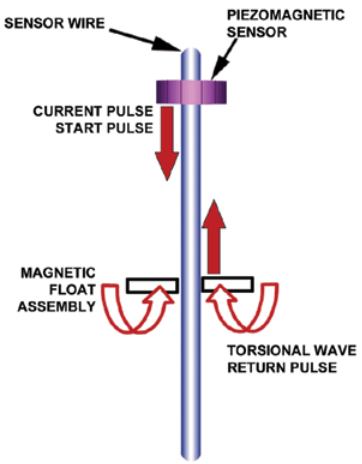

Figure 40: Magnetostrictive Level Transmitters

The float should be located, in order to achieve it the transmitter sends a short current pulse down the sensor wire, this affects setting up a magnetic field along the length of the tube. At the same time a timing circuit is triggered ON. The overall effect is reflected when during a brief time the current flow, a torsional force is produces in the wire, which travels back to the sensor at a characteristic speed. At the time that the sensor detects the torsional wave, it is produced an electrical signal, which means that it is the moment to stop the timing circuit OFF. After knowing the TOF is easy to determine the float location. [38]

Although the method has some advantages, there is not a lot of information about this technique, because of that it is not possible to know the effect of this method in the area of the cascade. Since there are other methods, which are more suitable for the requirements of the experiment, this method will not be implemented. Although it is rejected, it could be an interesting method in future investigations.

5 Measurement Concept

5.1 Election of the Concept

After explaining all the possible techniques that have been researched, the election of the concept for the measurement system will be explained in this section of the project. The following three combinations have been chosen due to the fact that they achieve the requirements of the concept settled in section 3.

1. Pitot Tube + Conductive Level Altimetry
2. Flow Visualization + Camera + Pitot Tube
3. PIV/PTV + Camera

5.1.1 Pitot Tube + Conductive Level Altimetry

This combination is the current state of the project, the velocity is measured by a Pitot tube, which it is already implemented in the laboratory, and the water lever measurement is measured with the Conductive level altimetry.

The main reasons because of that this current combination is rejected have been already explained in sections 2.3., 4.1.3 and 4.2.3.

In light of the above mentioned, it is necessary to say that this option is the worst one of the three proposed due to its lack of accuracy.

5.1.2 Flow Visualization + Pitot tube + Camera

In the second combination, the velocity would be measured with the previous mentioned technique: flow visualization + Pitot tube and the water level measurement would be measured by a high resolution camera.

The high resolution camera used for the water level measurement will be the same one which is going to be used for the flow visualization technique, which as it has been before commented, it is available in TU Darmstadt.

5.1.2.1 Polyethylene Foils Concept

This concept was commented in section 4.1.8., it was the very first idea for the flow visualization. After researching different materials which were solid, flexible and had a similar water density ($1\ g/$

cm^3), there were found two options: Low Density Polyethylene (LDP), which has a density between $(0.92 - 0.94\ g/cm^3)$ and High Density Polyethylene (HDP), which has a density between $(0.93 - 0.97\ g/cm^3)$.

Although HDP has a more similar density to the water, the elected material was LDP due to its flexibility. After validating LDP, it can be said that LDP is enough stable in the water, which means that the foils were not sinking nor floating.

Some bands of polystyrene $(0.96 - 1.04\ g/cm^3)$ were added to the polyethylene foils in order to make them more consistent and heavier.

The foils will be coupled in the following assembly:

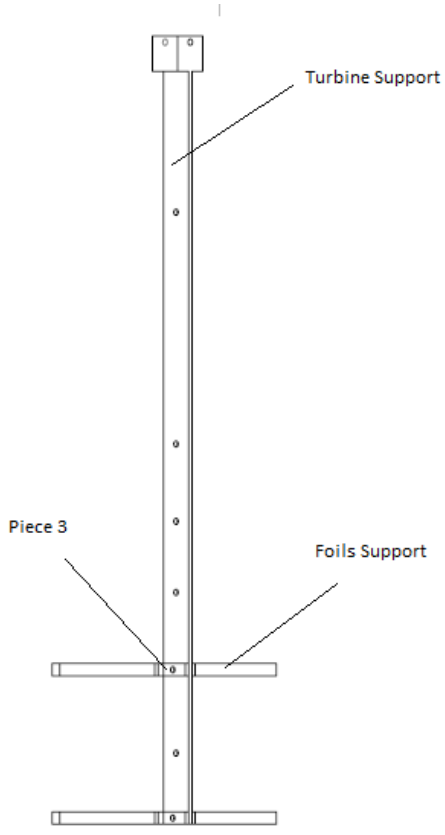

Figure 41: Turbine Structure

The assembly is formed by two pieces called foils support, the turbine support and four pieces (3). Each foil support is coupled to the turbine support by two pieces (3), through the holes there will be a screw fixing the elements.

The foils will be fixed to the foils support, as it can be observed in Figure 29, and it won't be necessary to remove then when changing the size of the turbine. So, the good point of this concept structure resides in the fact that when using perforated plates with different width, it will be only necessary to screw the foils support to a different hole of the turbine support.

It will only be necessary to screw when changing the size of the turbine, but not when changing the type of resistance of the perforated plate, which is quite interesting in order to speed up the process of collecting data from the measurement.

The main reason of using pieces (3) is to give rigidity to the structure. The first idea was to weld the foils support positioned below to the turbine support, (this foil support will be fixed) in contrast with the upper one, which is movable. At the end, this idea was rejected. By using two pieces (3) the structure is way more stable and rigid than before.

Technical Drawings of all the components of Figure 41 are attached in section 10: Appendix B

After discussing this concept with Prof. Dr.-Ing. Peter Pelz and Dr.-Ing. Gerhard Ludwig, it has been decided to reject the idea of using foils, because the presence of the foil will produce uncontrollable forces which are not negligible. That means that when measuring, the error produce will be too high.

Although it is an inaccurate concept and it cannot be used to measure the velocity, the medium line and the width of the streamtube, it can be used in order to visualize the flow's behaviour.

Because of that it has been decided to carry through this concept and just use it when it is necessary to show the flow's behaviour to other people or institutions.

5.1.2.2 Hydrogen Bubbles Generation Concept

Although the Foils concept has been refused, it was decided to keep working in a concept related to flow visualization.

The other main measurement system commented in section 4.1.8. is the generation of hydrogen bubbles in order to measure the velocity, the medium line and the width of the streamtube. The idea is to generate bubbles from a wire by electrolysis and take pictures in order to visualize the behaviour of the flow.

The high resolution camera, previously commented (see Figure 34), will be used for two tasks: to take pictures of the hydrogen bubbles and to measure the water level altimetry. The water level measurement has been explained in section 4.2.1. The idea of the measurement resides in doing a lot of pictures to the flow and then interpolating these values to get an average value of the altimetry, which should be accurate and cost-effective.

Hydrogen bubbles will be generated with the following electronic system:

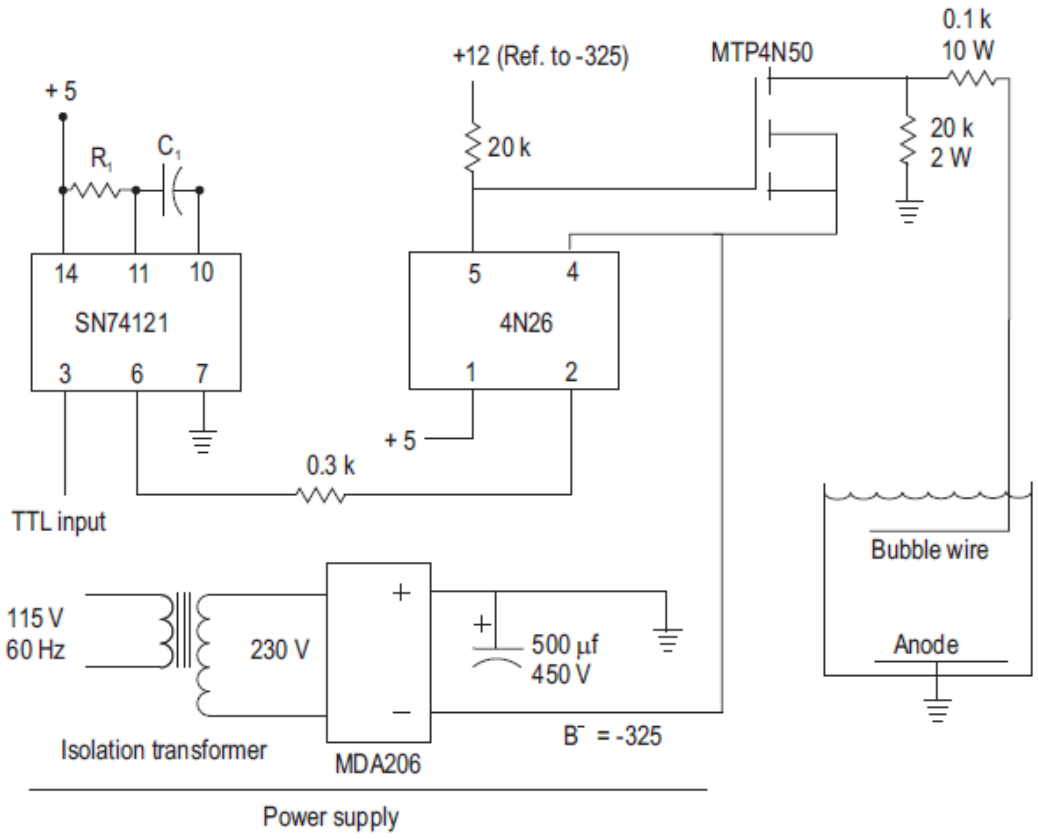

Figure 42: Electric Circuit for Hydrogen Bubble Generation. [34]

As it has been studied in [32] and [34] for a wire length of 250 mm it is necessary a range of 0-300 V at a maximum current of 2 A. As two wires are used in this experiment, it will be necessary to construct an electric circuit for each wire probe.

So de basic requirements will be the variable voltage DC power supply, a rectifier, an Opto-isolator and the transistor MOSFET, which allow generating a pulse in order to create “time lines” of hydrogen bubbles, which are necessary to measure the velocity behaviour.

One of the advantages of pulse voltage is the possibility to determine the average velocity directly from the pulse frequency if there is a pulsed voltage of two wires separated by a known streamtube distance. [32]

Usually the pulsing process is achieved by the usage of square wave generator transistor-transistor logic (TTL) signal, which enables to gate the voltage signal from DC power supply via a power MOSFET. This TTL signal can be controlled with the frequency of the time line generation and the duty cycle of the generating bubbles. [34]

The incoming TTL signal triggers the Multivibrator to generate a second TTL pulse, which can be controlled by its width τ.

$$\tau = 0.7 \cdot R_1 \cdot C_1 \quad \text{(Eq. 30)}$$

The resistor R_1 and the capacitor C_1 cannot be bought yet because their values will depend on the pulse width, which would be decision of the responsible person of doing the measurements.

The Opto-isolator will oversee isolating the TTL signal from the rest of the circuit, which is referenced to $B_- = -325\,V$. The output will be configured as a switch, which means that for each input pulse, there will be a pulse generated in output 5 of $B_+ = 12\,V$. Finally, this pulse goes through the MOSFET transistor, which is also used as a switch to supply -325 V pulses to the bubble wire. [34]

The safety system is really important in this kind of circuits, working with electrolysis. It will be placed a circuit breaker of maximum current (2A) after the isolated transformer.

In order to implement one of the electric circuits is necessary to buy the following components:

- Isolated Transformer: N73A (Triad Magnetics) - 36.51 euros (Digikey)
- Rectifier: MDA206G-B - 0.562 euros (Mouser)
- Opto-isolator. 859-4N26 - 0.417 euros (Mouser)
- Multivibrator monostable: SN74121D - 3.38 euros (Digikey)
- Transistor MOSFET: MTP4N50 – 10.21 euros (Octopart)
- Capacitor of 500 µF and 450 V: E36D451LPN500TA54M - 9.38 euros (Mouser)
- Resistor of 0.3 kΩ: RC04022JR-07300RL - 0.08 euros (Digikey)
- Resistor of 20 kΩ: RC0201FR-0720KL - 0.08 euros (Digikey)
- Resistor of 0.1 kΩ and 10 W: RC0603FR-07100RL – 0.08 euros (Digikey)
- Resistor of 20 kΩ and 2W: 352120KFT - 0.57 euros (Digikey)
- Circuit Breaker of 2 A: 9926251902 – 19.37euros (Digikey)

All these components represent one electric circuit. As in our experiment we are using two bubble wires, it is necessary to buy each component twice.

All the components with its prices are set in section 9.3 (Economic Budget).

As it was commented in section 4.1.8., it is necessary to clean the wires. A possible solution is reversing the polarity of the power supply during 6-10 seconds with a voltage lower than 50 V. In order to reverse the polarity the following circuit should be used. [33]

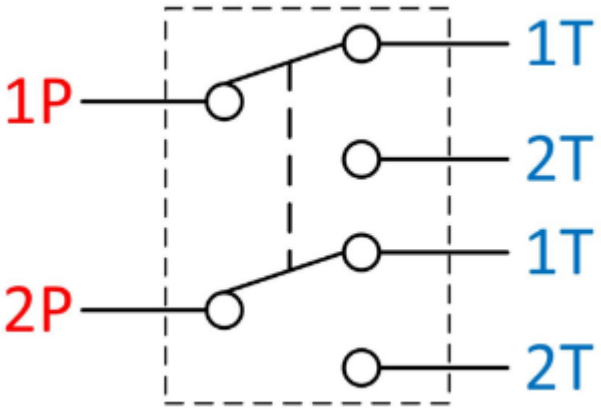

Figure 43: Polarity switch for cleaning

In terms of improving the visualization quality of the hydrogen bubbles, it is highly recommended to add 0.12 grams of sodium sulphate per litre of water. By adding this component it is created an electrolyte concentration, which improves the visualization. Another possibility in case this additive is not available could be sodium chloride (table salt), although it will have worse results than sodium sulphate. The last possibility could be to add a really small quantity of hydrochloric acid (0.3 ppm), which will also control algae growth and maintain the water clear and clean. [32]

Note that the concentration of the additives must be calibrated by trial and error. A low concentration means that it is need a higher voltage, whereas a high concentration could lead to big size bubbles.

As it was before mentioned in section 4.1.8., the flow has a turbulent behaviour because of the high Reynolds number, due to this fact we need very little bubbles. The diameter of the bubbles is directly proportional to the diameter of the wire probes. Even though, it has been decided to use $50\ \mu m$ diameter so that the structure will be more rigidity and the wire probe will be more resistant to failure. It is necessary to take into account that bubbles size will be bigger than with 25 μm diameter wire probes.

The length of the wire probe is going to be the same as the total energy in the entrance H_1 $(250\ mm)$ .See Eq. 16.

When choosing the material of the wire probe, there are some possibilities: platinum, steel, stainless steel, aluminium and tungsten.

As some electrolyte additives have been added there could be problems of oxidation with steel and aluminium, which will lead to a wire failure. Stainless steel and tungsten are defined as strong materials, but the quality of the bubbles generated is not so good. So, the best option in terms of quality, price and strength is the platinum wire, which is the one selected in this concept. Some other

advantages of platinum are the lack of corrosion, the effectiveness when welding components and the appropriate conductivity necessary to generate hydrogen bubbles. [32]

As the calibration is really tough and usually there are some wire failures. It is necessary to buy at least 3 m of platinum wire $50\ \mu m$ diameter. In buyplatinumwire.com there is offered a platinum wire of $50\ \mu m$ diameter per 3,048 metres, which cost 99.52 euros.

Both wire probes will be vertical (Figure 31) in order to measure the width, the medium line of the streamtube and the local velocity. As it is detailed in section 5.2, each wire probe will be placed 30 mm away from the turbine support one to the right and the other one to the left. The supporting tubes will be made of Brass.

The interesting point of vertical wire probe is that some of the bubbles will collide with the perforated plate and explode, but the ones which follow the streamtube will not collide and by doing pictures with a high-resolution camera, we are able to measure the velocity, medium line and width of the streamtube, which are the objectives.

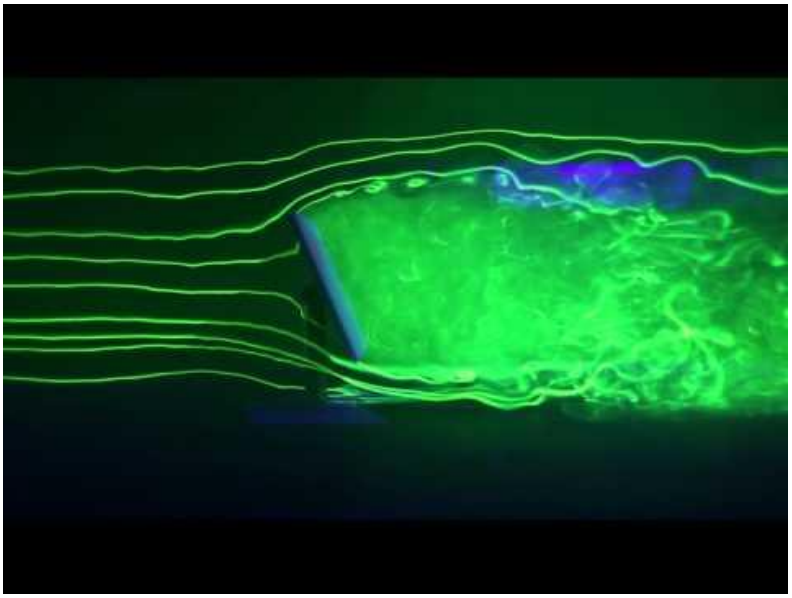

Figure 44: Flow Visualization

The supporting wire probe, which will be used, is the one in Figure 45.

It is not necessary that the whole supporting wire is made of brass, the part inside the water should be brass, but the rest could be without any problem a common cable.

The technical drawings of this piece are set in section 10 (Appendix B).

The platinum wire must be tensed in order to create a clean sheet of bubbles, determining the right tension must be calibrated with the trial and error method. Sometimes too much tension can

occasion failure of the wire. In [33], there are some methods proposed in order to weld with a correct tension the wire and the wire support.

The wire probe will be vertical in the first attempt, but it is important to mention that when using horizontal probes, it is necessary to calibrate the angle of attack. If the angle is too large the cross tubbing of the probe will interfere with the line of vision of the bubble sheet from above, but this is not a big deal because the camera will be placed in the lateral side. If the angle is too small, the cross tubing can produce shedding forces which is undesirable. This angle should be also calibrated when testing the wire. Note that bigger angles of attack are preferable. [32]

Figure 45: Vertical Wire

It will be necessary 3 metres of brass round bar 4 mm diameter in order to make the support of the wires. This diameter has been chosen in order to avoid shedding forces. The relation between the length of the wire and the radio of the round bar should be between 40 and 50.

In the company Metalandplastic.co is possible to buy a brass round bar rod 4mm x 3M for 7.99 pounds. It is important that the round bars of brass are completely insulated, so that the hydrogen bubbles are only generated on the platinum wire. Normally the insulation process includes shrink-fit tubing and a commercial liquid tape.

The shrink-fit should be positioned around the brass and must be applied before welding the wire to the supporting wire. The liquid tape should be sprayed at the final part of the wire supports, because when welding, high temperatures can produce the melt of the shrink tubing.

The department of FST of FB 16 (TU Darmstadt) should have these two insulating components. In the case of the Shrink tubing, Mouser offers RT-770-1/4-0-SP (1.51 euros) the issue is that the minimum quantity to buy it is 1.000 items.

Another important aspect is the illumination. In this experiment high power LEDs projectors are the one chosen owing to the fact that they have less power requirements and infrared emissions than a standard source of light. See Figure 32. [32]

In order to select the proper LED, it is necessary to calculate the quantity of lumens appropriated for this task. In the area of interest the area illuminated is 0.2m x 0.4 m = 0.16m^2.

$$1\ lux = 1\ lumen/\mathrm{m}^2 \quad \text{(Eq. 31)}$$

In the reference [39], it is recommended a quantity of lux between 10.000 and 15.000 for indoor places with performance of very special visual tasks of extremely low contrast and small size, this leads to a quantity of lumens between 1.600 and 2.400 for our area of interest.

The position of the LEDs should also be taken into account when calibrating by trial and error. Usually the LEDs are placed in an oblique angle or at the bottom of the channel. Here two options are provided with its prices.

Here there are several possibilities that could be done:

- Single LED of 1.600 lumens placed at the bottom of the channel: CXM-14-30-95-36-AA00-F2-3 - 6.74 euros (Mouser).
- Single LED of 1.120 lumens placed at the bottom of the channel XHP50B-00-0000-0D0BJ450E – 5.75 euros (Mouser) and 2 x LEDS of 400 lumens placed in an oblique position to the wire probes: XPLAWT-00-0000-000BV20E3 – 2.69 euros (Mouser)

The second possibility seems to be more efficient in terms of illumination and it is the one recommended, but it won't be too expensive to test both illumination systems.

It is also important to make a contrast of the background, in our case the camera is going to be placed at the side of the channel. An interesting decision could be to position a black poster in the other side of the channel in order to make contrast.

It is also common to illuminate the hydrogen bubbles with laser sheets, in this experiment this will not be a possibility but maybe in future works it would be a possible improvement of the measurement system. [36]

5.1.3 PIV/PTV + Camera Concept

The concept of the hydrogen bubble flow visualization should be enough in order to measure the velocity between the points (-) and (2). Even though, it is necessary to say that if we want to take a leap of quality in the measurement, PIV or PTV techniques would be the right option.

In this combination the velocity is measured by PIV or PTV, whereas the water level altimetry is measured with the same camera used for the optical methods.

As it was explained in sections 4.1.1 and 4.1.2., the big disadvantage of these systems, except for the price (which will not be a problem, the material is already available in TU Darmstatd) is the hard implementation, calibration and analyse of all the data. To overcome these difficulties it is needed a great knowledge about the topic and its instrumentation.

The camera which is currently in TU Darmstadt is the Sensicam 370 KD from PCO, which has a resolution of 1280 x 1024 pixels.

It is important to make sure that the strokes number of the particles used in this technique is below 0.1 so that the tracer particles can follow the streamlines of the flow. If this condition is not achieved, the tracer particles would not follow the streamtube and therefore all the data collected will not be accurate enough.

So it is necessary to calculate the strokes number of the particles. As it was explained in section 2.1.4., u_0 is the velocity far away from the turbine that means a Froude number between 0.3-0.5. The velocity can be calculated with Eq. 19. l_0 is the height of the turbine, in this case it would vary between 5 cm and 40 cm.

It is important that the density of the particles is similar to the water, so that the particle will be stable and will not sink or float. As it was also commented in section 4.1.1., the material of the tracer particles should be glass microspheres or particles of polystyrene in order to have a similar density as the water. Also, the diameter of the particles should be really low in this case the particles diameter is 0.25 mm.

By using Eq. 14 and Eq. 15.:

$$t_0 = \frac{\rho_p \cdot d_p^2}{\mu_{H20}} = \frac{1000 \cdot (0.2510^{-3})^2}{1 \cdot 10^{-3}} = 0.0625$$

$$Stk = \frac{t_0 \cdot u_0}{l_0} = \frac{0.0625 \cdot (0.22 \div 0.465)}{0.05 \div 0.25} = 0.055 \div 0.58$$

This range means that when using PIV or PTV, we should be careful at the time of choosing the height of the turbine and the Froude numbers of the flow. It is recommendable to use as large height turbines as possible and as low Froude numbers as possible.

Therefore, as the range could be low enough to work with this technique, it is highly recommended to investigate if there is a possibility of using PIV or PTV techniques in order to measure the velocity, the medium line and the width of the streamtube.

5.2 Design of the Construction of the Measurement System.

The concept which will be implemented relies on a camera placed on the lateral side of the channel, the hydrogen bubbles generation system (wire probe, supporting wire and electrical console) and a pitot tube placed just in front of the perforate plate.

The Pitot tube will be accomplished to the following structure:

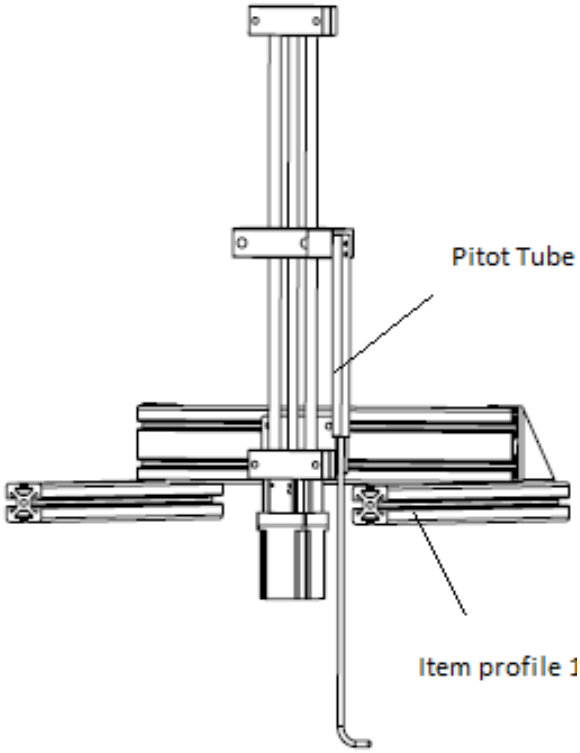

Figure 46: Pitot tube Structure

As it is observed in the Figure 46, by using this structure the Pitot tube can be moved vertically due to the ball screw and the stepper motor, which will be explain in detail in section 5. The idea of using the Pitot tube is to measure the velocity at the entrance of the perforated plate. As the velocity profile is constant through the width of the channel, it would be only necessary to measure the velocity at the centre of the channel (See Figure 2).

It is also important to notice that the Pitot tube could also measure the velocity between the points (1) and (+) by changing the position of the items profiles 1, by doing these changes it is possible to get the whole distribution of the velocity between (1) and (+).

There are components which are not marked because they will be explained in detail in section 5. The main function of these pieces resides in the Turbine Concept although they are also used in the construction of the Pitot tube structure in order to profit the design of the pieces.

Note that the Pitot tube shown in Figure 46, is already set in the laboratory, the original technical drawings were not available in the database of TU Darmstadt, so piece 12 is just an imitation of it.

As it has been previously commented the two vertical supporting wire probes will be fixed in the profile item 1 as it is shown in the following assembly: Both wire probes will be installed at a distance of 15 mm, each in one side of the Turbine support. The supporting wire probe will be then screwed to the item profile 1, shown in Figure 46. It is important to note that the distances between the end of the item profile 1 and the adaptor 1 must be kept, if not the wire probe will touch the wall of the channel test rig. By using this structure, the supporting wire probe will be fixed always.

The technical drawings of the wire support and the adaptor 3 are attached in section 10. (Appendix B).

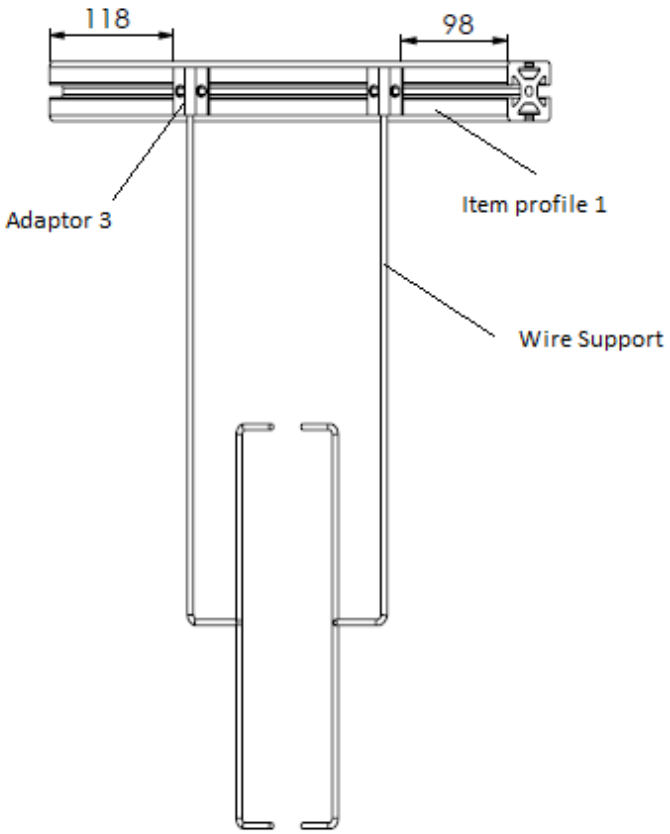

Figure 47: Wire Probes Support

6 Turbine Concept

The requirements of the Turbine concept were settled in section 3. The turbine concept should change automatically the perforated plate height position and should make easier the removable of the turbine resistances and the perforated plate size (height) as it is explained in section 2.3.

There should be at least three different perforated plate resistances and each perforated plate should have at least four different heights.

Also, the system should combine the Turbine structure with the Pitot tube structure in order to have the technical drawings of the complete measurement system.

6.1 Election of the Turbine Concept

The Turbine Concept that is proposed in this thesis is composed of a Ball Screw from Igus, which enables the turbine to move vertically in combination with the Stepper motor and the gear box

By using this concept it is quite easy to control the height position of the perforated plate by codding in Labview and using a controller, which will be placed in out of the test rig. Programming the Labview code is beyond this thesis but should be done by the person in charge of running the measurement.

The combination of these components allows measuring the required parameters many different points. Furthermore it allows collecting more data in less time in comparison with the current state of the Turbine concept. Currently, the perforated plate's height position can only be changed by screwing the perforated plate in a different hole of the turbine support (see Figure 41.

With this concept, it will only be necessary to screw at the time of changing the perforated plate to another one with different size. So the correct process of our measurement will be to collect all the data of a single perforated plate size in different height positions and different turbine resistances and then change the perforated plate size.

Currently it is necessary to screw every time that is necessary to change the height position, the resistances and the perforated plate size.

Another advantage of this structure is that when changing the perforated plate size, it is possible to position the turbine in the maximum height and screw in a more comfortable way. Nowadays it is really uncomfortable because as it is shown in Figure 18, the turbine is fixed inside the test rig.

The turbine support will be longer than before, so that if it is necessary to change the size of the perforated plate, it would be possible to screw outside of the test rig on the condition that the turbine is positioned in the maximum height.

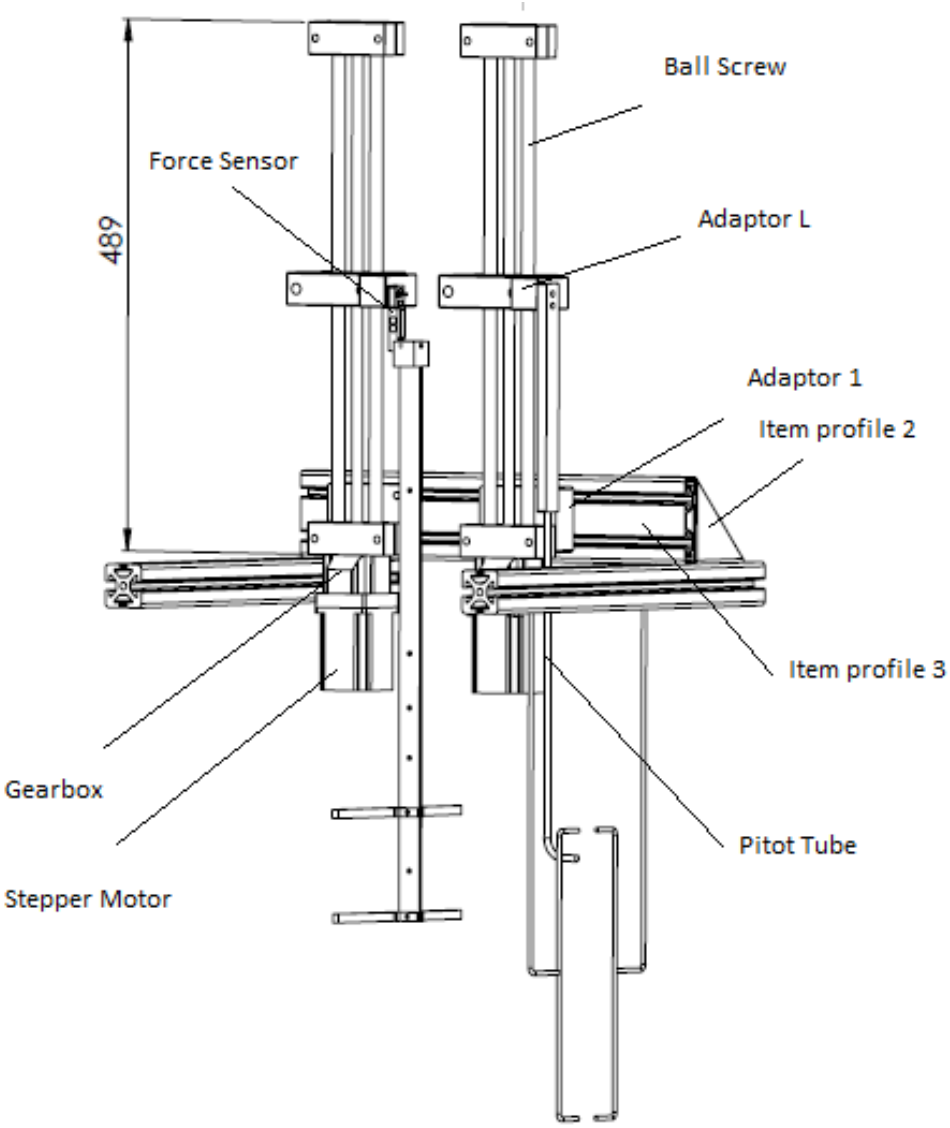

Figure 48: Lateral Turbine Concept

The technical drawing of the Adaptor L, Adaptor 1 and the colour version of Figure 48 are attached in section 10 (Appendix B).

All the pieces which are attached in the Appendix B are pieces that do not exist currently and should be fabricated in TU Darmstadt. The rest of pieces do not have technical drawings because they already exist and are placed in the channel test rig. The majority of them were bought from Igus and Rose&Krieger.

The item profiles shown in Figure 48 are from Rose&Krieger, the main function of them is to position the structure in the centre of the test rig, they are not relevant to the functioning of the system.

It is important to talk about the force sensor (See section 2.2.).

In Figure 51, there are two red lines, which cannot be exceeded by any piece. This fact is really important because if any piece touches the zone between both red lines the force sensor does not work properly. Therefore, the turbine support and the Adaptor L must be design in a way that never touch this area. This sensor will be the component in charge of measuring the force, which the flow is producing in the perforated plate. As it has been previously commented, the sensor works greatly with a measurement uncertainty of 0.1%

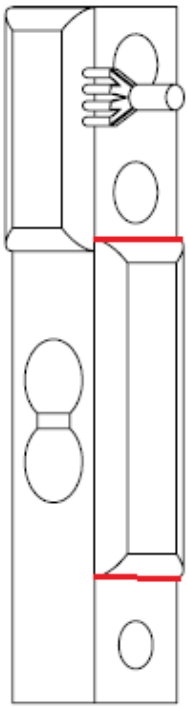

Figure 49: Force Sensor

Adaptor L is used to fix the turbine system to the ball screw, it must be deep enough so that the turbine support does not touch the stepper motor, its shape places the turbine structure frontally, but the ball screw is fixed laterally. Adaptor 1 is used to fix the ball screw to the item profiles, which are fixed to the rest of the test rig, it must also be deep enough in order to avoid collision between item profile 3 and the stepper motor.

One of the advantages of this concept is that by placing the ball screw laterally, we avoid the structure bending when high velocities are used in the test rig. This fact is produced because the surface which is normal to the flow is smaller than the transversal surface. This gives more rigidity to the structure.

Although the lateral option is efficient, as it is placed in the lateral side of the test rig, it appears a momentum, which is not desirable. To confront this con, it was decided to design the structure with the minimum distance between the turbine structure and the ball screw: 5 cm. That means that the momentum will not be that powerful to interfere in the measurement accuracy. The velocities that we are working with are not going to be higher than 1.3 m/s.

There is another option which could also be test, a frontal structure with almost the same components. It will move also vertically by using a ball screw a stepper motor, gearbox and a controller which will be placed outside the test rig. The vertical movement will be programmed by Labview.

The following picture shows the frontal concept

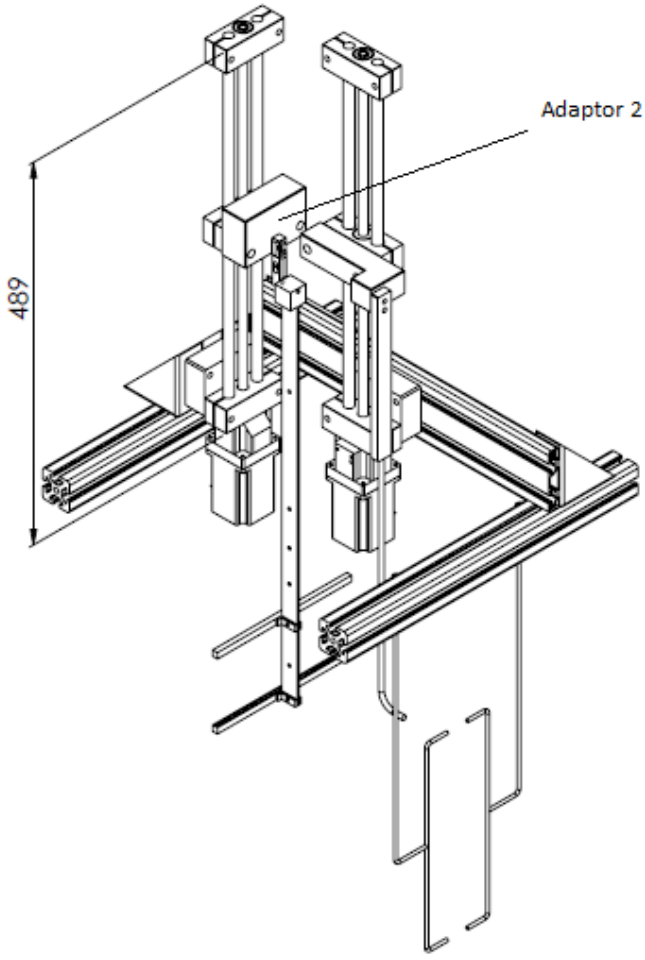

Figure 50: Frontal Turbine Concept

The only two differences with the lateral structure are the use of Adaptor 2 instead of Adaptor L and the fact that the ball screw will be fixed to item profile 2 without using item profile 3 (See Figure 50).

The coloured version of Figure 50 is attached in section 10 (Appendix B).

In this option it does not appear a momentum because the turbine is fixed to an item profile positioned normal to the flow. The main problem of this concept is that if the flow has high velocities, the force produced may be too high and therefore the whole frontal structure could bend, producing undesirable errors in the measurement parameters, because the turbine will change the position and then the hydrogen bubbles will also change the path of the streamtube.

Although the Lateral option is the concept chosen, both, frontal and lateral structures have almost the same pieces, this have been done so that both can be tested and therefore observe in the experimentation which one works better.

6.2 Election Turbine Resistances

Turbine Resistances are defined as the shape of the perforated plate. It is directly related with the dissipated energy of the turbine. There are plenty of different possibilities when choosing the shape of the perforated plate, for instance square holes, round holes, vertical lines, etc.

The dissipated energy is of high importance in this experiment. As it was commented in section 2.1., it does not matter what kind of energy is dissipated, but what really matters is the amount of the dissipated energy. For this experiment is necessary to achieve a wide range of dissipated energy.

In this case a high upper limit of the range is easy to achieve, so we should focus on the lower limit, and try to make it as low as possible. In order to achieve this purpose, ξ is defined as the resistance coefficient, which is the force caused by an obstacle placed against a water flow. It is usually expressed in kg/m^2. [40]

The lower the resistance coefficient is, the lower the perforated plate dissipates energy.

In Eq. 32 is defined the resistance coefficient. [40]

With the conditions that $Re > 10^5$ just after the turbine and that the coefficient $\frac{l}{D_h} = 0 \div 0.015$

In our case $Re_{max} = 2.4 \cdot 10^5$ and $\frac{l}{D_h} = \frac{2}{320} = 0.00625$

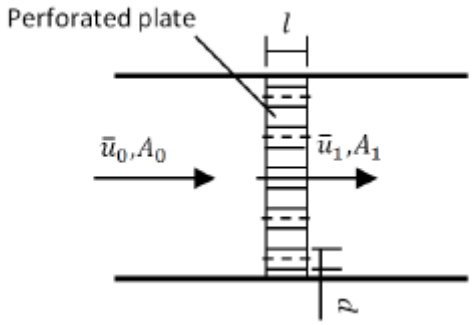

Figure 51: Sketch of turbine resistance [40]

$$\xi = (0.707\sqrt{1-\varphi} + 1 - \varphi)^2 \cdot \frac{1}{\varphi^2} \quad \text{(Eq. 32)}$$

This coefficient depends on the cross-section coefficient $\bar{f}$, the Reynolds number and the shape of its orifices.

The cross-section coefficient is defined in the following equation.

$$\varphi = \frac{A_{open}}{A_{close}} \quad \text{(Eq. 33)}$$

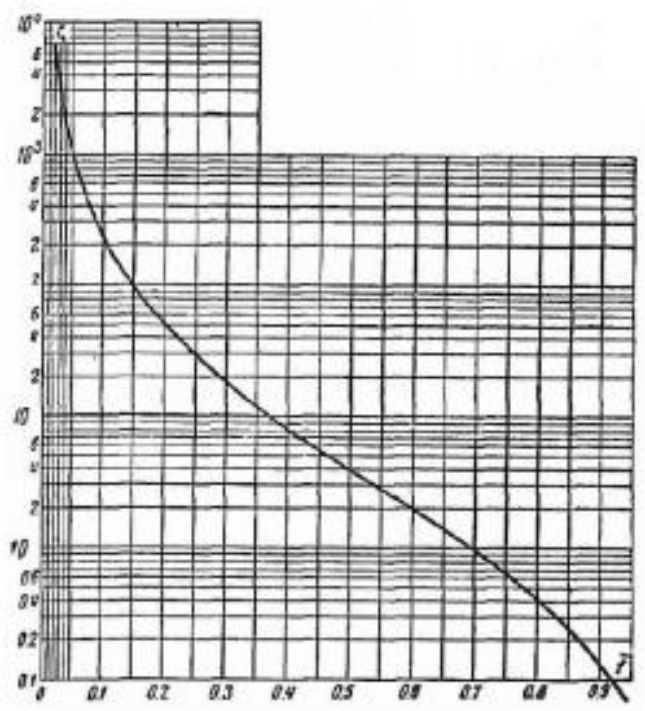

Figure 52: Values of the resistance coefficient in function of the cross-section coefficient [40]

As it has been explained, the objective is to analyse the measurement with low energy dissipation, this is achieved with a low resistance coefficient. By increasing the cross-section coefficient, it is achieved a diminution of the resistance coefficient.

The only solution then is to make bigger the open area, it is recommend to use square holes instead of round holes in the perforated plate, with this orifices shape, the perforated plate dissipates lower energy which was the objective.

There will be six different perforated plate sizes, the width will be always 200 mm but the height will be of 50 mm, 100 mm, 150mm, 200mm, 250 mm (which is H_1) and one perforated plate size, which blocks the whole channel of 400 mm.

The holes sizes that are proposed are:

- 5 mm square hole with a separation between the centres of 8 mm (1000x2000)
- 8 mm square hole with a separation between the centres of 12 mm (1000x2000)
- 10 mm square hole with a separation between the centres of 15 mm (1000x2000)

The material will be steel due to its low price. The perforated plates can be bought in Shopmetal.de.

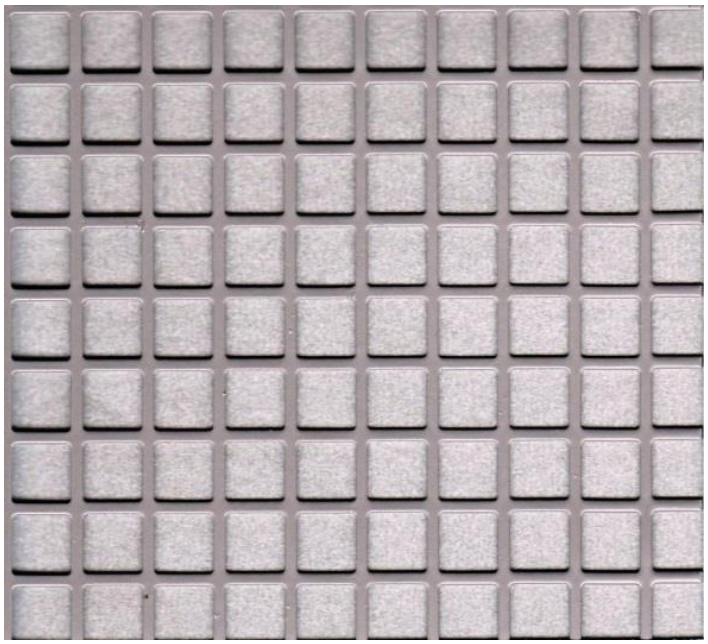

Figure 53: Square perforated plates (Turbine resistances)

7 Summary and Outlooks

7.1 Summary

In light of the above mentioned, it is important to make some conclusions of the present bachelor thesis.

The elected Measurement system can be divided in velocity measurement and water level altimetry measurement.

The velocity will be measured with a Flow visualization technique, more concretely with the hydrogen bubble method, the electric circuit used in order to generate the bubbles by electrolysis is the one shown in Figure 42, the wire will be of platinum and the wires support od brass with an insulation of shrink-fit, the illumination will consist of one LED in the bottom of the channel and other two oblique to the area of interest. By using this technique, it will be possible to measure the distribution of the velocity between points (-) and (2) as well as the medium line and the width of the streamtube.

A Pitot tube will be used to measure the velocity before the perforated plate. Also, the foils concept explained previously will be used just to show the flow's behaviour to other people or institutions.

The water level altimetry will be measured with the same high-resolution camera used in the velocity measurement. At TU Darmstadt there is already a Charge Coupled Device (CCD) Camera: Sensicam qe. By making a lot of pictures and interpolating it will not be difficult to measure the shape of the water flow altimetry. By using this technique, it would be possible to measure the water level altimetry as well as the static pressure, which depends directly on the height.

The turbine system, which has been designed in the present thesis consist of a ball screw, a stepper motor, a gearbox and a controller. The vertical movement of this system will be coded in Labview. This concept allows measuring the required parameters in different height positions without screwing in the turbine support. Also, it will not be necessary to screw when changing the perforated plate resistances. The only moment that will be necessary to screw is when changing the size of the perforated plate.

By implementing the proposed turbine system, it is gained velocity at the time of collecting data and comfortability when changing the resistances or sizes of the perforated plates.

The turbine system will have a lateral structure (Figure 48) in order to avoid a bending force produced by the water flow, the distance between the ball screw and the turbine support will be minimal in order to avoid an undesirable momentum.

As the pieces used in the construction of the lateral structure are almost the same as the ones that could be used to construct a frontal structure (Figure 50) it could be interesting to test both experimentally and then choose the most efficient structure. Even though, the frontal structure could present bending forces and could change the position of the turbine, resulting in inaccurate measurements.

7.2 Outlooks

Although the hydrogen bubble technique should work efficiently, if it is wanted a leap of quality in the project it would be recommendable to use PIV or PTV techniques, which are way more accurate than the hydrogen bubble method. The material is available in TU Darmstadt. The main disadvantage of these techniques is the hard implementation.

In this case the water level altimetry measurement will consist of the same camera used for the optical method. It is the same concept that the one present in this thesis.

If the future path does not follow immediately the PIV or PTV techniques, it would be a good idea to invest in a laser sheet in order to illuminate the area of interest where the camera will focus on the hydrogen bubbles. This laser sheet will be also necessary in the PIV or PTV techniques, so it would be nice to start with this step.

The person responsible of running the measurement should consider that is necessary the calibration of the signal TTL by calibrating the components R_1 and C_1 as well as the angle of LEDs position.

In the turbine system, it is also necessary to program the code of Labview to move vertically the Pitot tube and the perforated plate.

8 References

[1] Renewables 2017 Global Status Report - Ren21, 2017.

[2] Lombardo, Crystal. The Advantages and Disadvantages of Tidal Energy Power - The Next Galaxy, 2015.

[3] Hermes, Jennifer. The present and Future of Tidal Power - Environmental leader, 2013.

[4] Pelz, P.F. *Upper Limit for Hydropower in an Open-Chanel Flow*. J. Hydraul. Eng., 137(11), 1536-1542. American Society of Civil Engineers. 2011.

[5] Pelz, P.F; Metzler M. An Analytic Approach to Optimization of Tidal Turbine Fields. ICEPE 2013 - 3rd International Conference on Energy Process Engineering. Frankfurt, Deutschland. 2013.

[6] J. Nieschlag. Experimentelle Untersuchung der Strömung um eine vertikal umströmte hydrokinetische Turbine, Darmstadt 2016

[7] D. Hernández Días. *Design and Construction of an Open Channel Test Rig.* Bachelor-Thesis. Darmstadt. 2013.

[8] Lehr, M. Aufbau eines Messsystems zur Strömungsvermessung am offenen Gerinneprüfstand. Master-Thesis. Darmstadt. 2014.

[9] M. Euler, A. Krah, M. Lehr, X. Li. *Design eines Messsystems für einen Gerinneprüfstand.* Advanced Design Project. Darmstadt. 2013.

[10] Deparment FST (Fluid System Technik) - TU Darmstadt.

[11] Çengel, Yunus A; Cimbala, John M. Fluid Mechanics [Fundamentals and Applications] 1st Edition in SI Units. New York Mc.Graw-Hills 2006.

[12] Shames, I.H. Mechanics of Fluids. New York McGraw-Hill Higher Education, 2004.

[13] Mott, Robert L.. *Applied Fluid Mechanics*. 6th Edition. New Jersey: Pearson Prentice Hall. 2006.

[14] Cameron Tropea; Alexander Yarin; John Foss (eds.). Springer Handbook of Experimental Fluid Mechanics. Springer.

[15] Starke, Oliver. Konstruktion eines Prüfstandes zur experimentellen Validierung von Gezeitenturbinenmodellen. Darmstadt 2017

[16] Froehlich, T. *Performance survey of an open channel test rig*. Master-Thesis. Darmstadt. 2015.

[17] Dr. R.B. Green. An introductory course for advanced experimental techniques used in fluid dynamics and aerodynamics. United Kingdom: University of Glasgow. 2009.

[18] Ronald J, Adrian. Particle-Imaging Techniques for Experimental Fluid Mechanics. University of Illinois. 1991.

[19] W. Nitsche, A. Brunn. *Strömungsmesstechnik*. Springer-Verlag. Berlin, Heidelberg. 2006.

[20] http://www.andor.com/learning-academy/piv-mode-for-istar-scmos-technical-article

[21] TH. Dracos. Three-Dimensional Velocity and Vorticity Measuring and Image Analysis Techniques, Zürich 1996.

[22] K. Rubner, D. Bohn. Verfahren für die Auswertung der Messergebnisse von Strömungs sonden durch mehrdimensionale Approximation der Eichkurven und Eichflächen. Zeit-schrift für Flugwissenschaften 20. 1972.

[23] http://ocw.metu.edu.tr/pluginfile.php/1871/mod_resource/content/0/AE547/AE47_9_Hotwire-son.pdf (20/08/2013)

[24] Dantec Dynamics. Probes for Hot-wire anemometry. Product Catalog.

[25] R. Markert. *Strukturdynamik*. Vorlesungsskript. Fachgebiet Strukturdynamik. Darmstadt. 2010.

[26] Durst, F.A. Melling; J.Whitelaw. Principles and Practices of Laser Doppler Anemometry. Academic Press. 1981.

[27] Dantec Dynamics. Measurement Principles of Laser Dopler Anemometry.

[28] Manoochehr M. Koochesfahani and Daniel G. Nocera. Molecular Tagging Velocimetry. Handbook of Experimental Fluid Dynamics, Chapter 5.4, editors: J. Foss, C. Tropea and A. Yarin, Springer-Verlag . 2007).

[29] C. R. Smith and R. D. Paxson. A Technique for Evaluation of Three-dimensional Behavior in Turbulent Boundary Layers Using Computer Augmented Hydrogen Bubble-wire Flow Visualization. Bethlehem. 1983.

[30] W. Merzkirch. Techniques of Flow Visualization, AGARD, editor: K.Gersten. Essen 1987.

[31] Taif M. Mansoor, Prof. Dr. Akram W. Ezzat. Water Flow Visualization And Velocity Measurement Using Hydrogen Bubble Generation Technique In Low Speed Open Channel. Baghdad 2012.

[32] Flow Visualization: Techniques and Examples, Edition: Second, Publisher: Imperial College Press, London, Editors: A. J. Smits, T.T. Lim, pp.19

[33] Mattingly, George E. The Hydrogen-Bubble, Flow Visualization Technique. Washington, D.C. :Dept. of the Navy, David Taylor Model Basin,1966.

[34] R. Budwig, R. Peattie. Two new Circuits for Hydrogen Bubble Flow Visualization. Moscow 1988.

[35] L.J.Lu, C.R.Smith Image processing of Hydrogen Bubble Flow Visualization for Determination of Turbulence Statistics and Bursting Characteristics. Bethlehem 1985.

[36] C.Magness, T. Utsch, D.Rockwell. Flow Visualization via Laser-Induced Reflection from Bubble Sheets. Bethlehem 1990.

[37] M. Löffler-Mang. *Optische Sensorik*. Springer-Verlag. Berlin, Heidelberg. 2012.

[38] Hopper, Henry. A Dozen Ways to Measure Fluid Level and How they work. Sensors|Online. 2004.

[39] Recommended Light Levels (Illuminance) for Outdoor and Indoor Venues

[40] Idel'chik. *Handbook of Hydraulic Resistance* [Coefficients of Local Resistance and of Friction]. Jerusalem: Israel Program for Scientific Translations. 1966.

9 Appendix A

9.1 List of Figures

9.2 List of Tables

9.3 Economic Budget

In this Section, it will be explained all the costs which have been surrounded in this thesis. It is considered that the student would have a salary of 12 €/ hour. It is also considered that the student has work in the thesis around 375 hours.

So, the **human cost** of the present bachelor thesis would be of **4.500 €**

In the following table, it is shown all the required components which must be bought by TU Darmstadt in order to make possible the realization of this thesis. As it can be observed the **material cost** is **539.79 €**

Component	Company	Nº of Reference	Price
Isolated Transformer x2	Digikey	N-73A (Triad Magnets)	73.02 euros
Rectifier x2	Mouser	MDA206G	1.12 euros
Opto-isolator x2	Mouser	859-4N26	0.84 euros
Multivibrator Monostable x2	Digikey	SN74121D	6.76 euros
Transistor MOSFET x2	Octopart	MTP4N50	20.42 euros
Capacitor 500 µF and 450 V x2	Mouser	E36D451LPN500TA54M	18.76 euros
Resistor 0.3 kΩ x2	Digikey	RC04022JR-07300RL	0.16 euros
Resistor 20 kΩ x2	Digikey	RC0201FR-0720KL	0.16 euros
Resistor 0.1 kΩ (10W) x2	Digikey	RC0603FR-07100RL	0.16 euros
Resistor 20 kΩ (2W) x2	Digikey	352120KFT	1.14 euros
Circuit breaker 2 A x2	Digikey	9926251902	38.74 euros
Wire Platinum	Buyplatinumwire.com	50 µm x 3,048 m	99.52 euros
Brass round bar	Metalandplastic	4mm x 3 m	8.83 euros
LED of 1120 lumens	Mouser	XHPTOB-00-0000-000BJ450E	5.75 euros
LED of 400 lumens x 2	Mouser	XPLAWT-00-0000-000BV20E3	5.38 euros
Perforated Sheet 5mm	Shopmetal	Lochblech aus Stahl roh DC/DD/S235 - QG 5-8 2x1000x2000	98.28 euros
Perforated Sheet 8mm	Shopmetal	Lochblech aus Stahl roh DC/DD/S235 - QG 8-12 2x1000x2000	78.47 euros
Perforated Sheet 10mm	Shopmetal	Lochblech aus Stahl roh DC/DD/S235 - QG 10-15 2x1000x2000	82.28 euros
Total			539.79 euros

In the following table, it is shown all the costs which have been involved in the realization of this project:

Resource	Cost (€)
Human Cost	4.500
Material Cost	539,79
General Cost	503,98
Industry Surcharge	453,58
IVA (21%)	1259,4435
Total	7.257

Consequently, the **Total Costs** of the project are estimated in **7.257 €**

9.4 Planning – Diagram of Gantt

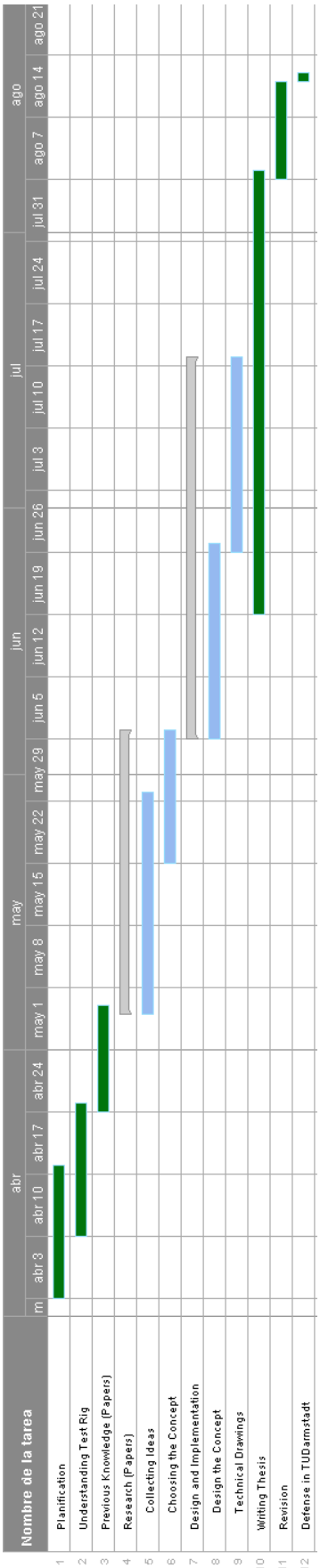

10 Appendix B – Technical Drawings

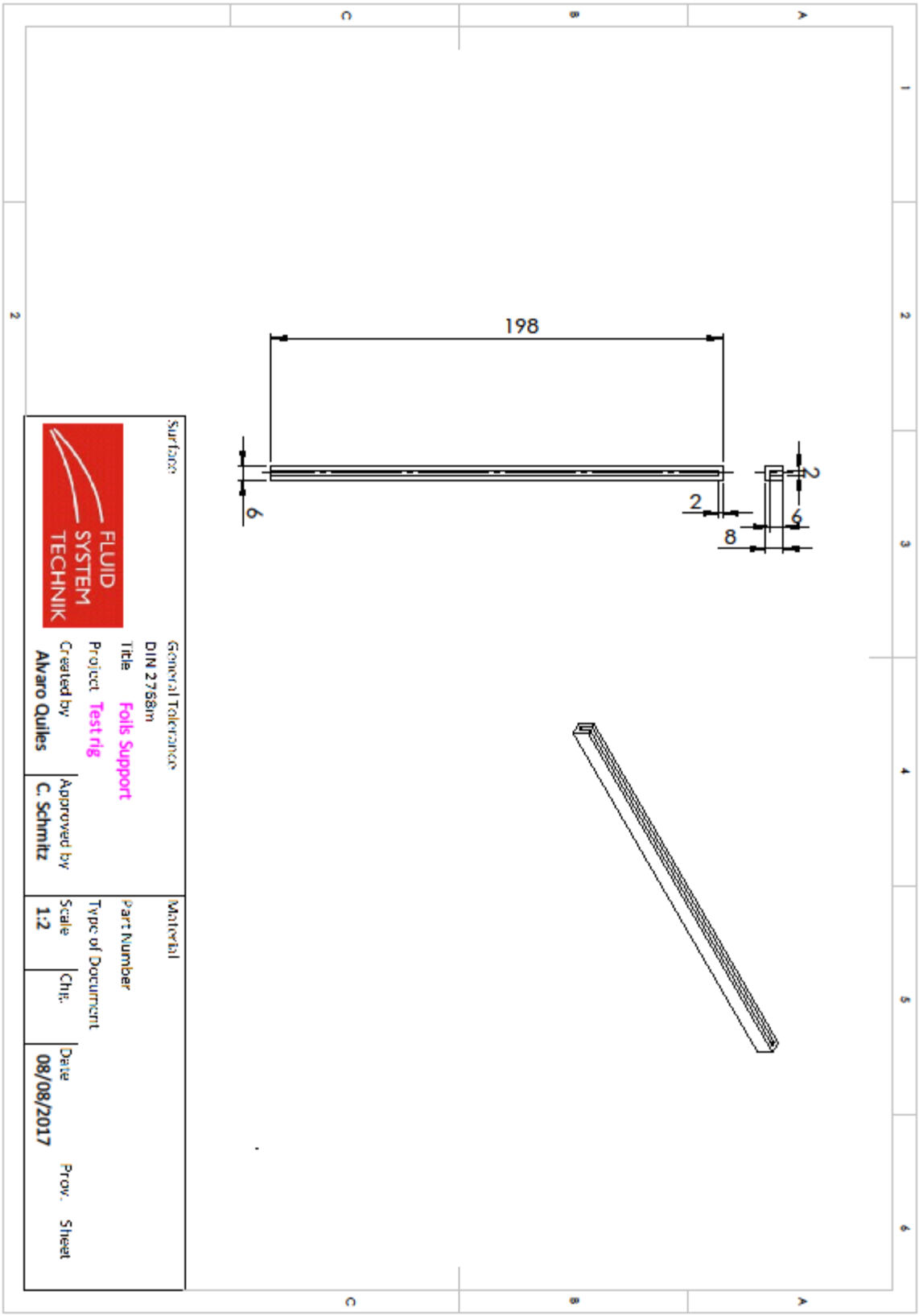

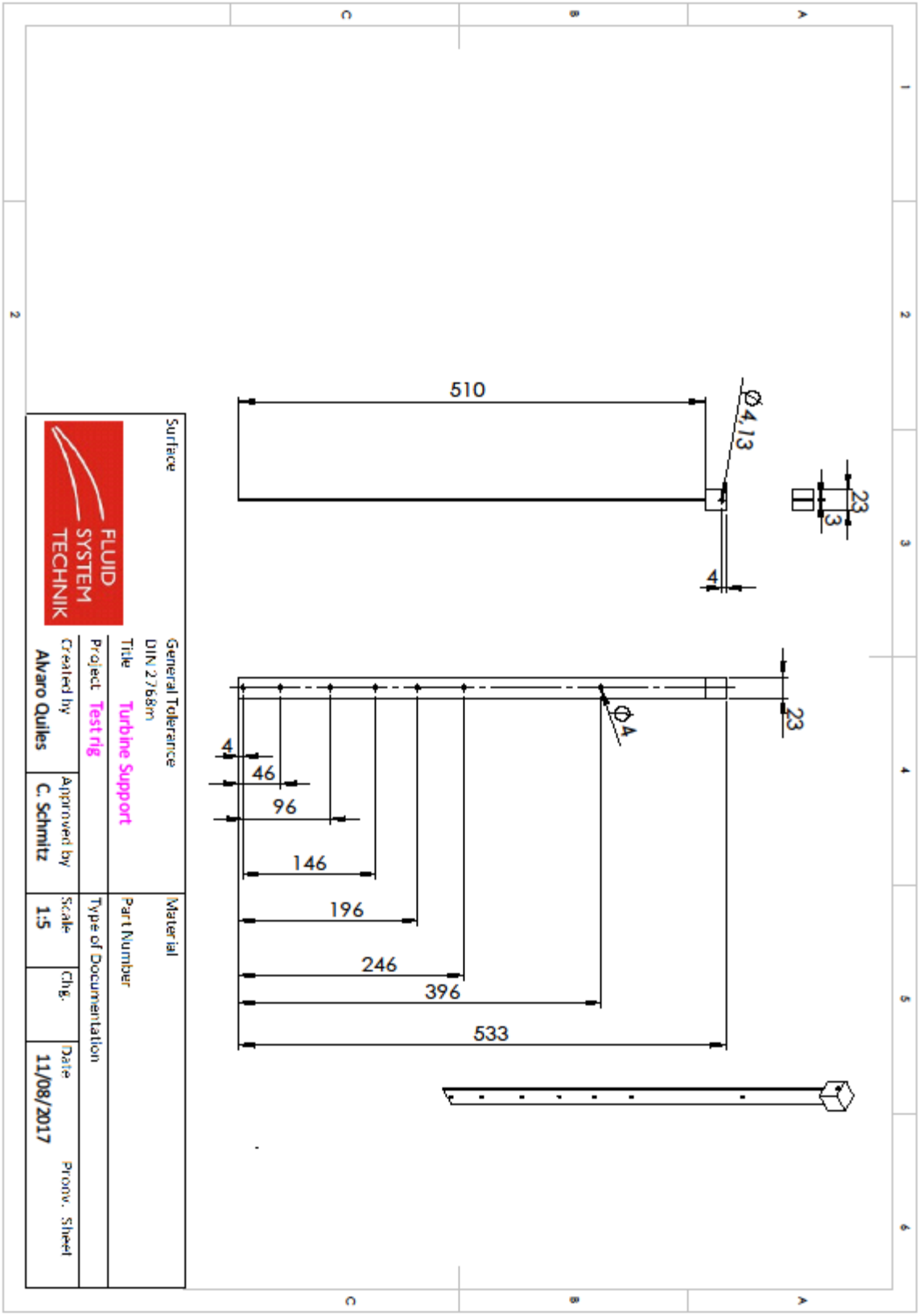
510
Ø4,13
23
3
4
Ø4
23
4
46
96
146
196
246
396
533
Surface
General Tolerance
DIN 2768m
Material
Title
Turbine Support
Part Number
Project
Test rig
Type of Documentation
Created by
Alvaro Quiles
Approved by
C. Schmitz
Scale
1:5
Chg.
Date
11/08/2017
Prom. Sheet
FLUID SYSTEM TECHNIK

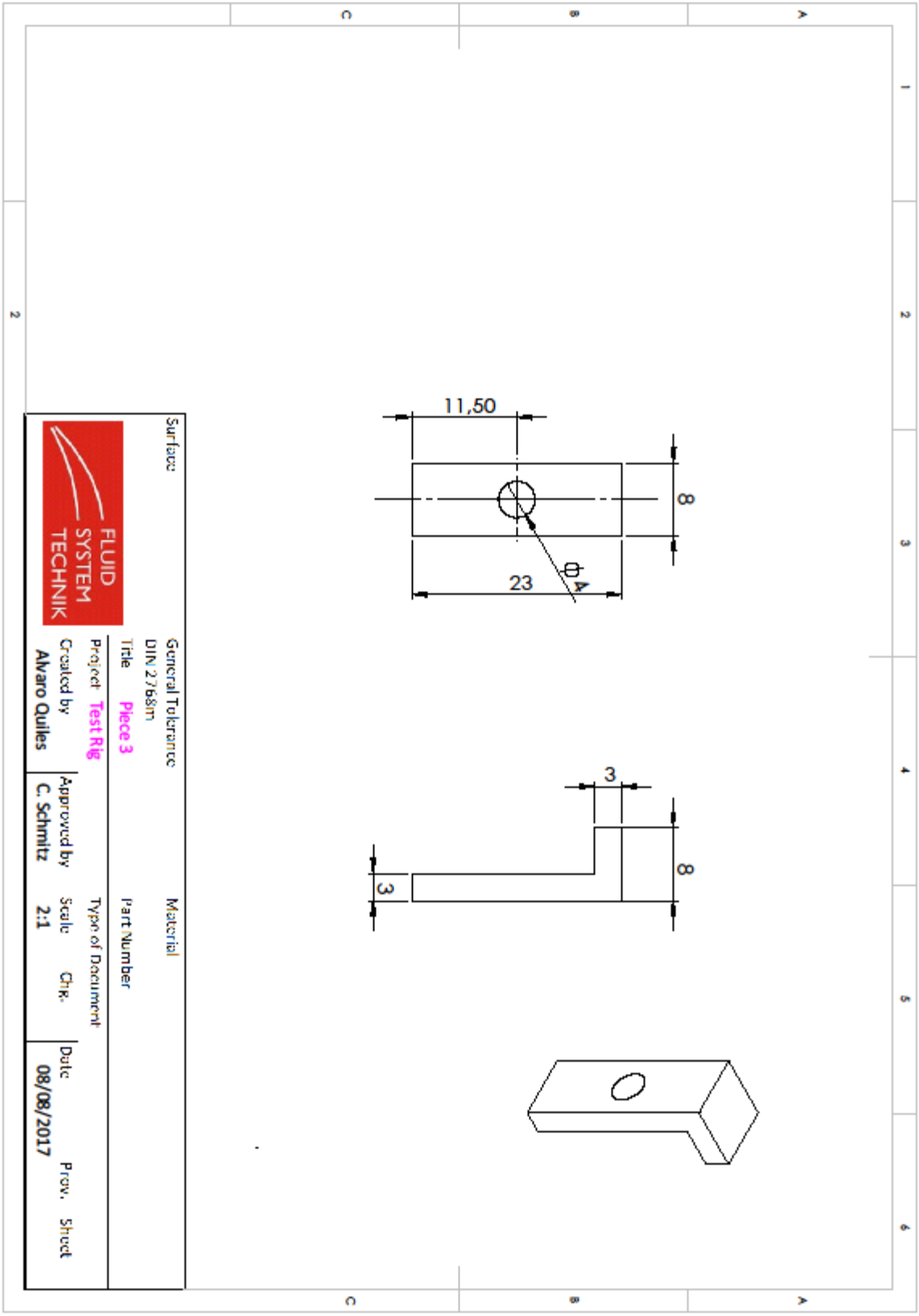
11,50
8
Ø4
23
3
3
8
Surface:
General Tolerance
DIN 2768m
Material
Title
Piece 3
Part Number
Project
Test Rig
Type of Document
Created by
Alvaro Quiles
Approved by
C. Schmitz
Scale
2:1
Chk.
Date
08/08/2017
Prov.
Sheet
FLUID SYSTEM TECHNIK

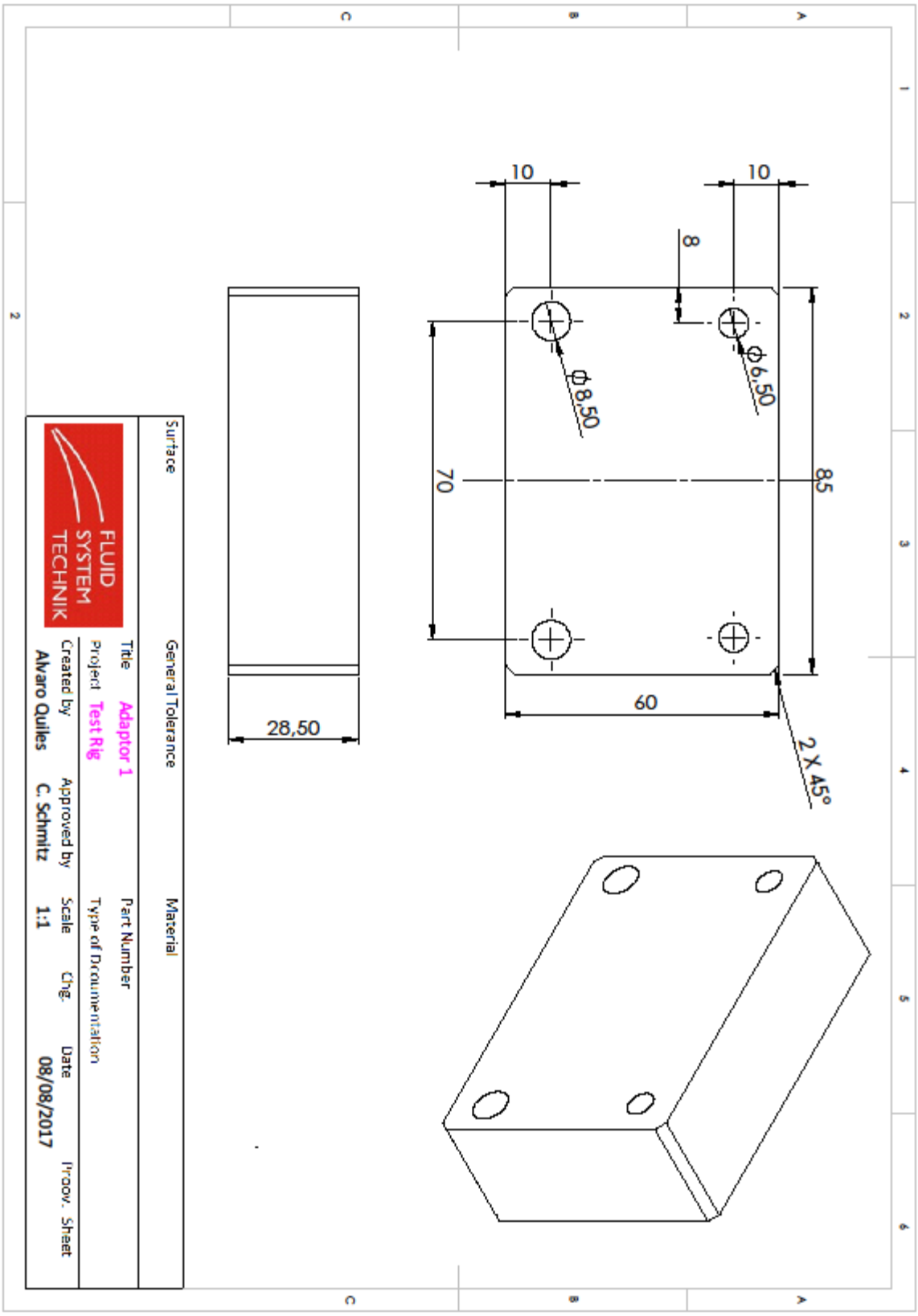
10
10
8
Φ6,50
Φ8,50
70
85
60
28,50
2 X 45°
Surface
General Tolerance
Material
FLUID SYSTEM TECHNIK
Title
Adaptor 1
Part Number
Project
Test Rig
Type of Documentation
Created by
Approved by
Scale
Chg.
Date
Prjov.
Sheet
Alvaro Quiles
C. Schmitz
1:1
08/08/2017

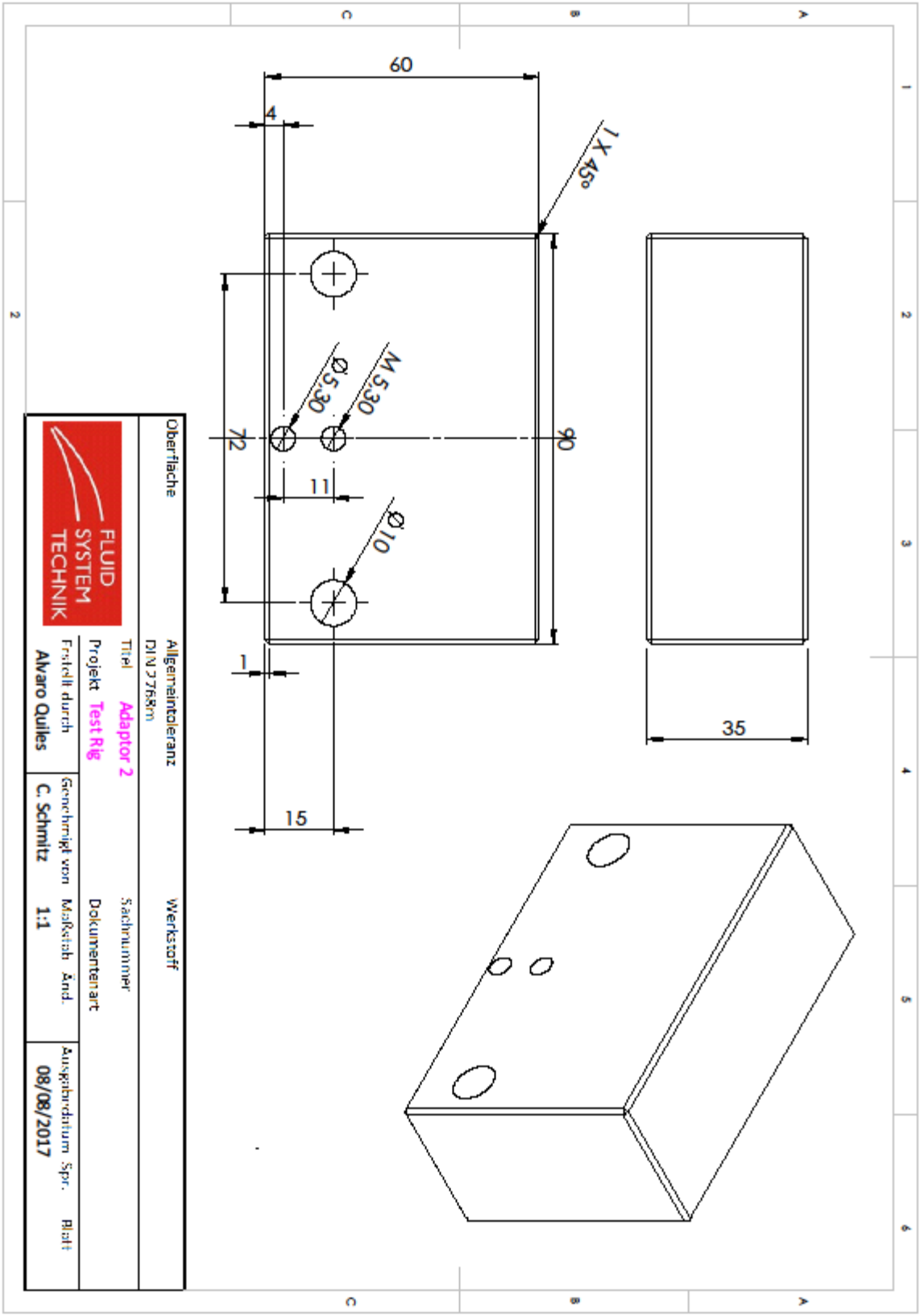
60
4
1 X 45°
M 5,30
Ø 5,30
72
90
11
Ø 10
1
15
35
Oberfläche
Allgemeintoleranz
DIN 7168m
Werkstoff
FLUID SYSTEM TECHNIK
Titel Adaptor 2
Projekt Test Rig
Sachnummer
Dokumentenart
Erstellt durch
Alvaro Quiles
Geprüft von
C. Schmitz
Maßstab
1:1
Änd.
Ausgabedatum
08/08/2017
Spr.
Blatt

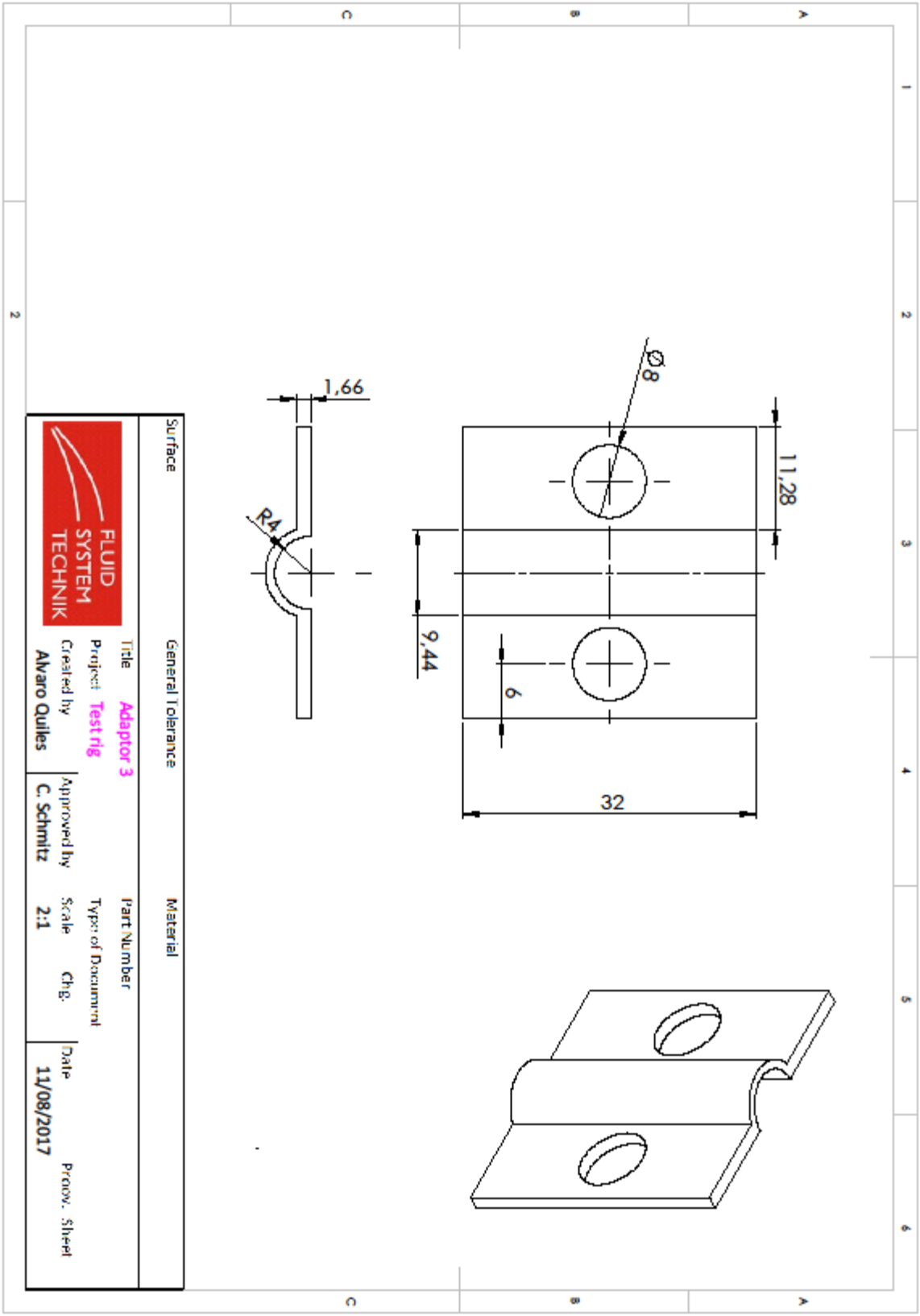
1,66
R4
Ø8
11,28
9,44
6
32
Surface
General Tolerance
Material
FLUID SYSTEM TECHNIK
Title Adaptor 3
Part Number
Project Test rig
Type of Document
Created by
Alvaro Quiles
Approved by
C. Schmitz
Scale
2:1
Chg.
Date
11/08/2017
Prooy. Sheet

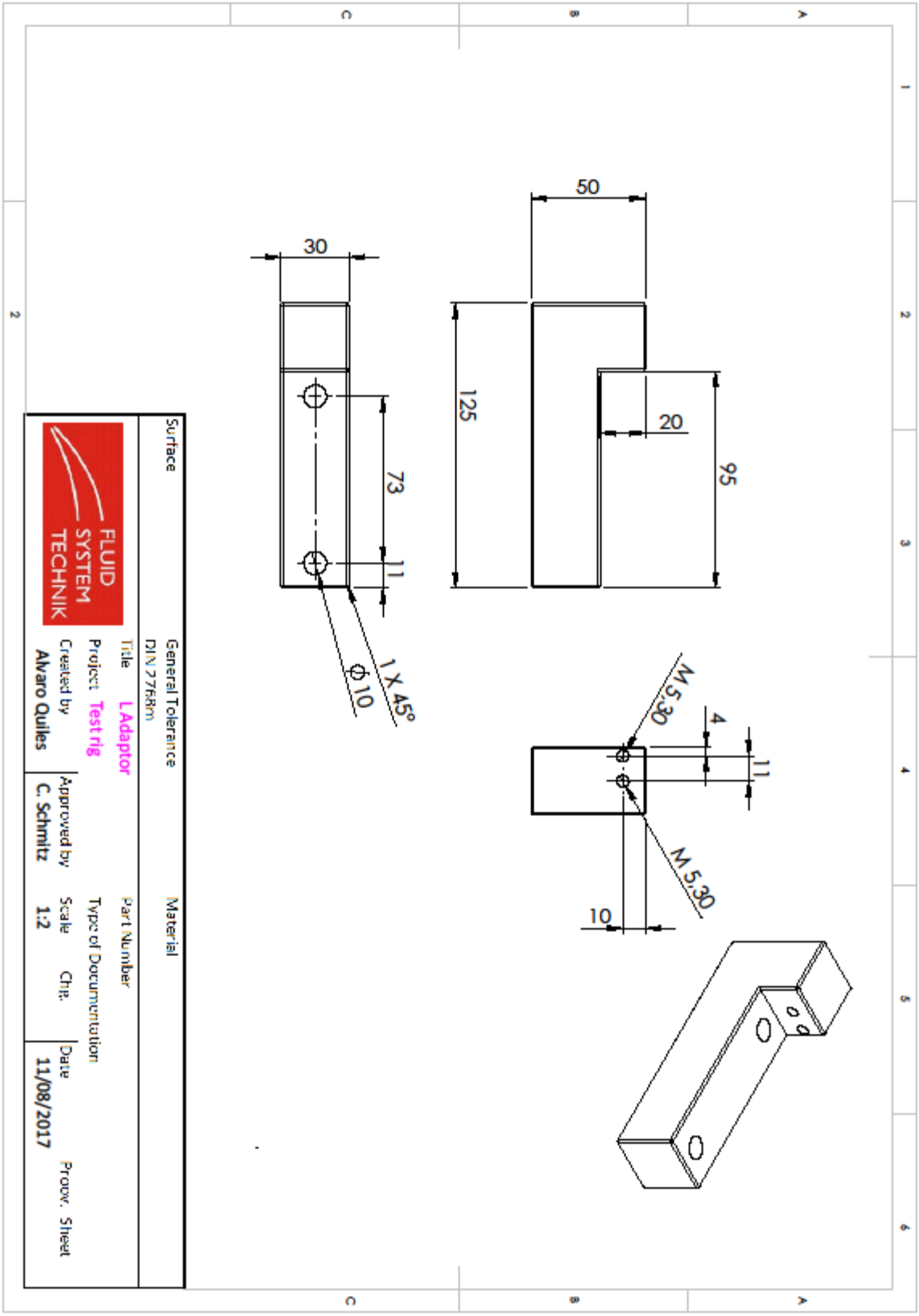
50
30
125
20
95
73
11
1 X 45°
Ø 10
M 5;30
4
11
M 5;30
10
Surface
General Tolerance
DIN 7168m
Material
FLUID SYSTEM TECHNIK
Title LAdaptor
Part Number
Project Test rig
Type of Documentation
Created by
Alvaro Quiles
Approved by
C. Schmitz
Scale
1:2
Chg.
Date
11/08/2017
Proov.
Sheet

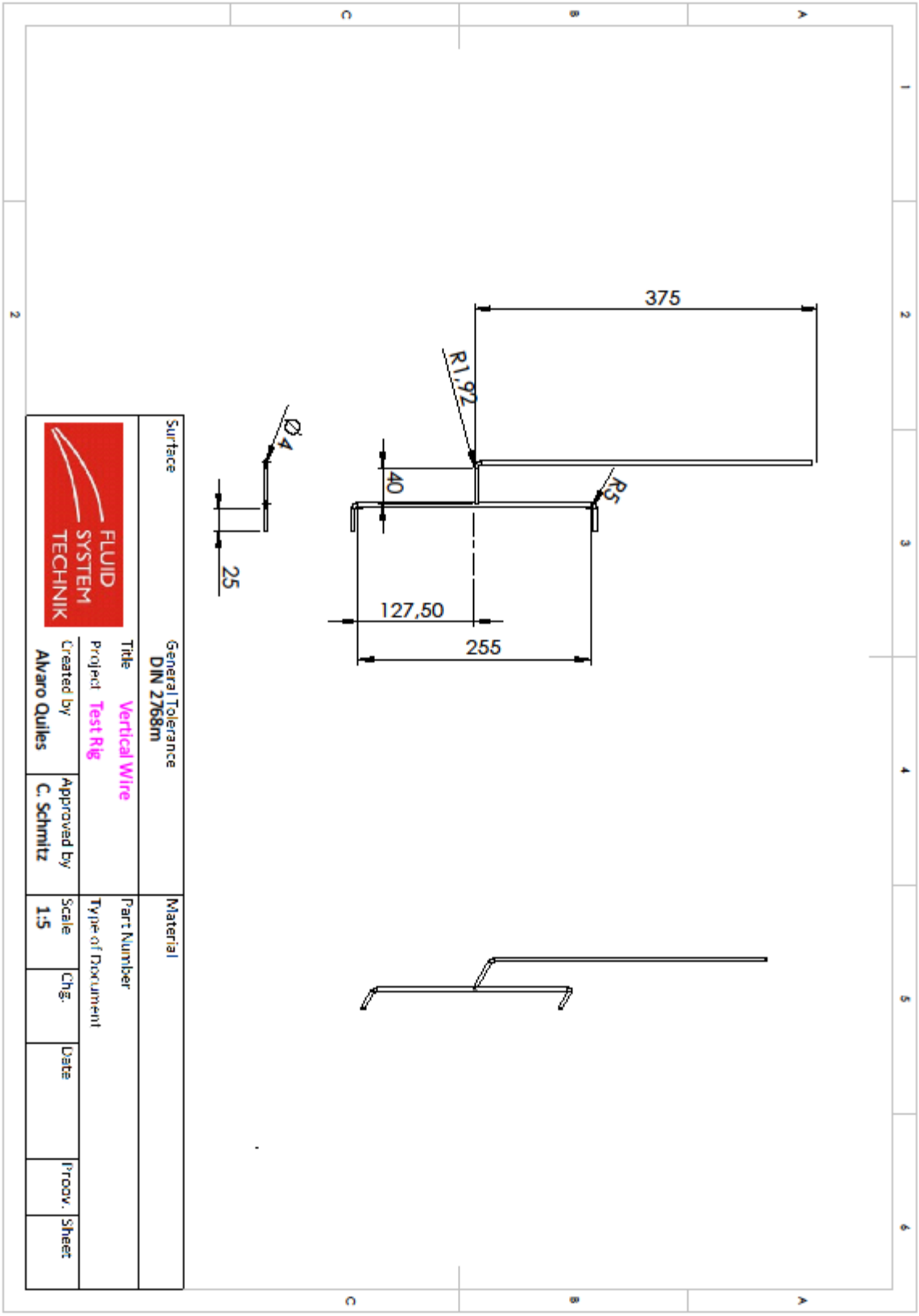
375
R1,92
Ø4
40
R5
25
127,50
255
Surface
General Tolerance
DIN 2768m
Material
FLUID SYSTEM TECHNIK
Title Vertical Wire
Project Test Rig
Part Number
Type of Document
Created by
Alvaro Quiles
Approved by
C. Schmitz
Scale
1:5
Chg.
Date
Proov.
Sheet

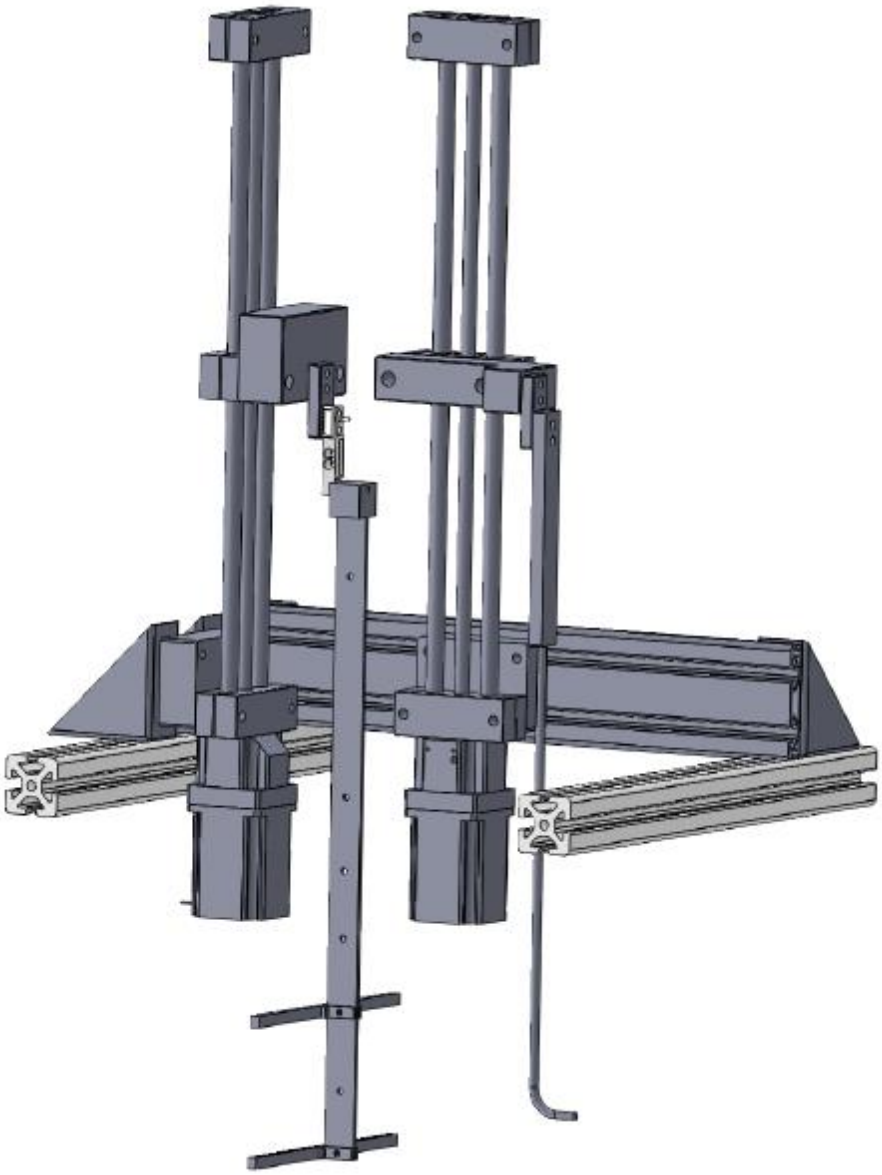

Figure: Frontal Turbine Concept

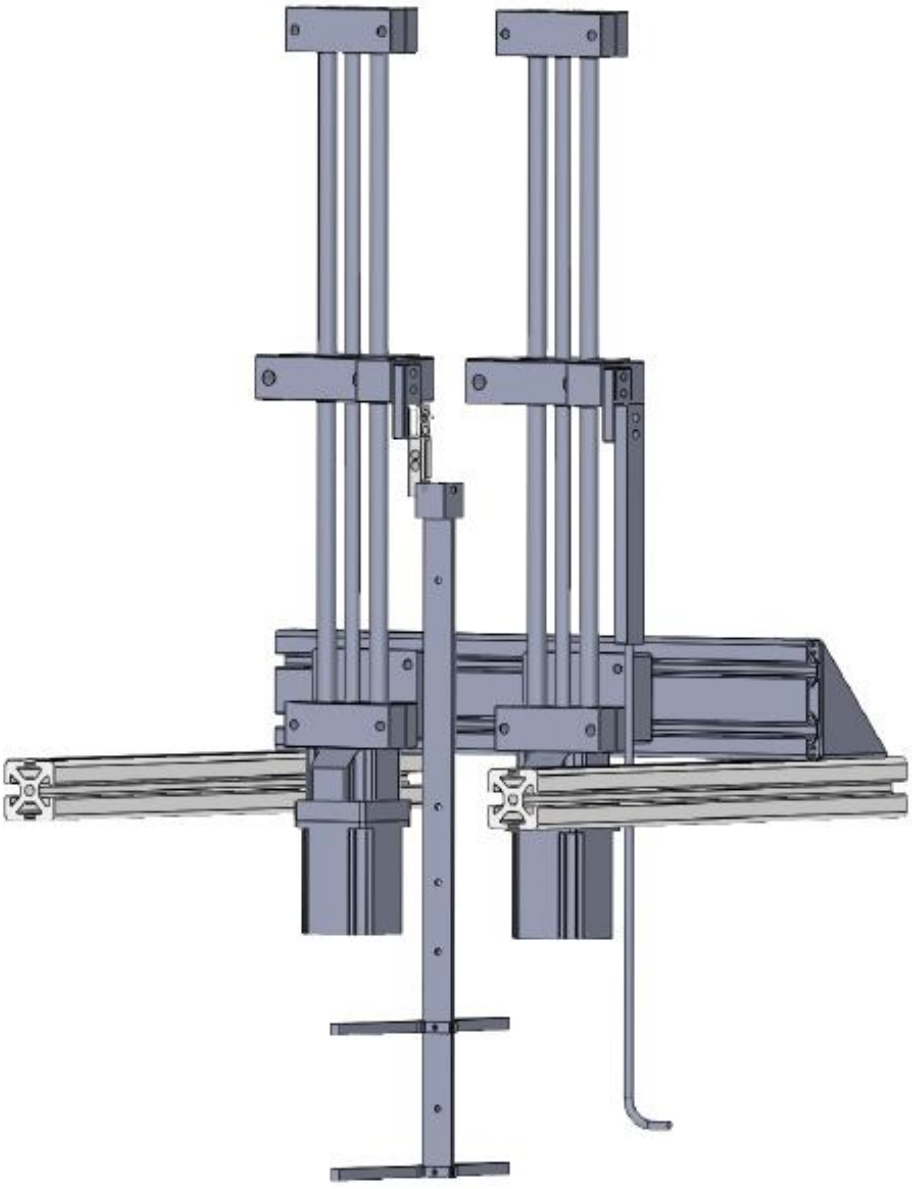

Figure: Lateral Turbine Concept.